REGION 1

Agno River Basin:

DREAM Flood Forecasting and Flood Hazard Mapping

TRAINING CENTER FOR APPLIED GEODESY AND PHOTOGRAMMETRY

2015

Published by the UP Training Center for Applied Geodesy and Photogrammetry (TCAGP)
College of Engineering
University of the Philippines Diliman
Quezon City
1101 PHILIPPINES

This research work is supported by the Department of Science and Technology (DOST) Grant-in-Aid Program and is to be cited as:

UP TCAGP (2015), Flood Forecasting and Flood Hazard Mapping for Agno River Basin, Disaster Risk and Exposure Assessment for Mitigation (DREAM) Program, DOST-Grants-in-Aid Program, 106 pp.

For questions/queries regarding this report, contact:

Alfredo Mahar Francisco A. Lagmay, PhD.
Project Leader, Flood Modeling Component, DREAM Program
University of the Philippines Diliman
Quezon City, Philippines 1101
Email: amfal2@yahoo.com

Enrico C. Paringit, Dr. Eng.
Program Leader, DREAM Program
University of the Philippines Diliman
Quezon City, Philippines 1101
E-mail: paringit@gmail.com

National Library of the Philippines
ISBN: 978-621-95189-7-0

Table of Contents

Table of Contents

List of Figures

List of Figures

List of Figures

List of Tables

List of Equations

List of Abbreviations

ACDP	Acoustic Doppler Current Profiler
AOI	Area of Interest
ARG	Automated Rain Gauge
AWLS	Automated Water Level Sensor
DAC	Data Acquisition Component
DEM	Digital Elevation Model
DOST	Department of Science and Technology
DPC	Data Processing Component
DREAM	Disaster Risk Exposure and Assessment for Mitigation
DTM	Digital Terrain Model
DVC	Data Validation Component
FMC	Flood Modelling Component
GDS	Grid Developer System
HEC-HMS	Hydrologic Engineering Center – Hydrologic Modeling System
LiDAR	Light Detecting and Ranging
PAGASA	Philippine Atmospheric, Geophysical and Astronomical Services Administration
RIDF	Rainfall Intensity Duration Frequency
SCS	Soil Conservation Service
SRTM	Shuttle Radar Topography Mission
UP-TCAGP	UP Training Center for Applied Geodesy and Photogrammetry

Introduction

Introduction

1.1 About the DREAM Program

The UP Training Center for Applied Geodesy and Photogrammetry (UP TCAGP) conducts a research program entitled "Nationwide Disaster Risk and Exposure Assessment for Mitigation (DREAM) Program" funded by the Department of Science and Technology (DOST) Grants-in-Aid Program. The DREAM Program aims to produce detailed, up-to-date, national elevation dataset for 3D flood and hazard mapping to address disaster risk reduction and mitigation in the country.

The DREAM Program consists of four components that operationalize the various stages of implementation. The Data Acquisition Component (DAC) conducts aerial surveys to collect Light Detecting and Ranging (LiDAR) data and aerial images in major river basins and priority areas. The Data Validation Component (DVC) implements ground surveys to validate acquired LiDAR data, along with bathymetric measurements to gather river discharge data. The Data Processing Component (DPC) processes and compiles all data generated by the DAC and DVC. Finally, the Flood Modeling Component (FMC) utilizes compiled data for flood modeling and simulation.

Overall, the target output is a national elevation dataset suitable for 1:5000 scale mapping, with 50 centimeter horizontal and vertical accuracies. These accuracies are achieved through the use of state-of-the-art airborne Light Detection and Ranging (LiDAR) technology and appended with Synthetic-aperture radar (SAR) in some areas. It collects point cloud data at a rate of 100,000 to 500,000 points per second, and is capable of collecting elevation data at a rate of 300 to 400 square kilometers per day, per sensor

1.2 Objectives and Target Outputs

The program aims to achieve the following objectives:

a) To acquire a national elevation and resource dataset at sufficient resolution to produce information necessary to support the different phases of disaster management,

b) To operationalize the development of flood hazard models that would produce updated and detailed flood hazard maps for the major river systems in the country,

c) To develop the capacity to process, produce and analyze various proven and potential thematic map layers from the 3D data useful for government agencies,

d) To transfer product development technologies to government agencies with geospatial information requirements, and,

e) To generate the following outputs
1) flood hazard map
2) digital surface model
3) digital terrain model and
4) orthophotograph.

1.3 General Methodological Framework

The methodology to accomplish the program's expected outputs are subdivided into four (4) major components, as shown in Figure 1. Each component is described in detail in the following section.

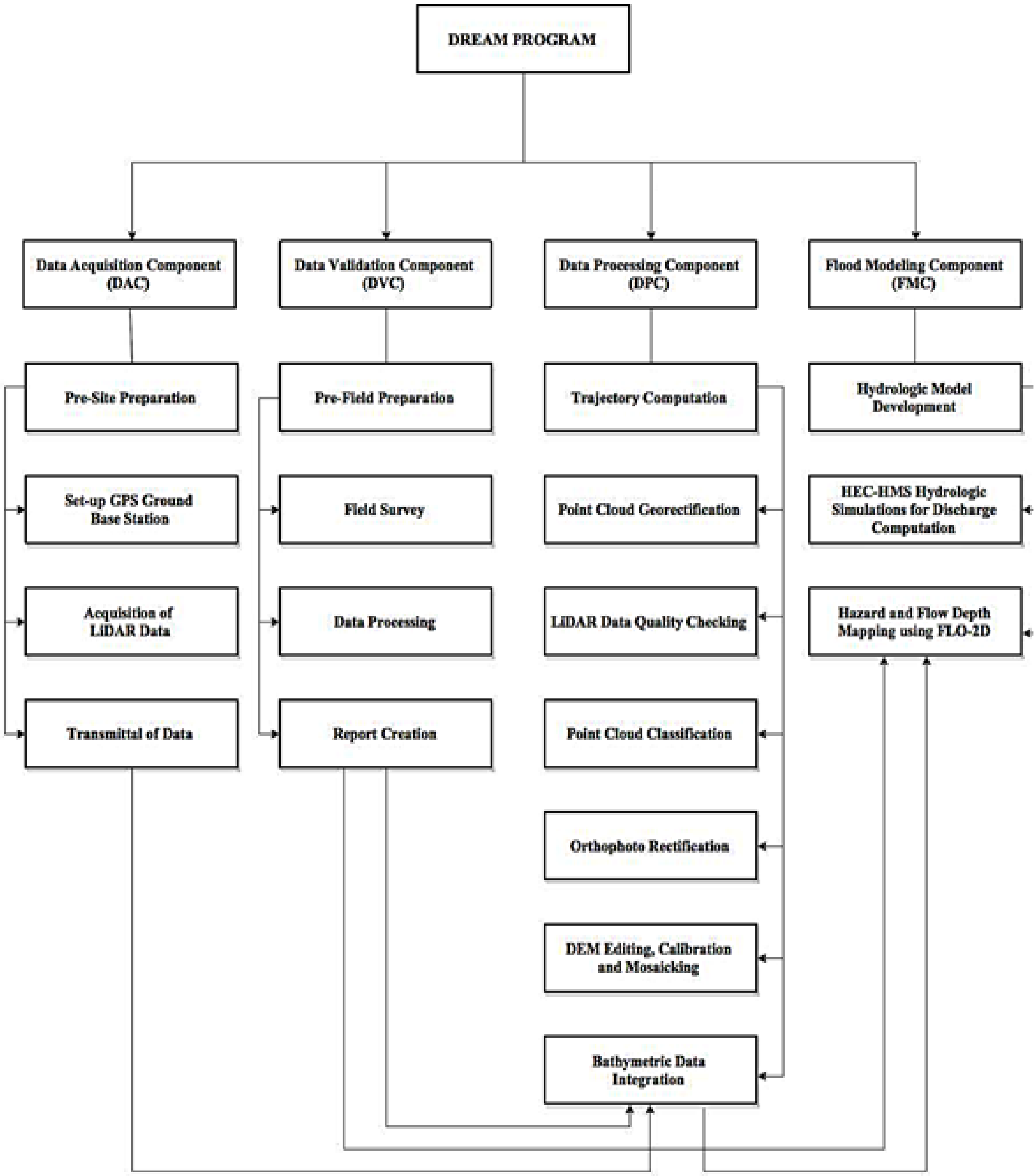

Figure 1. The general methodological framework of the program

1.4 Scope of Work of the Flood Modeling Component

The scope of work of the Flood Modeling Component is listed as the following:

a) To develop the watershed hydrologic model of the Agno River Basin;

b) To compute the discharge values quantifying the amount of water entering the floodplain using HEC-HMS;

c) To create flood simulations using hydrologic models of the Agno floodplain using FLO-2D GDS Pro; and

d) To prepare the static flood hazard and flow depth maps for the Agno river basin.

1.5 Limitations

This research is limited to the usage of the available data, such as the following:

1. Digital Elevation Models (DEM) surveyed by the Data Acquisition Component (DAC) and processed by the Data Processing Component (DPC)
2. Outflow data surveyed by the Data Validation and Bathymetric Component (DVC)
3. Observed Rainfall from ASTI sensors

While the findings of this research could be further used in related-studies, the accuracy of such is dependent on the accuracy of the available data. Also, this research adapts the limitations of the software used: ArcGIS 10.2, HEC-GeoHMS 10.2 extension, WMS 9.1, HEC-HMS 3.5 and FLO-2D GDS Pro.

1.6 Operational Framework

The flow for the operational framework of the Flood Modeling Component is shown in Figure 2.

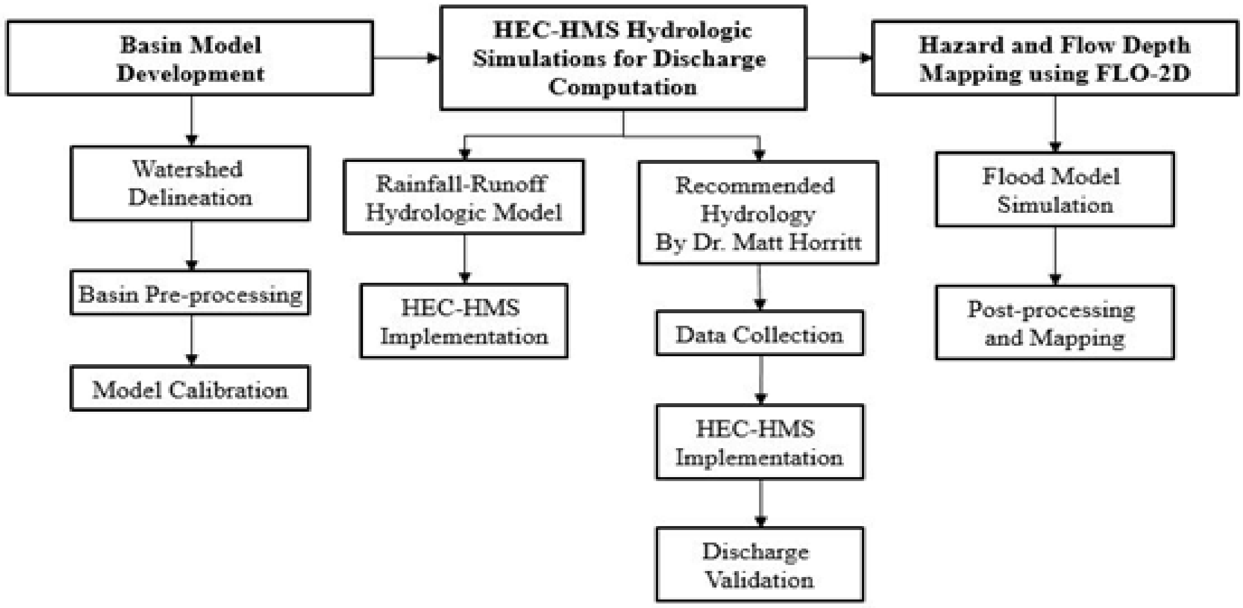

Figure 2. The operational framework and specific work flow of the Flood Modeling Component

The Agno River Basin

The Agno River Basin

The Agno River Basin is situated in Luzon and is the fifth largest river basin in the Philippines, with an estimated basin area of 5,852 square kilometers. The Agno River is also considered as the third largest in Luzon, with its river system having a length of 270 kilometers, 90 kilometers of which runs through mountainous terrain and canyons. The location of the Agno River Basin is as shown in Figure 3.

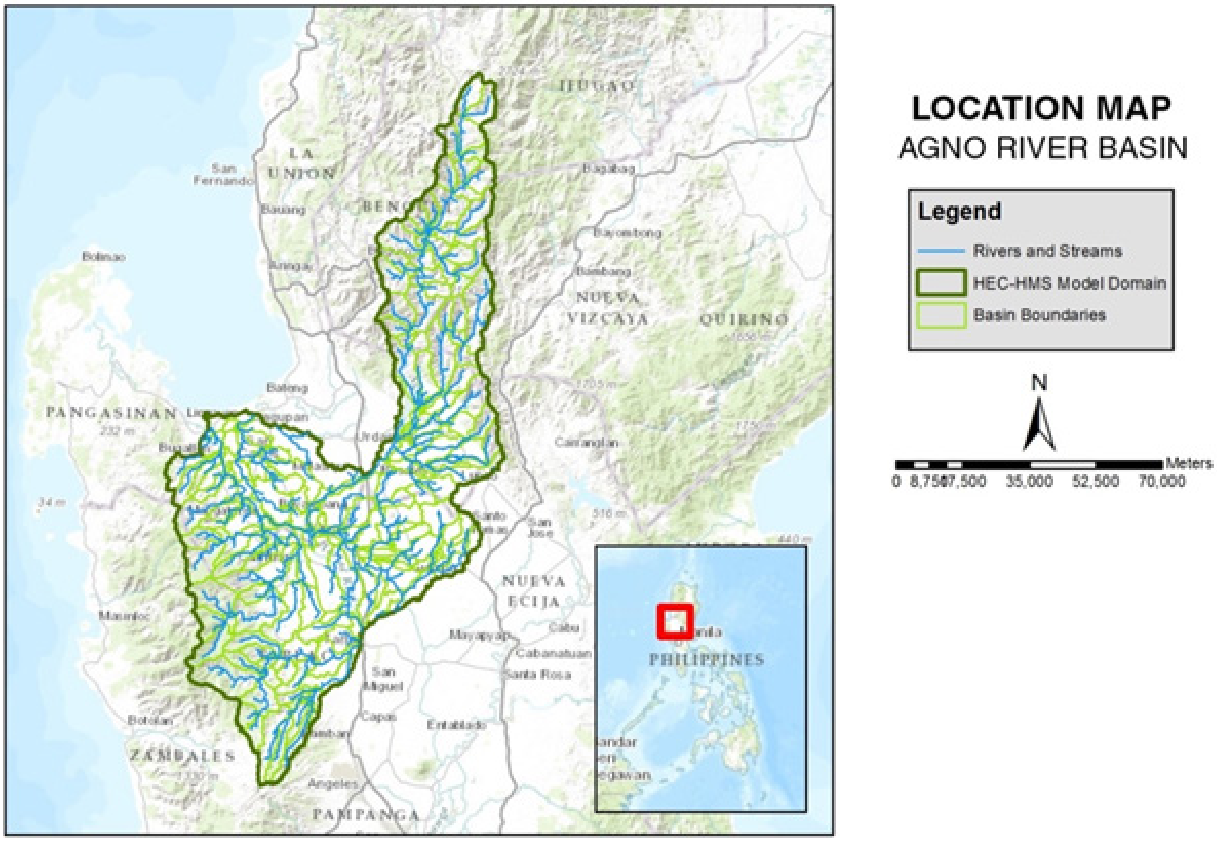

Figure 3. Agno River Basin Location Map

The headwaters of the Agno River are at the Cordillera Mountains and drains about 6.6 cubic kilometres of fresh water into the Lingayen Gulf in Pangasinan, becoming the largest Philippine river in terms of water discharge. It has 4 principal tributaries-- Tarlac River, which is the main branch, the Pila River, the Camiling River, and the Ambayoan River. It drains the western portion of the island and a large part of its catchment is located in Pangasinan. According to the Agno River Basin Development Commission (ARBDC), the river basin covers 68 municipalities and 5 cities in the provinces of Benguet, Tarlac and Pangasinan.

The land and soil characteristics are important parameters used in assigning the roughness coefficient for different areas within the river basin. The roughness coefficient, also called Manning's coefficient, represents the variable flow of water in different land covers (i.e. rougher, restricted flow within vegetated areas, smoother flow within channels and fluvial environments). 5+

The Agno River Basin

The shape files of the soil and land cover were taken from the Bureau of Soils, which is under the Department of Environment and Natural Resources Management, and National Mapping and Resource Information Authority (NAMRIA). The soil and land cover of Agno River Basin are shown in Figures 4 and 5, respectively.

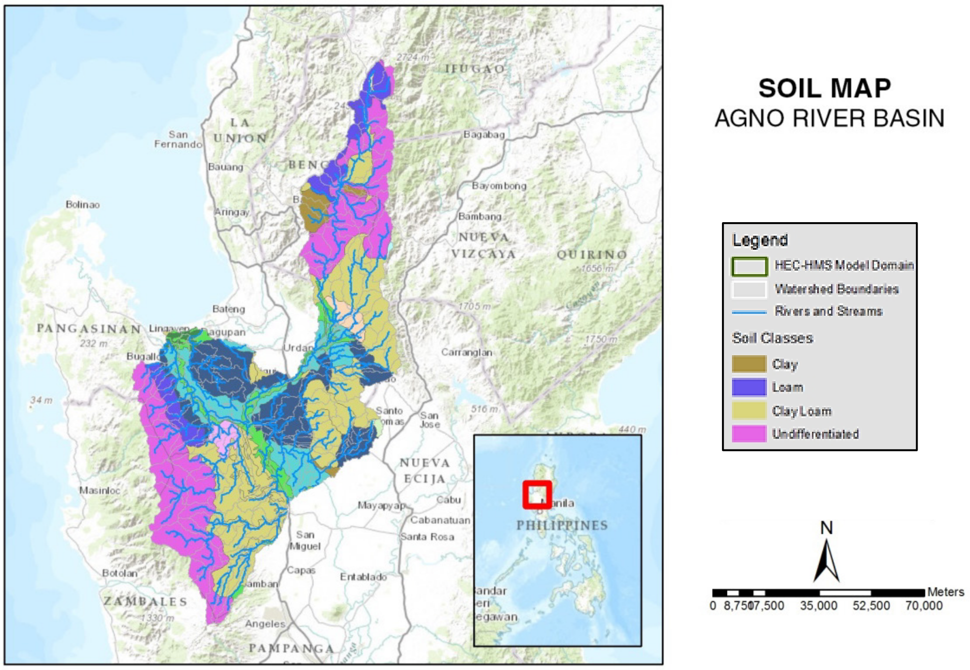

Figure 4. Agno River Basin Soil Map

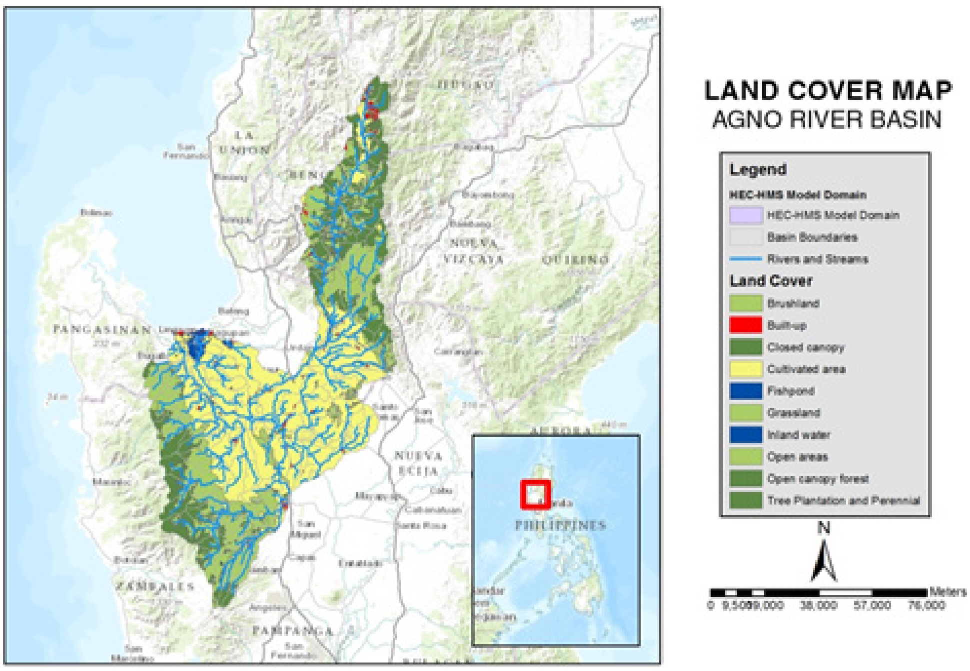

Figure 5. Agno River Basin Land Cover Map

Methodology

Methodology

3.1 Pre-processing and Data Used

Flood modeling involved several data and parameters to achieve realistic simulations and outputs. Figure 6 shows a summary of the data needed to for the research.

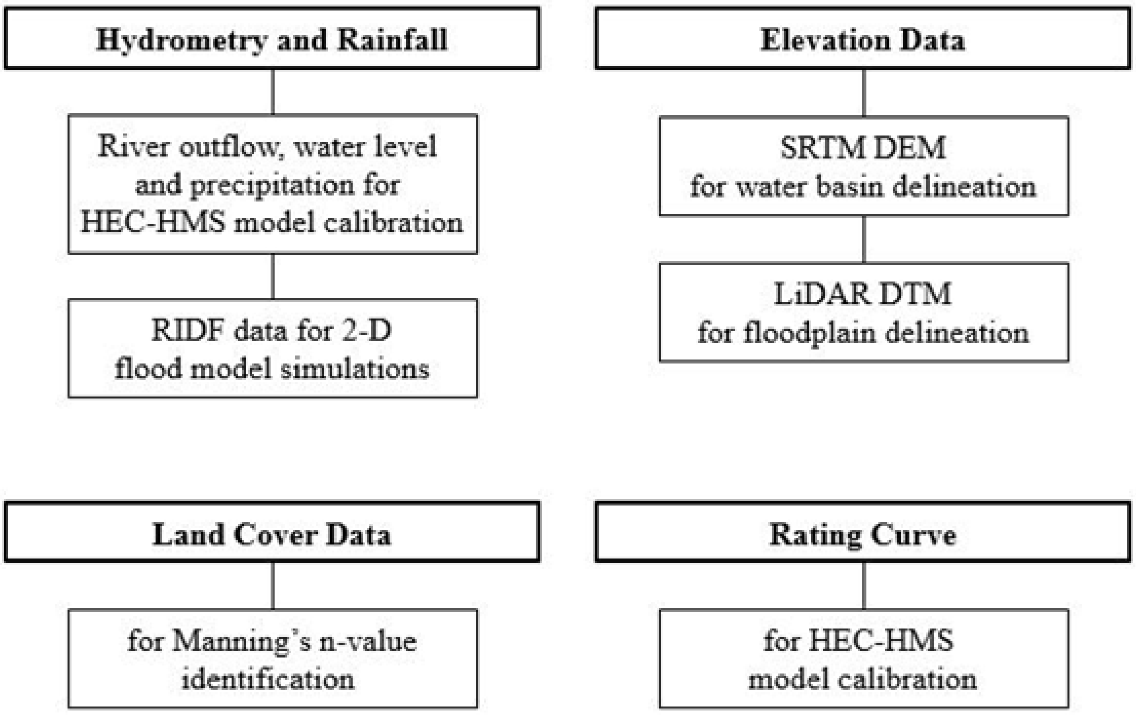

Figure 6. Summary of data needed for the purpose of flood modeling

3.1.1 Elevation Data

3.1.1.1 Hydro Corrected SRTM DEM

With the Shuttle Radar Topography Mission Digital Elevation Model (SRTM DEM) data as an input in determining the extent of the delineated water basin, the model was set-up. The Digital Elevation Model (DEM) is a set of elevation values for a range of points within a designated area. SRTM DEM has a 90 meter spatial mosaic of the entire country. Survey data of cross sections and profile points were integrated to the SRTM DEM for the hydro-correction.

3.1.1.2 LiDAR DEM

LiDAR was used to generate the Digital Elevation Model (DEM) of the different floodplains. DEMs used for flood modeling were already converted to digital terrain models (DTMs) which only show topography, and are thus cleared of land features such as trees and buildings. These terrain features would allow water to flow realistically in the models.

Figure 7 shows an image of the DEM generated through LiDAR.

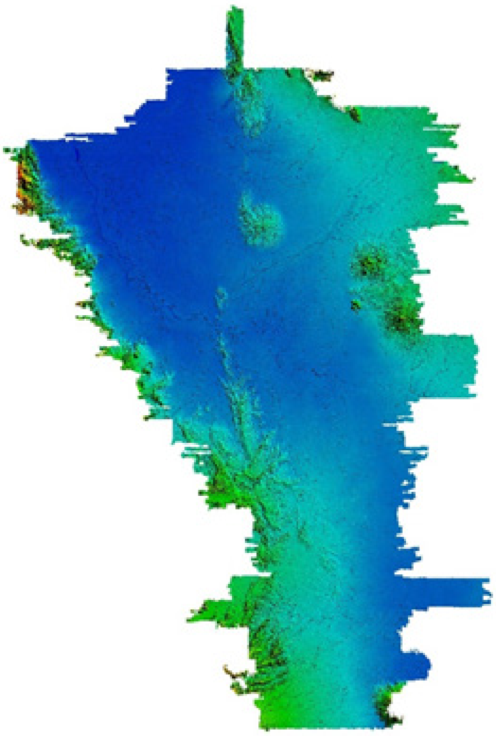

Figure 7. Digital Elevation Model (DEM) of the Agno River Basin using Light Detection and Ranging (LiDAR) technology

Elevation points were created from LiDAR DTMs. Since DTMs were provided as 1-meter spatial resolution rasters (while flood models for Agno were created using a 10-meter grid), the DTM raster had to be resampled to a raster grid with a 10-meter cell size using ArcGIS.

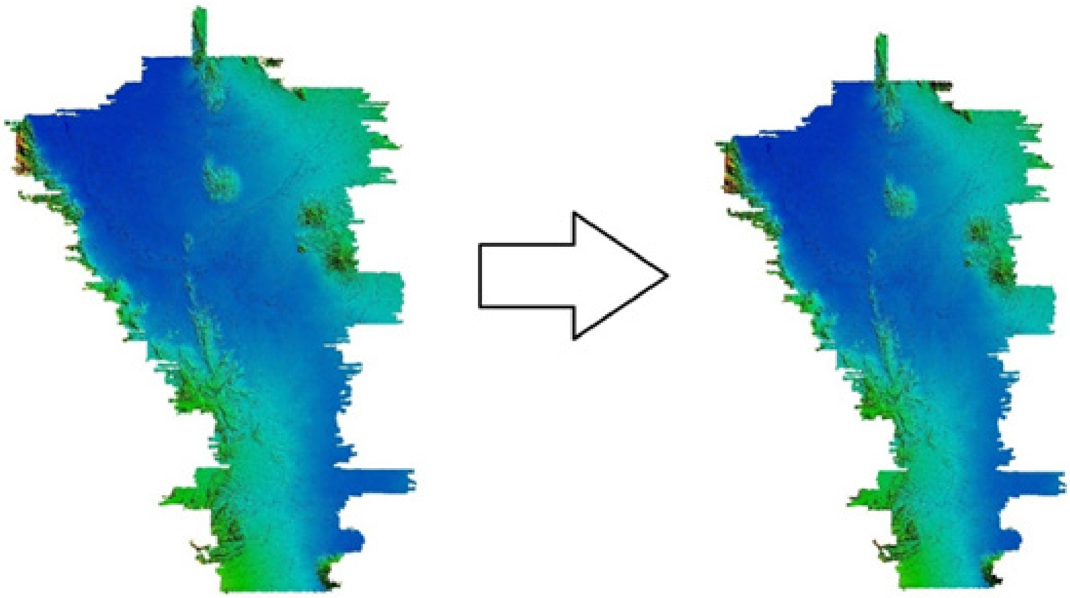

Figure 8. The 1-meter resolution LiDAR data resampled to a 10-meter raster grid in GIS software to ensure that values are properly adjusted

3.1.2 Land Cover and Soil Type

The land and soil characteristics are important parameters used in assigning the roughness coefficient for different areas within the river basin. The roughness coefficient, also called Manning's coefficient, represents the variable flow of water in different land covers (i.e. rougher, restricted flow within vegetated areas, smoother flow within channels and fluvial environments).

A general approach was done for the Agno floodplain. Streams were identified against built-up areas and rice fields. Identification was done visually using stitched Quickbird images from Google Earth. Areas with different land covers are shown on Figure 9. Different Manning n-values are assigned to each grid element coinciding with these main classifications during the modeling phase.

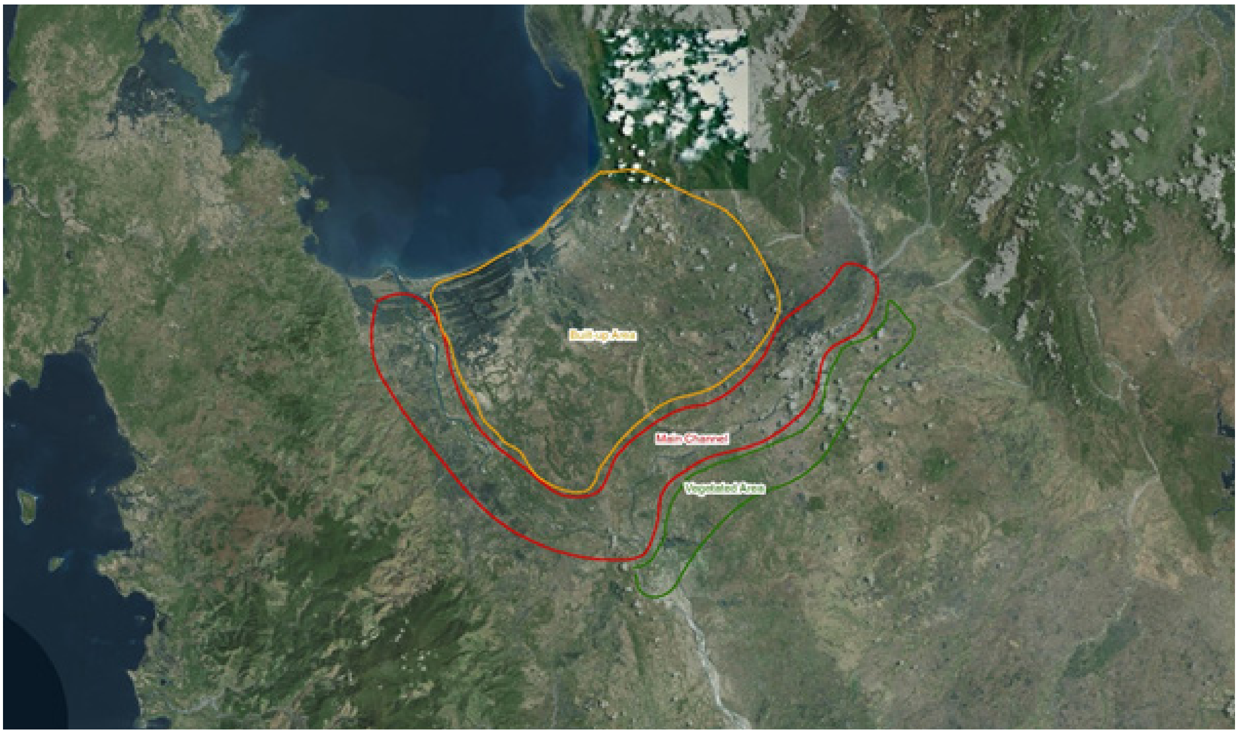

Figure 9. Stitched Quickbird images for the Agno floodplain

3.1.3 Hydrometry and Rainfall Data

3.1.3.1 Hydrometry for different discharge points

3.1.3.1.1 Hector Mendoza/Calvo bridge, Pangasinan

The river outflow was computed using the derived rating curve equation. This discharge was used to calibrate the HEC-HMS model. It was taken from Hector Mendoza Bridge, Pangasinan (15°50'6.01"N, 120°30'1.27"E). The recorded peak discharge is around 417.5 cms at 10:20 AM, September 6, 2013.

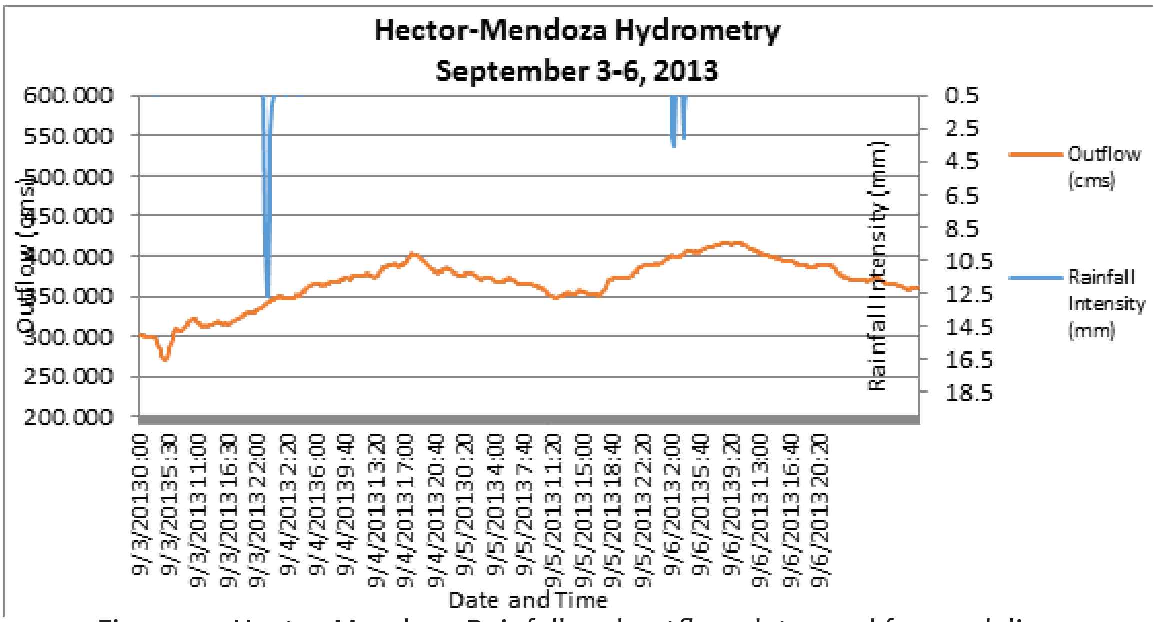

Figure 10. Hector Mendoza Rainfall and outflow data used for modeling

3.1.3.1.2 Banela Bridge, Pangasinan

The river outflow was computed using the derived rating curve equation. This discharge was used to calibrate the HEC-HMS model. It was taken from Banela Bridge, Pangasinan (15 56' 23.99"N, 120 50' 25.5"E). The recorded peak discharge is around 28.8 cms at 4:10 PM, September 5, 2013.

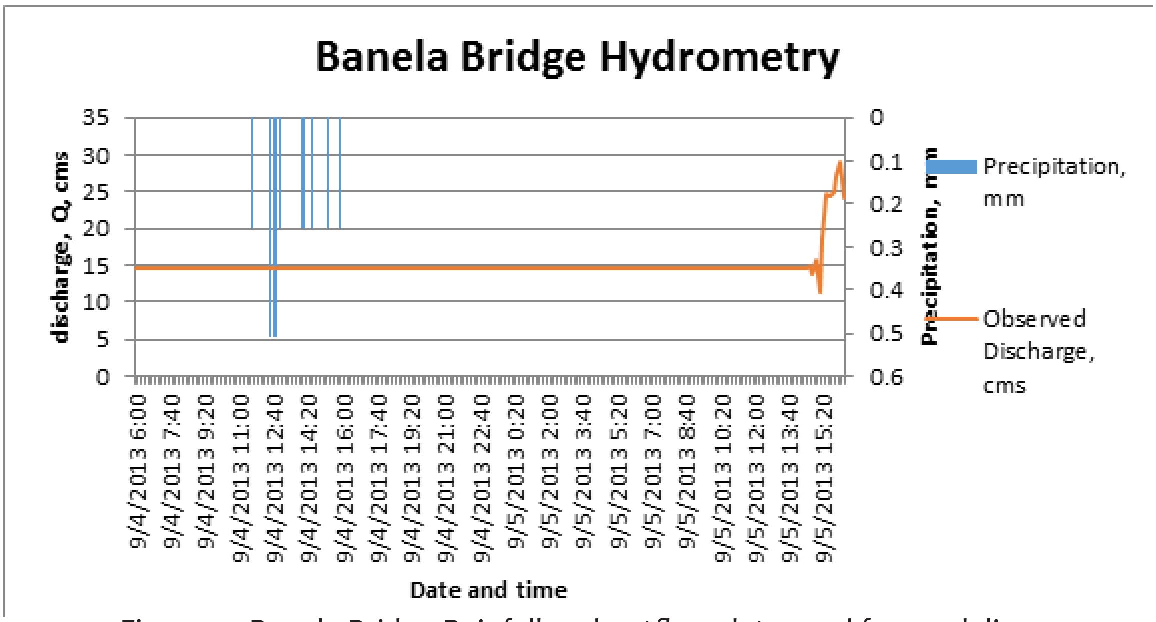

Figure 11. Banela Bridge Rainfall and outflow data used for modeling

3.1.3.1.3 Magallanes Bridge, Pangasinan

The river outflow was computed using the derived rating curve equation. This discharge was used to calibrate the HEC-HMS model. It was taken from Magallanes Bridge, Pangasinan (16°0'48.3"N, 120°44'13.8"E). The recorded peak discharge is 68.8 cms at 6.20 AM, October 12, 2013.

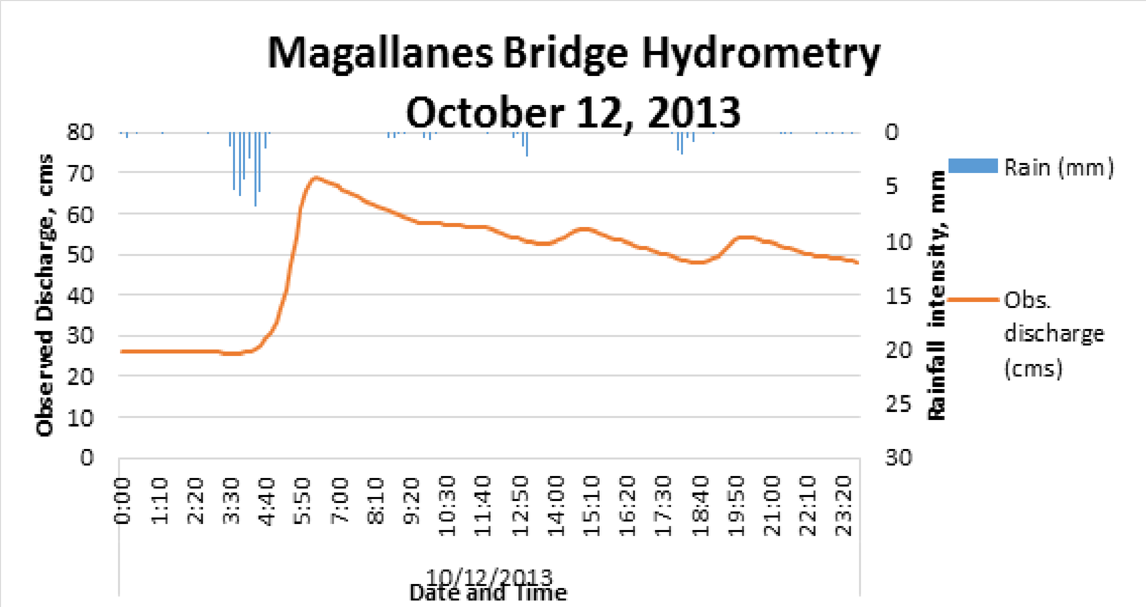

Figure 12. Magallanes Bridge Rainfall and outflow data used for modeling

3.1.3.1.4 Viray Bridge, Pangasinan

The river outflow was computed using the derived rating curve equation. This discharge was used to calibrate the HEC-HMS model. It was taken from Viray Bridge, Pangasinan (16°1'56.33"N, 120°48'0.36"E). The recorded peak discharge is 38.1 at 11:00 PM, September 29, 2013.

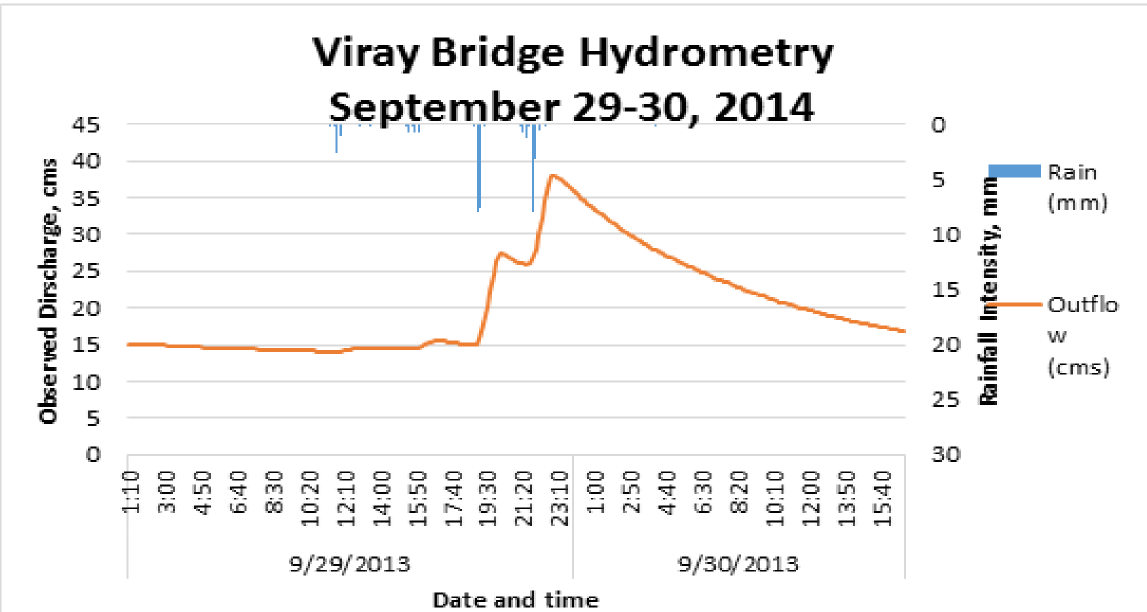

Figure 13. Viray Bridge rainfall and Outflow data for Modeling

3.1.3.1.5 Dipalo Bridge, Pangasinan

The river outflow was computed using the derived rating curve equation. This discharge was used to calibrate the HEC-HMS model. It was taken from Dipalo Bridge, Pangasinan (16°0'25.66"N, 120°48'23.98"E). The recorded peak discharge is 3.3cms at 11:00 PM, September 29, 2013.

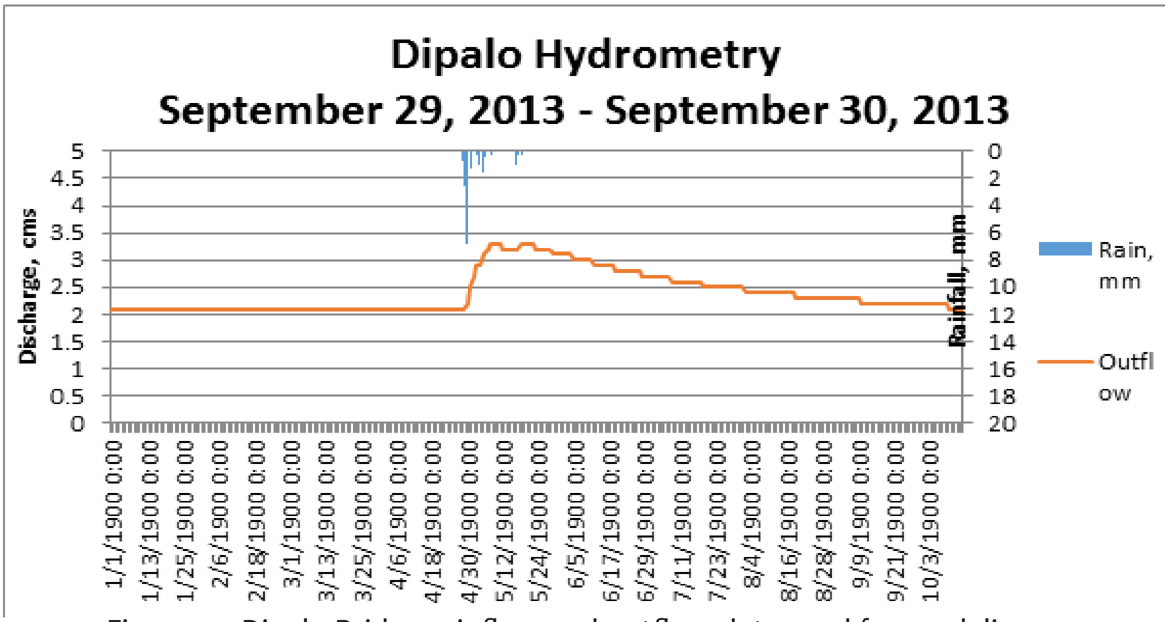

Figure 14. Dipalo Bridge rainflow and outflow data used for modeling

3.1.3.2 Rainfall Intensity Duration Frequency

The Philippine Atmospheric Geophysical and Astronomical Services Administration (PAGASA) computed Rainfall Intensity Duration Frequency (RIDF) values for the Baguio and Dagupan Rain Gauge. This station was chosen based on its proximity to the Agno watershed. The extreme values for this watershed were computed based on a 57-year record.

Five return periods were used, namely, 5-, 10-, 25-, 50-, and 100-year RIDFs. All return periods are 24 hours long and peaks after 12 hours.

Figure 15. Thiessen Polygon of Rain Intensity Duration Frequency (RIDF) Stations for the whole Philippines

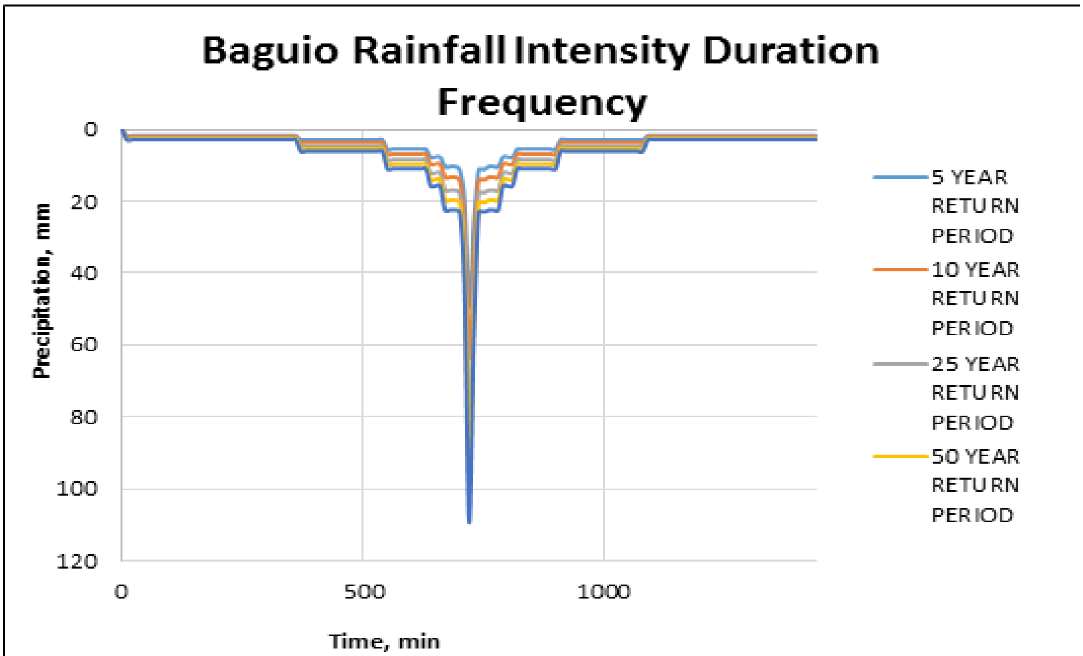

Figure 16. Baguio Rainfall-Intensity Duration Frequency (RIDF) curves

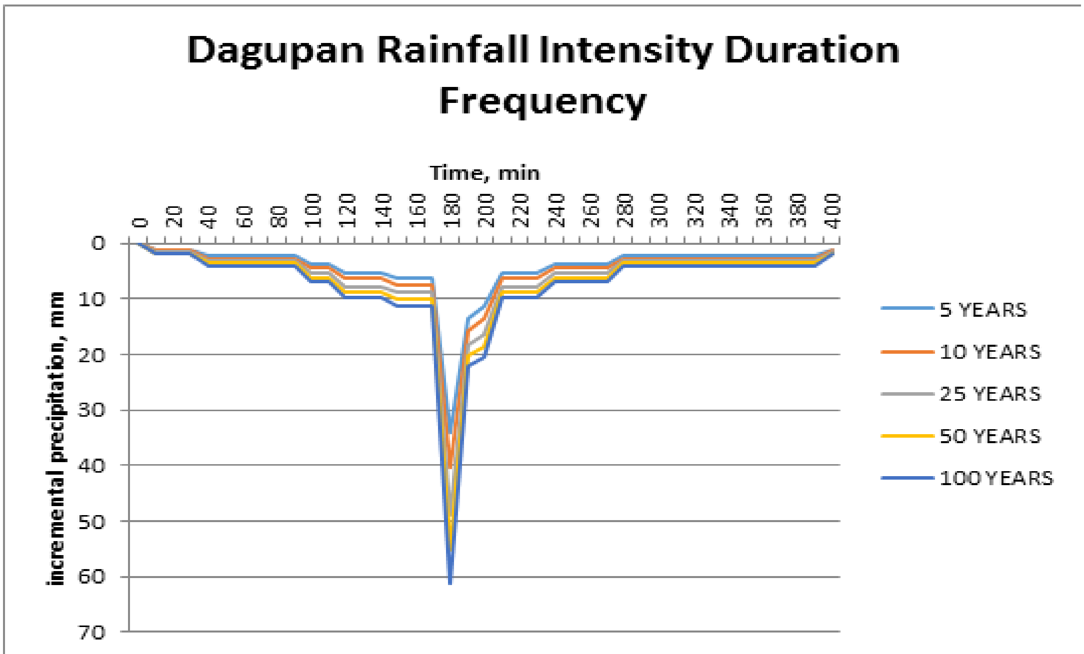

Figure 17. Dagupan Intensity Duration Frequency (RIDF) Curves

The outflow values at the discharge points in the Agno river basin were computed for the five return periods, namely, 5-, 10-, 25-, 50-, and 100-year RIDFs.

3.1.4 Rating Curves

Rating curves were provided by DVC. This curve gives the relationship between the observed water levels from the AWLS used and outflow watershed at the said locations.

Rating curves are expressed in the form of Equation 1 with the discharge (Q) as a function of the gauge height (h) readings from CDO Bridge AWLS and constants (a and n).

$$Q = a^{nh}$$

Equation 1. Rating Curve

3.1.4.1 Hector Mendoza/ Calvo Bridge, Pangasinan Rating Curve

For Hector Mendoza Bridge, the rating curve is expressed as $Q = 1.22E{+}01e^{2.19E-04x}$ as shown in Figure 18.

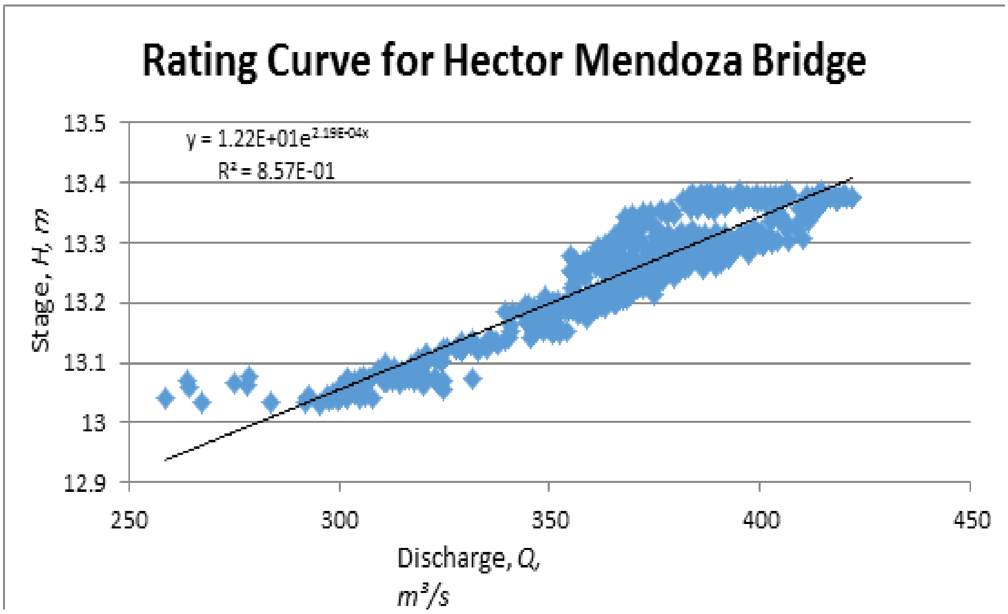

Figure 18. Water level vs. Discharge Curve for Hector Mendoza Bridge

3.1.4.2 Banela Bridge, Pangasinan Rating Curve

For Banela Bridge, the rating curve is expressed as $Q = 3E\text{-}22e^{5.18659h}$ as shown in Figure 19.

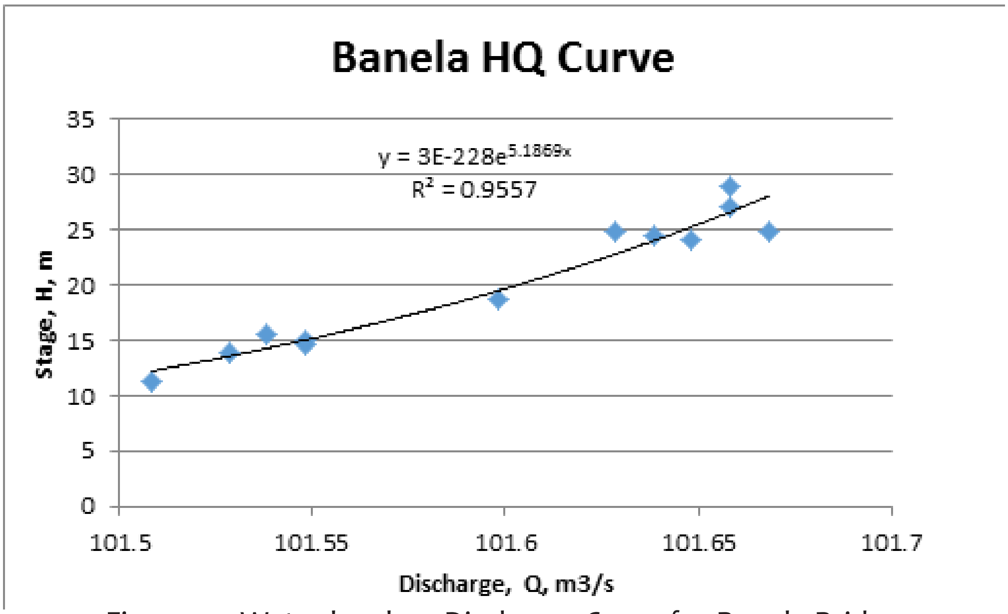

Figure 19. Water level vs. Discharge Curve for Banela Bridge

3.1.4.3 Magallanes Bridge, Pangasinan Rating Curve

A rating curve was developed at Magallanes Bridge, Pangasinan. For Magallanes Bridge, the rating curve is expressed as $Q = 6E\text{-}90e^{4.1219h}$ as shown in Figure 20.

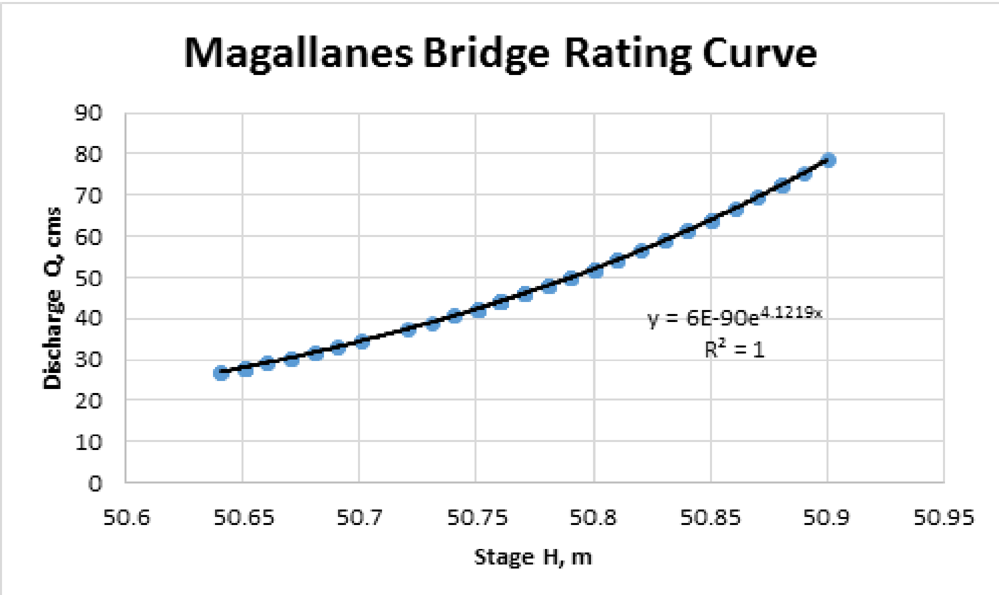

Figure 20. Water level vs. Discharge Curve for Magallanes Bridge

3.1.4.4 Viray Bridge, Pangasinan Rating Curve

A rating curve was developed at Viray Bridge, Pangasinan. For Viray Bridge, the rating curve is expressed as $Q = 6E\text{-}90e^{4.1219h}$ as shown in Figure 21.

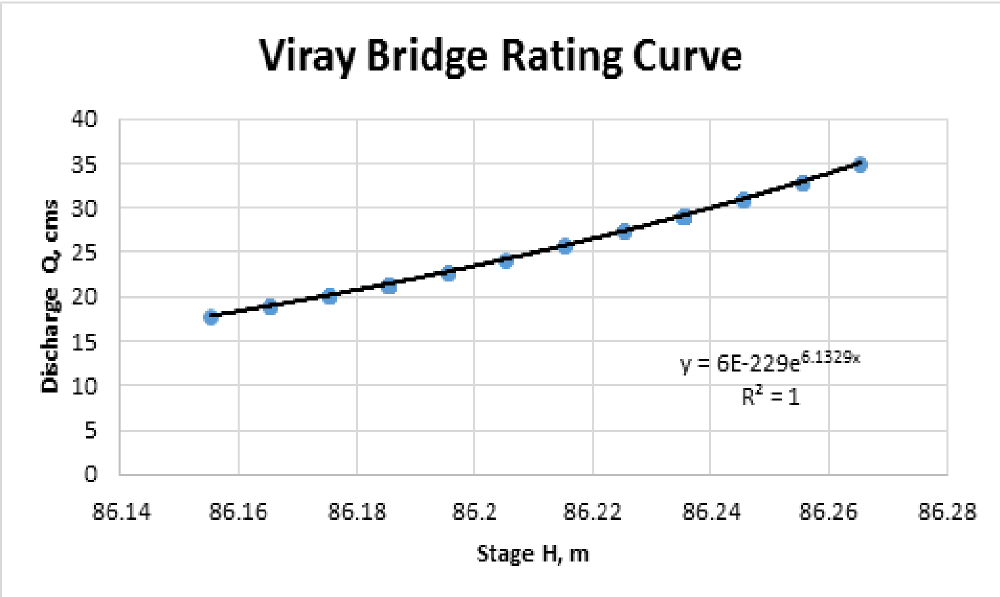

Figure 21. Water level vs. Discharge Curve for Viray Bridge

3.1.4.5 Dipalo Bridge, Pangasinan Rating Curve

A rating curve was developed at Dipalo Bridge, Pangasinan . For Dipalo Bridge, the rating curve is expressed as $Q = 1E\text{-}17e^{0.475h}$ as shown in Figure 22.

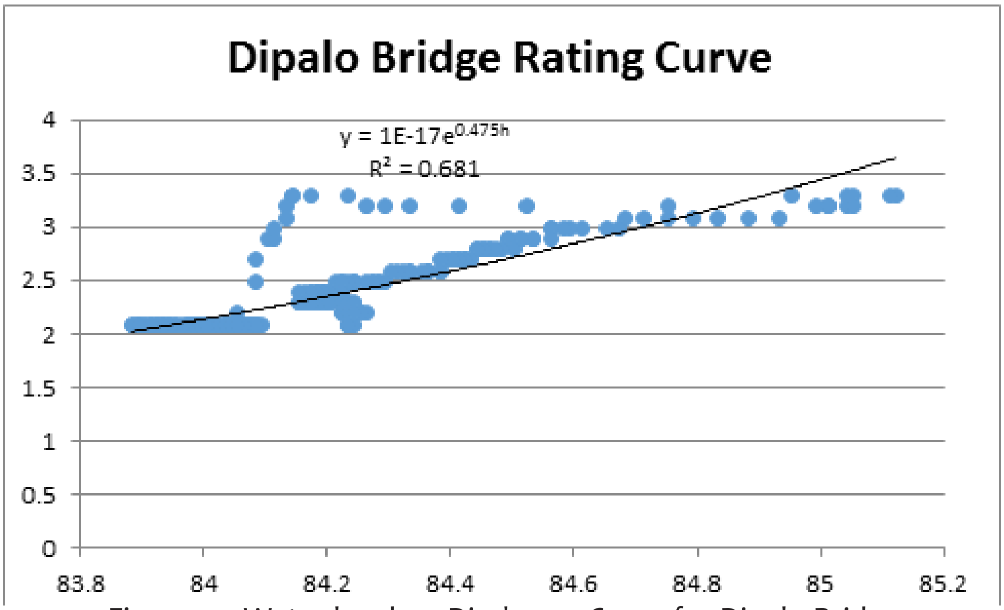

Figure 22. Water level vs. Discharge Curve for Dipalo Bridge

3.2 Rainfall-Runoff Hydrologic Model Development

3.2.1 Watershed Delineation and Basin Model Pre-processing

The hydrologic model of Agno River Basin was developed using Watershed Modeling System (WMS) version 9.1. The software was developed by Aquaveo, a water resources engineering consulting firm in United States. WMS is a program capable of various watershed computations and hydrologic simulations. The hydrologic model development follows the scheme shown in the Figure 23.

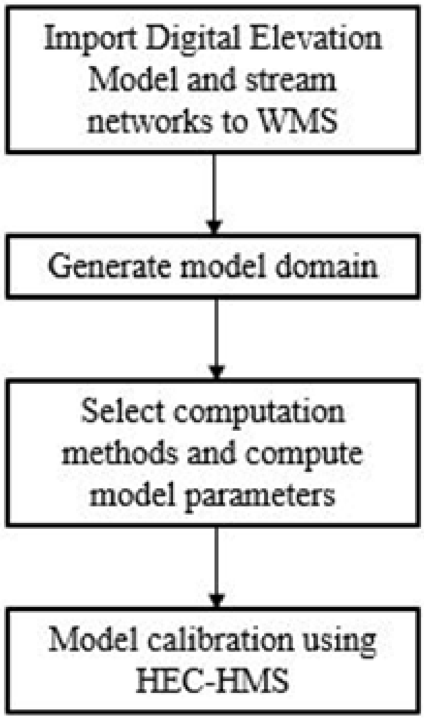

Figure 23. The Rainfall-Runoff Basin Model Development Scheme

Hydro-corrected SRTM DEM was used as the terrain for the basin model. The watershed delineation and its hydrologic elements, namely the subbasins, junctions and reaches, were generated using WMS after importing the elevation data and stream networks.

The parameters for the subbasins and reaches were computed after the model domain was created. There are several methods available for different calculation types for each subbasin and reach hydrologic elements. The methods used for this study is shown in Table 1. The necessary parameter values are determined by the selected methods. The initial abstraction, curve number, percentage impervious and manning's coefficient of roughness, n, for each subbasin were computed based on the soil type, land cover and land use data. The subbasin time of concentration and storage coefficient were computed based on the analysis of the topography of the basin.

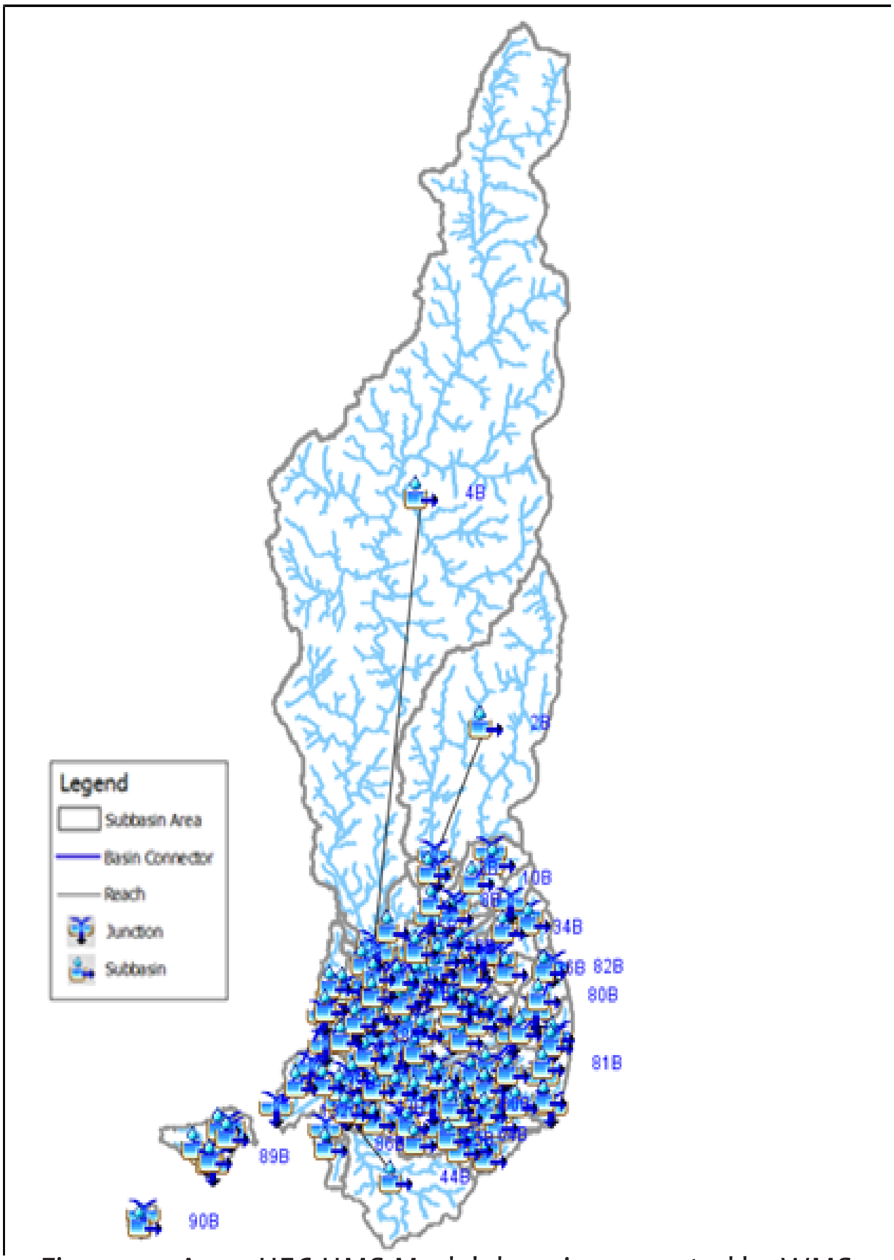

Figure 24. Agno HEC-HMS Model domain generated by WMS

Table 1. Methods used for the different calculation types for the hydrologic elements

Hydrologic Element	Calculation Type	Method
Subbasin	Loss Rate	SCS Curve Number
	Transform	Clark's unit hydrograph
	Baseflow	Bounded recession
Reach	Routing	Muskingum-Cunge

3.2.2 Basin Model Calibration

The basin model made using WMS was exported to Hydrologic Modeling System (HEC-HMS) version 3.5, a software made by the Hydrologic Engineering Center of the US Army Corps of Engineers, to create the final rainfall-runoff model. The developers described HEC-HMS as a program designed to simulate the hydrologic processes of a dendritic watershed systems. In this study, the rainfall-runoff model was developed to calculate inflow from the watershed to the floodplain.

Precipitation data was taken from three sensor, an automatic rain gauge (ARGs) installed by the Department of Science and Technology – Advanced Science and Technology Institute (DOST-ASTI). The location of the ARG is seen in Figure 25.

For the calibration of the downstream-most discharge point which is at Hector Mendoza Bridge, the total rain is 52.40mm for one day. It peaked to 8.60mm on 04 September 2013, 15:50.

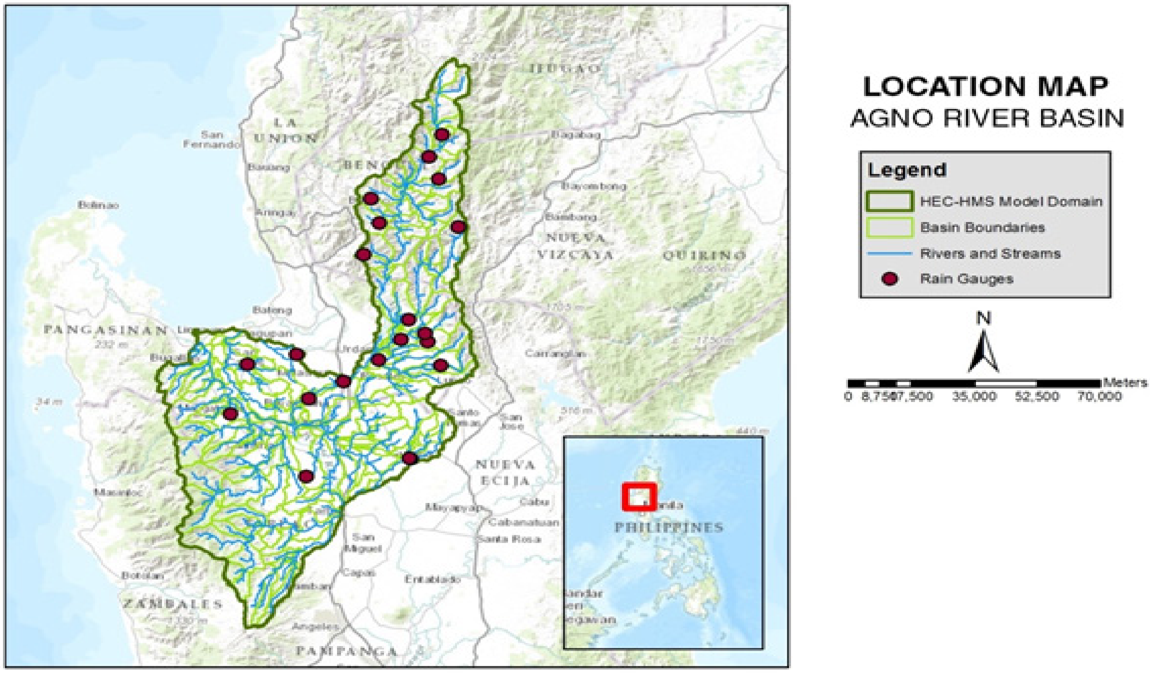

Figure 25. Location of rain gauge used for the calibration of Agno HEC-HMS Model

The outflow hydrograph for the downstream-most discharge point with field data was also encoded to the model as a basis for the calibration. Using the said data, HEC-HMS could perform rainfall-runoff simulation and the resulting outflow hydrograph was compared with the observed hydrograph. The values of the parameters were adjusted and optimized in order for the calculated outflow hydrograph to appear like the observed hydrograph. Acceptable values of the subbasin and reach parameters from the manual and past literatures were considered in the calibration.

3.3 HEC-HMS Hydrologic Simulations for Discharge Computations using PAGASA RIDF Curves

3.3.1 Discharge Computation using Rainfall-Runoff Hydrologic Model

The calibrated rainfall-Runoff Hydrologic Model for the Agno River Basin using WMS and HEC-HMS was used to simulate the flow for for the five return periods, namely, 5-, 10-, 25-, 50-, and 100-year RIDFs. Time-series data of the precipitation data using the Baguio and Dagupan RIDF curves were encoded to HEC-HMS for the aforementioned return periods, wherein each return period corresponds to a scenario. This process was performed for all discharge points – Hector Mendoza Bridge, Banela Bridge, Magallanes Bridge, Viray Bridge and Dipalo Bridge. The output for each simulation was an outflow hydrograph from that result, the total inflow to the floodplain and time difference between the peak outflow and peak precipitation could be determined.

3.3.2 Discharge Computation using Dr. Horritt's Recommended Hydrological Method

The required data to be accumulated for the implementation of Dr. Horrit's method is shown on Figure 26.

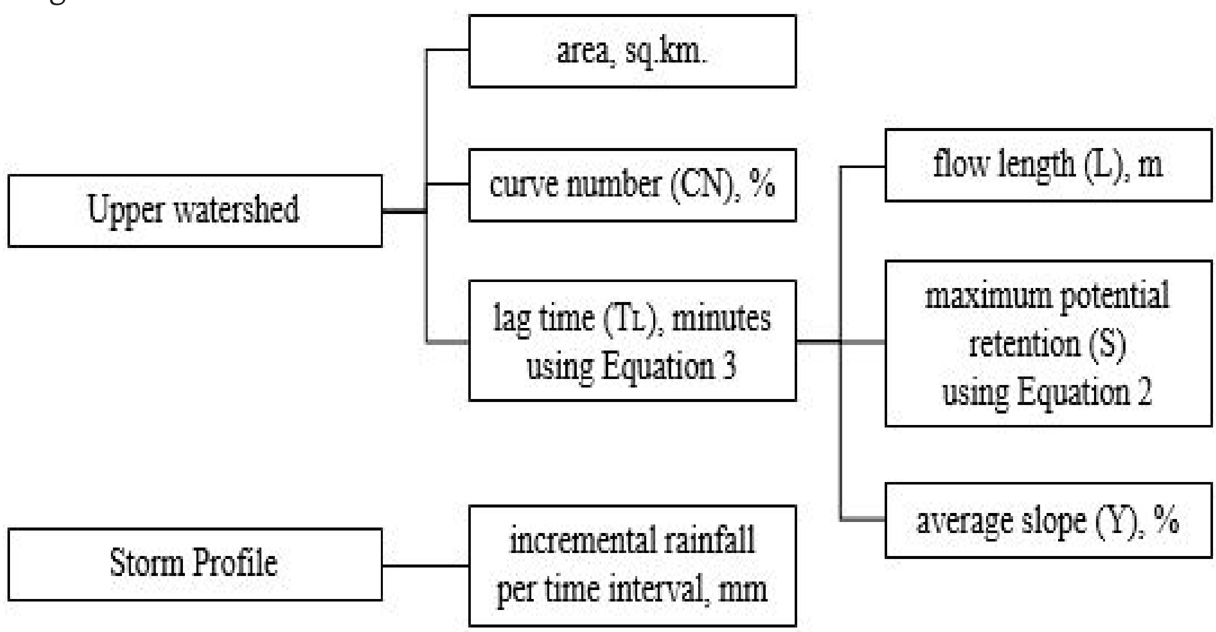

Figure 26. Different data needed as input for HEC-HMS discharge simulation using Dr. Horritt's recommended hydrology method

Flows from streams were computed using the hydrology method developed by the flood modeling component with Dr. Matt Horritt, a British hydrologist that specializes in flood research. The methodology was based on an approach developed by CH2M Hill and Horritt Consulting for Taiwan which has been successfully validated in a region with meteorology and hydrology similar to the Philippines. The method utilizes the SCS curve number and unit hydrograph method to have an accurate approximation of river discharge data from measurable catchment parameters.

3.3.2.1 Determination of Catchment Properties

RADARSAT DTM data for the different areas of the Philippines were compiled with the aid of ArcMap. RADARSAT satellites provide advance geospatial information and these were processed in the forms of shapefiles and layers that are readable and can be analyzed by ArcMap. These shapefiles are digital vectors that store geometric locations.

The watershed flow length is defined as the longest drainage path within the catchment, measured from the top of the watershed to the point of the outlet. With the tools provided by the ArcMap program and the data from RADARSAT DTM, the longest stream was selected and its geometric property, flow length, was then calculated in the program.

The area of the watershed is determined with the longest stream as the guide. The compiled RADARSAT data has a shapefile with defined small catchments based on mean elevation. These parameters were used in determining which catchments, along with the area, belong in the upper watershed.

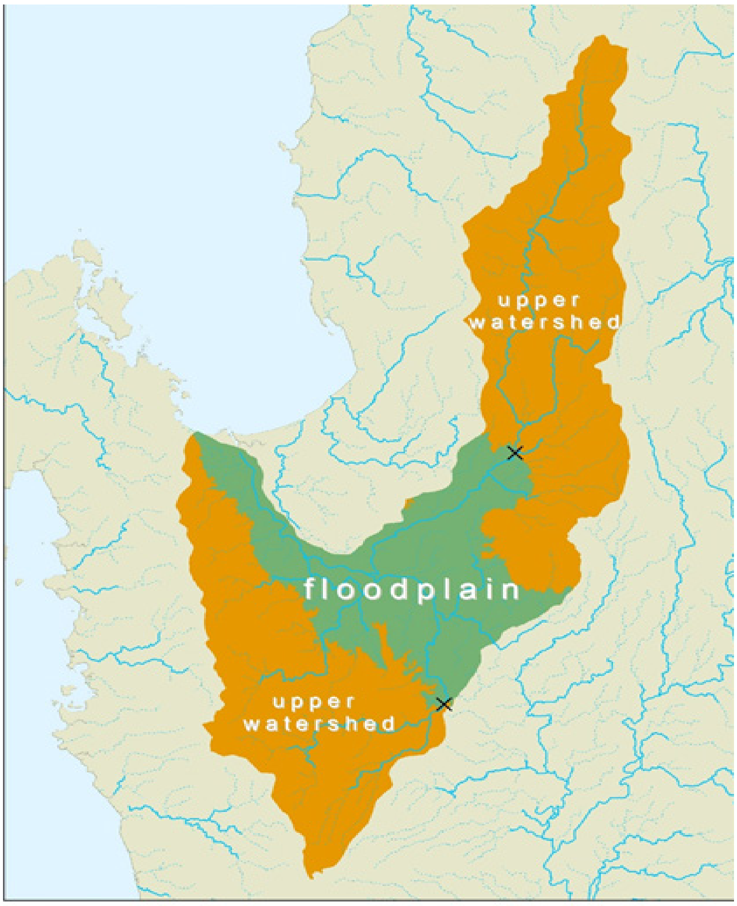

Figure 27. Delineation of upper watershed for Agno floodplain discharge computation

The value of the curve number was obtained using the RADARSAT data that contains information of the Philippine national curve number map. An ArcMap tool was used to determine the average curve number of the area bounded by the upper watershed shapefile. The same method was implemented in determining the average slope using RADARSAT with slope data for the whole country.

After determining the curve number (CN), the maximum potential retention (S) was determined by Equation 2.

$$S = \frac{1000}{CN} - 10$$

Equation 2. Determination of maximum potential retention using the average curve number of the catchment

The watershed length (L), average slope (Y) and maximum potential retention (S) are used to estimate the lag time of the upper watershed as illustrated in Equation 3.

$$T_L = \frac{L^{0.8}(S+1)^{0.7}}{560Y^{0.5}}$$

Equation 3. Lag Time Equation Calibrated for Philippine Setting

Finally, the final parameter that will be derived is the storm profile. The synoptic station which covers the majority of the upper watershed was identified. Using the RIDF data, the incremental values of rainfall in millimeter per 0.1 hour was used as the storm profile.

3.3.2.2 HEC-HMS Implementation

With all the parameters available, HEC-HMS was then utilized. Obtained values from the previous section were used as input and a brief simulation would result in the tabulation of discharge results per time interval. The maximum discharge and time-to-peak for the whole simulation as well as the river discharge hydrograph were used for the flood simulation process. The time series results (discharge per time interval) were stored as HYD files for input in FLO-2D GDS Pro.

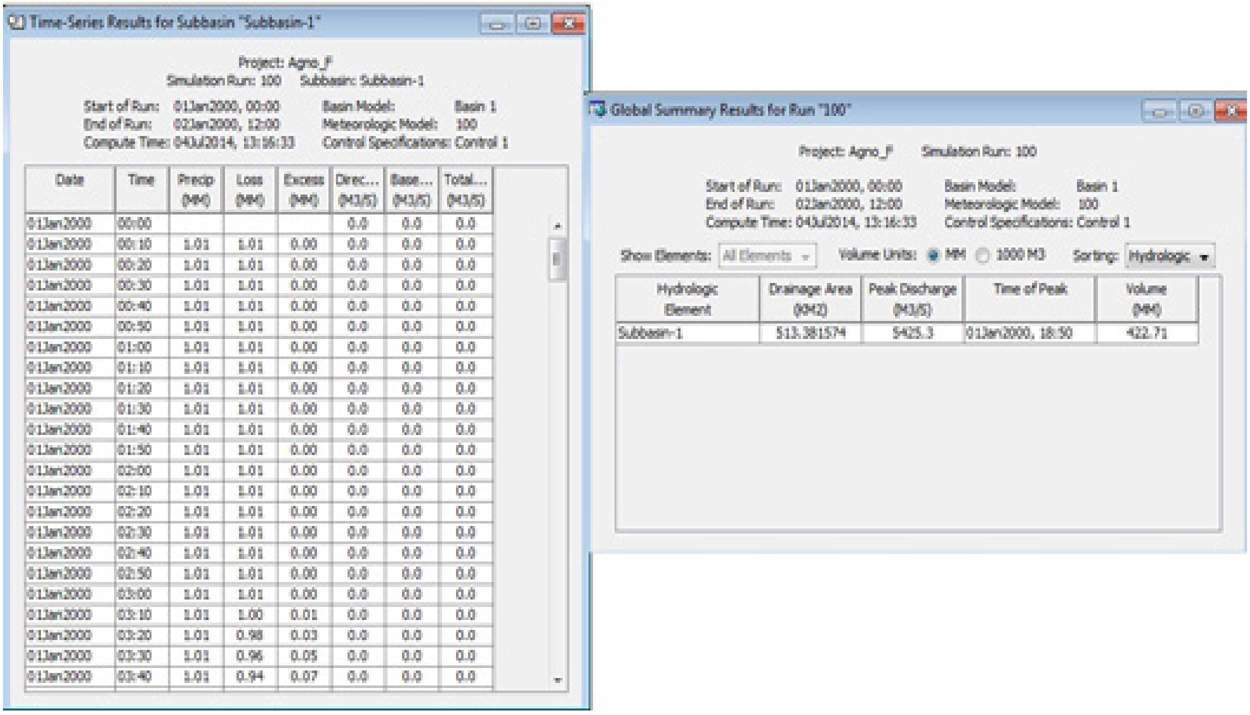

Figure 28. HEC-HMS simulation discharge results using Dr. Horritt's Method

3.3.2.3 Discharge validation against other estimates

As a general rule, the river discharge of a 2-year rain return, Q_{MED}, should approximately be equal to the bankful discharge, $Q_{bankful}$, of the river. This assumes that the river is in equilibrium, with its deposition being balanced by erosion. Since the simulations of the river discharge are done for 5-, 25-, and 100-year rainfall return scenarios, a simple ratio for the 2-year and 5-year return was computed with samples from actual discharge data of different rivers. It was found out to have a constant of 0.88. This constant, however, should still be continuously checked and calibrated when necessary.

$$Q_{MED} = 0.88Q_{5yr}$$

Equation 4. Ratio of river discharge of a 5-year rain return to a 2-year rain return scenario from measured discharge data

For the discharge calculation to pass the validation using the bankful method, Equation 5 must be satisfied.

$$50\%\, Q_{bankful} \leq Q_{MED} \leq 150\%\, Q_{bankful}$$

Equation 5. Discharge validation equation using bankful method

The bankful discharge was estimated using channel width (w), channel depth (h), bed slope (S) and Manning's constant (n). Derived from the Manning's Equation, the equation for the bankful discharge is by Equation 6.

$$Q_{bankful} = \frac{(wh)^{\frac{5}{3}} S^{\frac{1}{2}}}{n(w+2h)^{\frac{2}{3}}}$$

Equation 6. Bankful discharge equation using measurable channel parameters

3.4 Hazard and Flow Depth Mapping using FLO-2D

3.4.1 Floodplain Delineation

The boundaries of subbasins within the floodplain were delineated based on elevation values given by the DEM. Each subbasin is marked by ridges dividing catchment areas. These catchments were delineated using a set of ArcMap tools compiled by Al Duncan, a UK Geomatics Specialist, into a single processing model. The tool allows ArcMap to compute for the flow direction and acceleration based on the elevations provided by the DEM.

Running the tool creates features representing large, medium-sized, and small streams, as well as large, medium-sized, and small catchments. For the purpose of this particular model, the large, medium-sized, and small streams were set to have an area threshold of 100,000sqm, 50,000sqm, and 10,000sqm respectively. These thresholds define the values where the algorithm refers to in delineating a trough in the DEM as a stream feature, i.e. a large stream feature should drain a catchment area totalling 100,000 sqm to be considered as such. These values differ from the standard values used (10,000sqm, 1,000 sqm and 100sqm) to limit the detail of the project, as well as the file sizes, allowing the software to process the data faster.

The tool also shows the direction in which the water is going to flow across the catchment area. This information was used as the basis for delineating the floodplain. The entire area of the floodplain was subdivided into several zones in such a way that it can be processed properly. This was done by grouping the catchments together, taking special account of the inflows and outflows of water across the entire area. To be able to simulate actual conditions, all the catchments comprising a particular computational domain were set to have outflows that merged towards a single point. The area of each subdivision was limited to 250,000 grids or less to allow for an optimal simulation in FLO-2D GDS Pro. Larger models tend to run longer, while smaller models may not be as accurate as a large one.

3.4.2 Flood Model Generation

The software used to run the simulation is FLO-2D GDS Pro. It is a GIS integrated software tool that creates an integrated river and floodplain model by simulating the flow of the water over a system of square grid elements.

After loading the shapefile of the subcatchment onto FLO-2D, 10 meter by 10 meter grids that encompassed the entire area of interest were created.

The boundary for the area was set by defining the boundary grid elements. This can either be done by defining each element individually, or by drawing a line that traces the boundaries of the subcatchment. The grid elements inside of the defined boundary were considered as the computational area in which the simulation will be run.

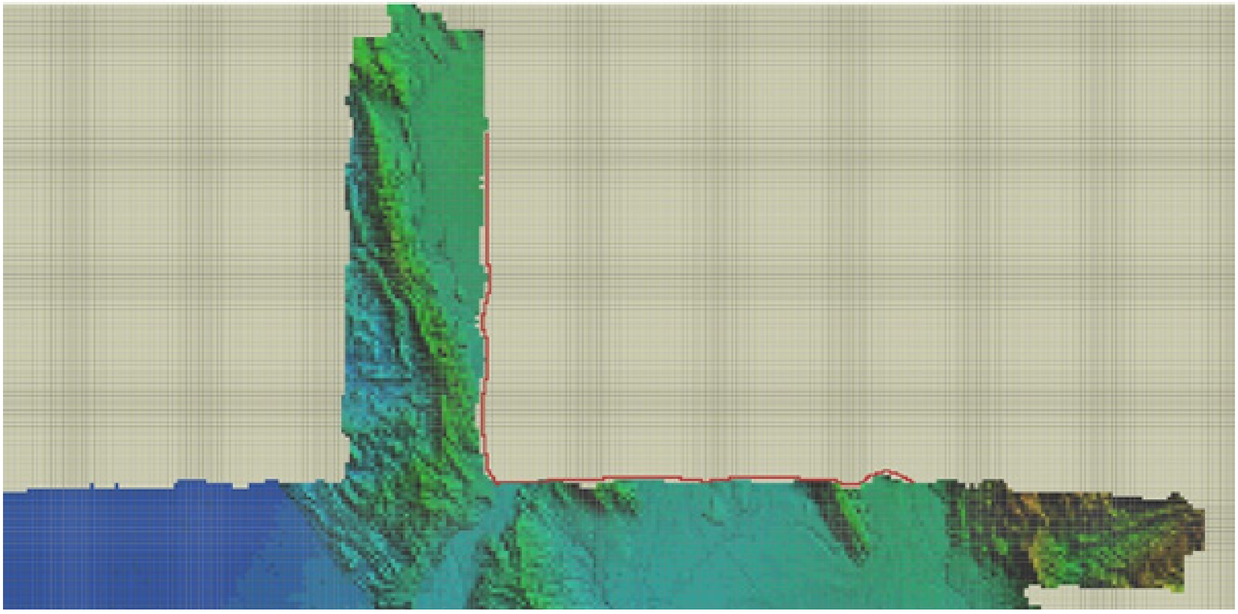

Figure 29. Screenshot showing how boundary grid elements are defined by line

Elevation data was imported in the form of the DEM gathered through LiDAR. These elevation points in PTS format were extrapolated into the model, providing an elevation value for each grid element.

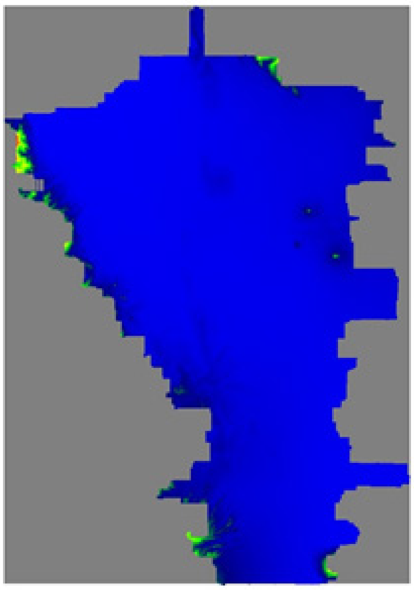

Figure 30. Screenshots of PTS files when loaded into the FLO-2D program

The floodplain is predominantly composed of rice fields, which have a Manning coefficient of 0.15. All the inner grid elements were selected and the Manning coefficient of 0.15 was assigned. To differentiate the streams from the rest of the floodplain, a shapefile containing all the streams and rivers in the area were imported into the software. The shapefile was generated using Al Duncan's catchment tool for ArcMap. The streams were then traced onto their corresponding grid elements.

These grid elements were all selected and assigned a Manning coefficient of 0.03. The DEM and aerial imagery were also used as bases for tracing the streams and rivers.

Figure 31. Areal image of Agno floodplain

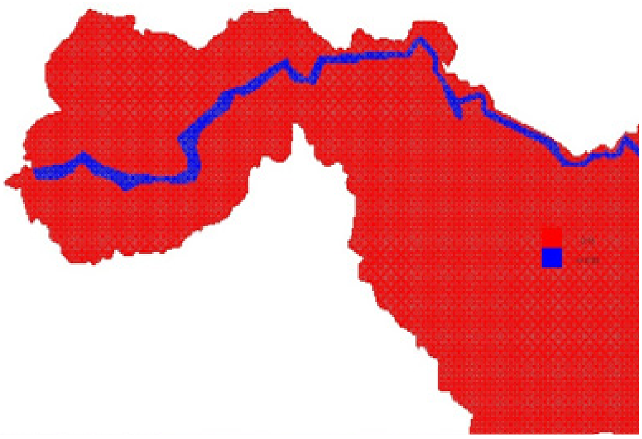

Figure 32. Screenshot of Manning's n-value rendering

After assigning Manning coefficients for each grid, the infiltration parameters were identified. Green-Ampt infiltration method by W. Heber Green and G.S Ampt were used for all the models. The initial saturations applied to the model were 0.99, 0.8, and 0.7 for 100-year, 25-year, and 5-year rain return periods respectively. These initial saturations were used in the computation of the infiltration value.

The Green-Ampt infiltration method by W. Heber Green and G.S Ampt method is based on a simple physical model in which the equation parameter can be related to physical properties of the soil. Physically, Green and Ampt assumed that the soil was saturated behind the wetting front and that one could define some "effective" matric potential at the wetting front (Kirkham, 2005). Basically, the system is assumed to consist of a uniformly wetted near-saturated transmission zone above a sharply defined wetting front of constant pressure head (Diamond & Shanley, 2003).

The next step was to allocate inflow nodes based on the locations of the outlets of the streams from the upper watershed. The inflow values came from the computed discharges that were input as hyd files.

Outflow nodes were allocated for the model. These outflow nodes show the locations where the water received by the watershed is discharged. The water that will remain in the watershed will result to flooding on low lying areas.

For the models to be able to simulate actual conditions, the inflow and outflow of each computational domain should be indicated properly. In situations wherein water flows from one subcatchment to the other, the corresponding models are processed one after the other. The outflow generated by the source subcatchment was used as inflow for the subcatchment area that it flows into.

The standard simulation time used to run each model is the time-to-peak (TP) plus an additional 12 hours. This gives enough time for the water to flow into and out of the model area, illustrating the complete process from entry to exit as shown in the hydrograph. The additional 12 hours allows enough time for the water to drain fully into the next subcatchment. After all the parameters were set, the model was run through FLO-2D GDS Pro.

3.4.3 Flow Depth and Hazard Map Simulation

After running the flood map simulation in FLO-2D GDS Pro, FLO-2D Mapper Pro was used to read the resulting hazard and flow depth maps. The standard input values for reading the simulation results are shown on Figure 33.

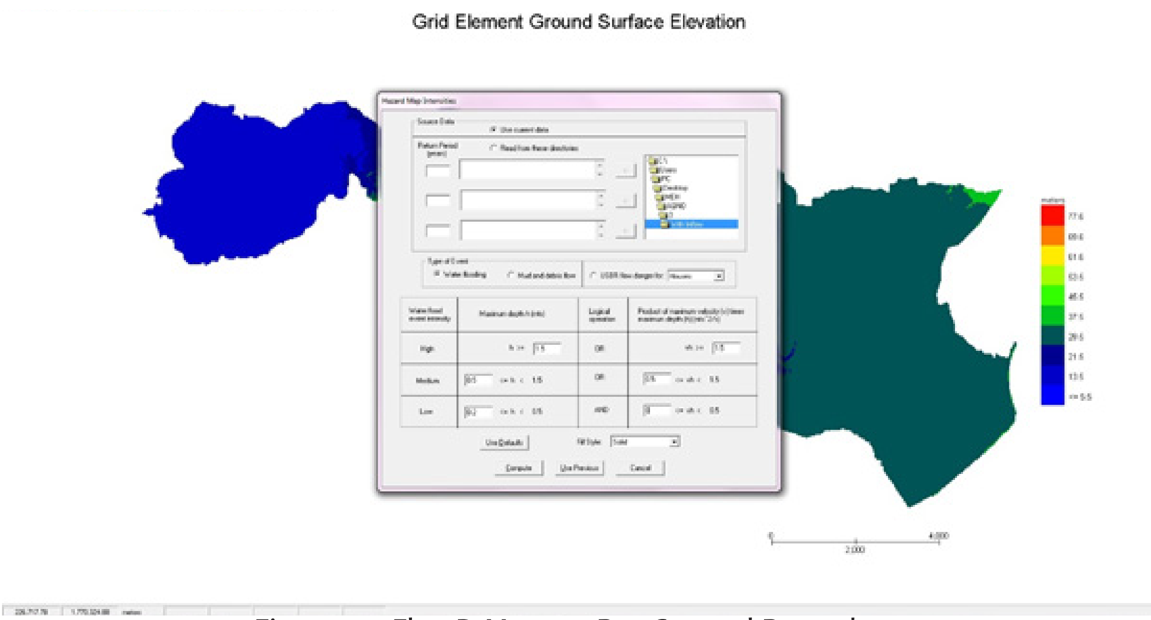

Figure 33. Flo-2D Mapper Pro General Procedure

In order to produce the hazard maps, set input for low maximum depth as 0.2 m, and vh, product of maximum velocity and maximum depth (m^2/s), as greater than or equal to zero. The program will then compute for the flood inundation and will generate shapefiles for the hazard and flow depth scenario.

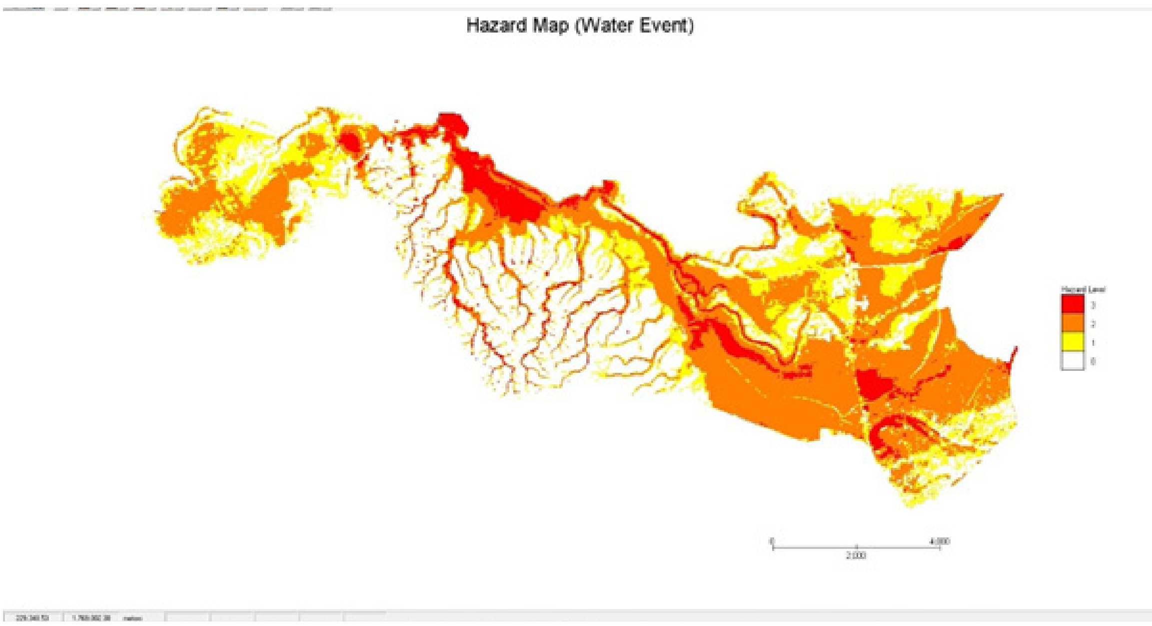

Figure 34. Agno Floodplain Generated Hazard Maps using FLO-2D Mapper

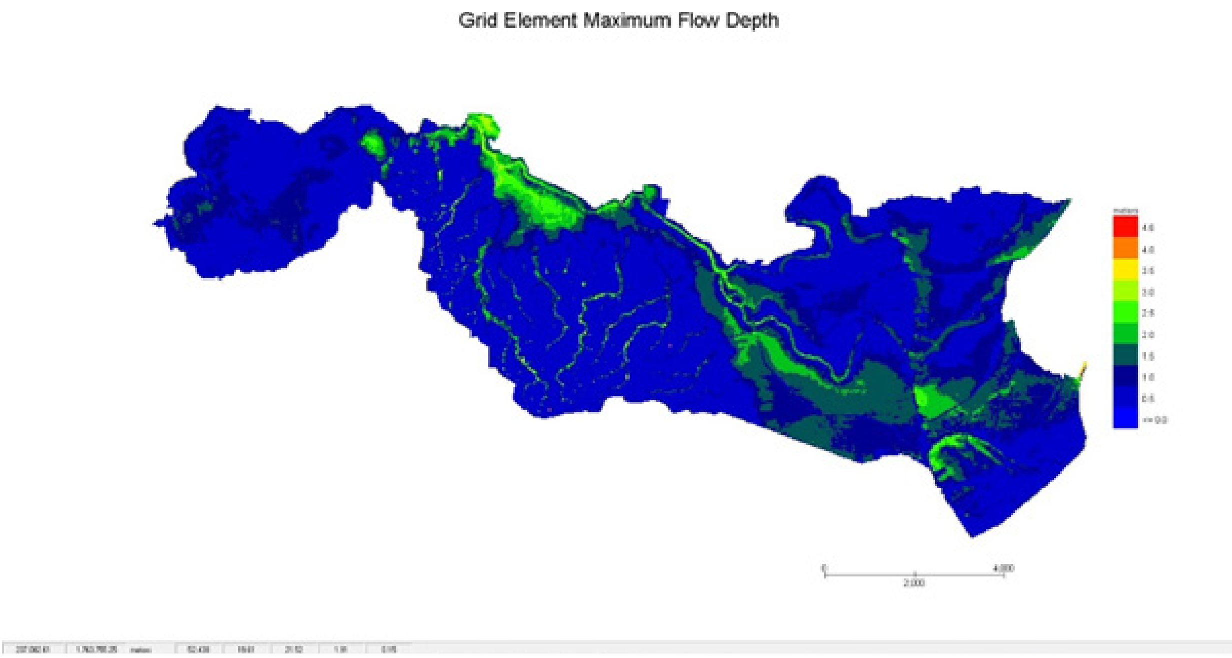

Figure 35. Agno floodplain generated flow depth map using FLO-2D Mapper

3.4.4 Hazard Map and Flow Depth Map Creation

The final procedure in creating the maps is to prepare them with the aid of ArcMap. The generated shapefiles from FLO-2D Mapper Pro were opened in ArcMap. The basic layout of a hazard map is shown in Figure 36. The same map elements are also found in a flow depth map.

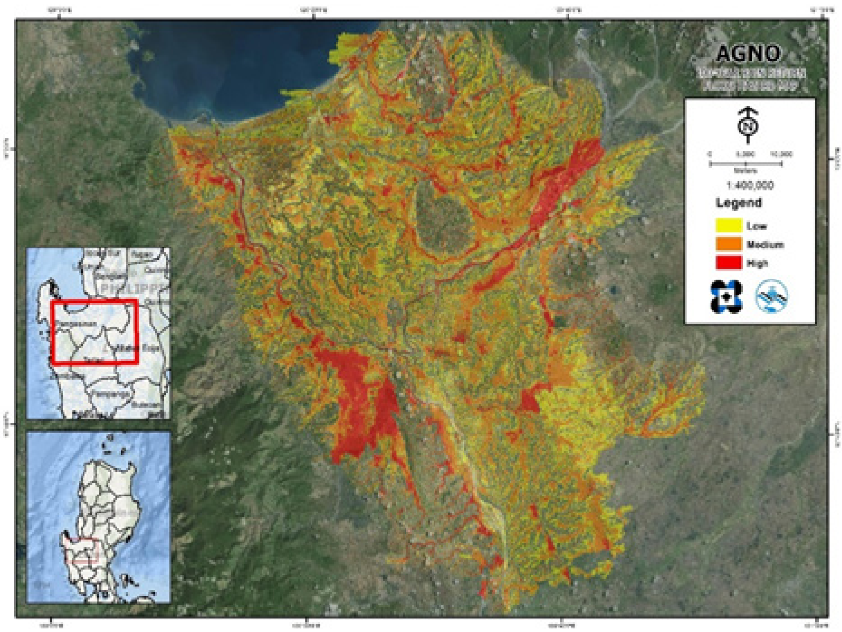

ELEMENTS
1. River Basin Name
2. Hazard/Flow Depth Shapefile
3. Provincial Inset
4. Philippine Inset
5. Hi-Res image of the area
6. North Arrow
7. Scale text and Bar

Figure 36. Basic Layout and Elements of the Hazard Maps

Results and Discussion

4.1 Efficiency of HEC-HMS Rainfall-Runoff Models calibrated based on field survey and gauges data

4.1.1 Hector Mendoza/Calvo Bridge, Pangasinan HMS Calibration Results

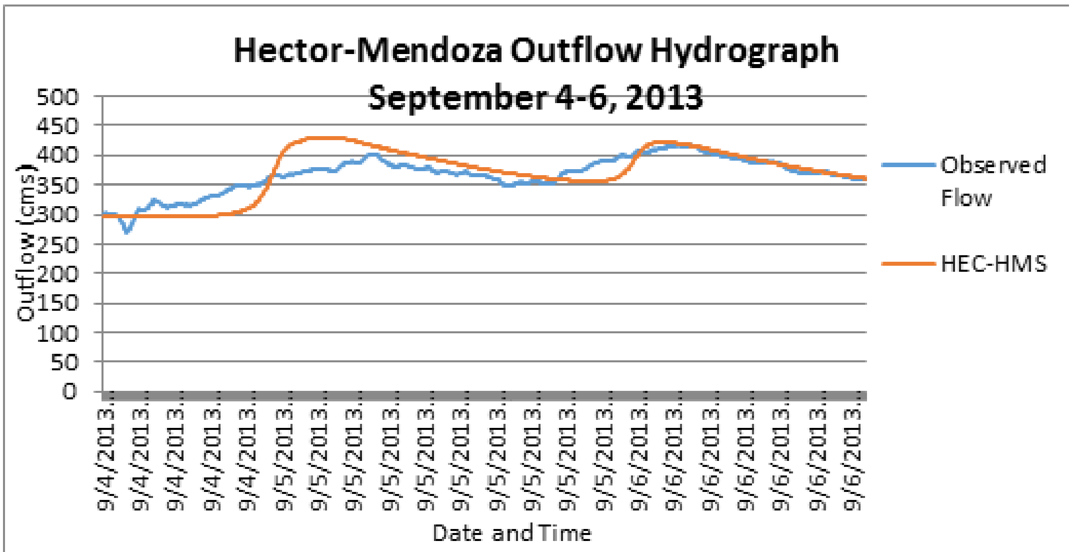

Figure 37. Hector Mendoza Bridge Outflow Hydrograph produced by the HEC-HMS model compared with observed outflow

After calibrating the Hector Mendoza HEC-HMS river basin model, its accuracy was measured against the observed values. Figure 37 shows the comparison between the two discharge data.

The Root Mean Square Error (RMSE) method aggregates the individual differences of these two measurements. It was identified at 0.982243937.

The Nash-Sutcliffe (E) method was also used to assess the predictive power of the model. Here the optimal value is 1. The model attained an efficiency coefficient of 0.99802742.

4.1.2 Banela Bridge, Pangasinan HMS Model Calibration Result

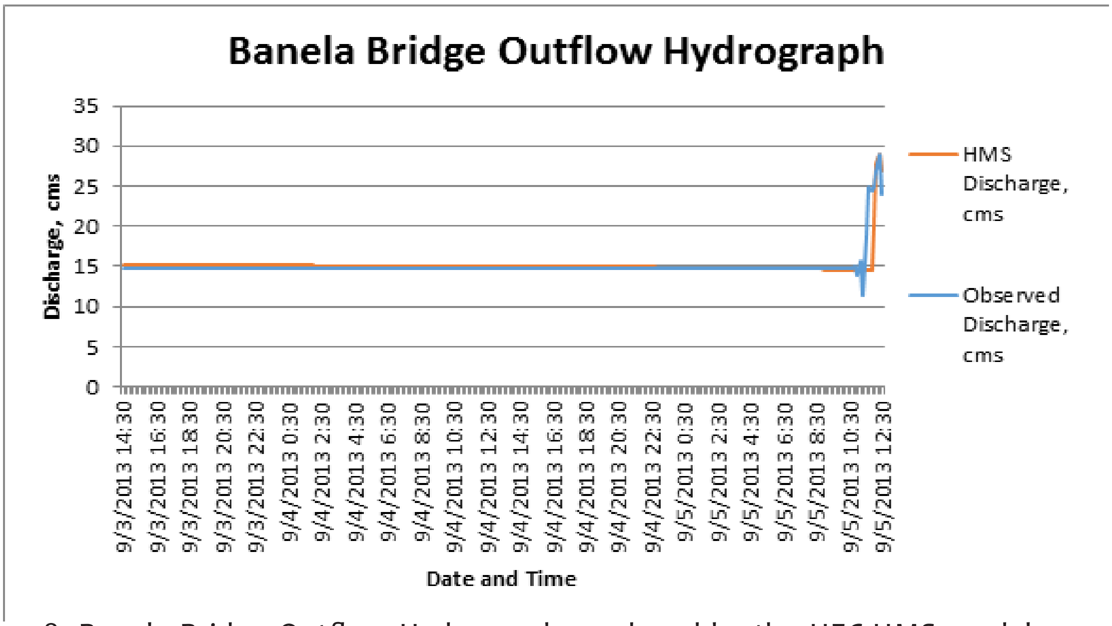

Figure 38. Banela Bridge Outflow Hydrograph produced by the HEC-HMS model compared with observed outflow

After calibrating the Banela HEC-HMS river basin model, its accuracy was measured against the observed values. Figure 38 shows the comparison between the two discharge data.

The Root Mean Square Error (RMSE) method aggregates the individual differences of these two measurements. It was identified at 1.0.

The Pearson correlation coefficient (r2) assesses the strength of the linear relationship between the observations and the model. This value being close to 1 corresponds to an almost perfect match of the observed discharge and the resulting discharge from the HEC HMS model. Here, it measured 0.2.

The Nash-Sutcliffe (E) method was also used to assess the predictive power of the model. Here the optimal value is 1. The model attained an efficiency coefficient of 0.47.

A positive Percent Bias (PBIAS) indicates a model's propensity towards under-prediction. Negative values indicate bias towards over-prediction. Again, the optimal value is 0. In the model, the PBIAS is 1.01.

The Observation Standard Deviation Ratio, RSR, is an error index. A perfect model attains a value of 0 when the error in the units of the valuable a quantified. The model has an RSR value of 0.73.

4.1.3 Magallanes Bridge, Pangasinan HMS model Calibration Results

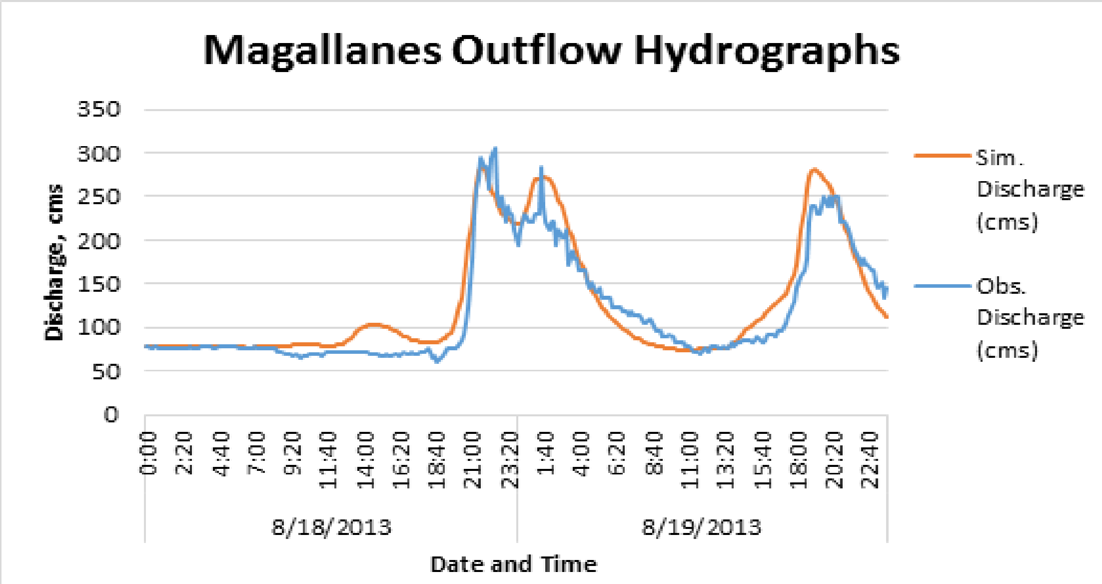

Figure 39. Magallanes Bridge Outflow Hydrograph produced by the HEC-HMS model compared with observed outflow

After calibrating the Magallanes HEC-HMS river basin model, its accuracy was measured against the observed values. Figure 39 shows the comparison between the two discharge data.

The Root Mean Square Error (RMSE) method aggregates the individual differences of these two measurements. It was identified at 22.5.

The Pearson correlation coefficient (r2) assesses the strength of the linear relationship between the observations and the model. This value being close to 1 corresponds to an almost perfect match of the observed discharge and the resulting discharge from the HEC HMS model. Here, it measured 0.95.

The Nash-Sutcliffe (E) method was also used to assess the predictive power of the model. Here the optimal value is 1. The model attained an efficiency coefficient of 0.87.

A positive Percent Bias (PBIAS) indicates a model's propensity towards under-prediction. Negative values indicate bias towards over-prediction. Again, the optimal value is 0. In the model, the PBIAS is -6.50.

The Observation Standard Deviation Ratio, RSR, is an error index. A perfect model attains a value of 0 when the error in the units of the valuable a quantified. The model has an RSR value of 0.35.

4.1.4 Viray Bridge, Pangasinan HMS Model Calibration Results

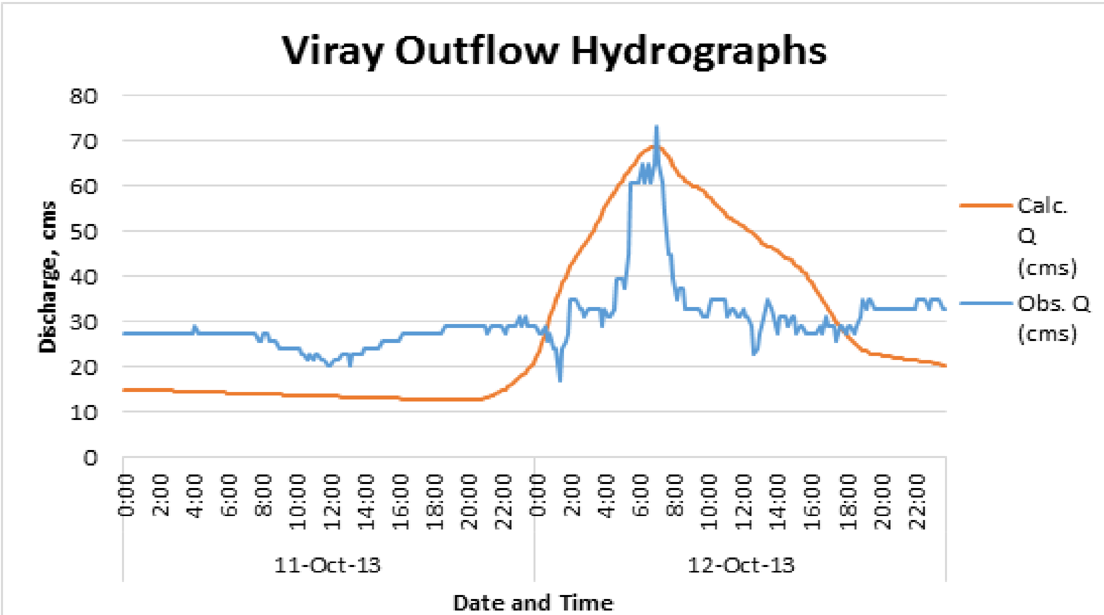

Figure 40. Viray Outflow Hydrograph produced by the Viray Bridge model compared with observed outflow

After calibrating the Viray HEC-HMS river basin model, its accuracy was measured against the observed values. Figure 40 shows the comparison between the two discharge data.

The Root Mean Square Error (RMSE) method aggregates the individual differences of these two measurements. It was identified at 14.3.

The Pearson correlation coefficient (r2) assesses the strength of the linear relationship between the observations and the model. This value being close to 1 corresponds to an almost perfect match of the observed discharge and the resulting discharge from the HEC HMS model. Here, it measured 0.67.

The Nash-Sutcliffe (E) method was also used to assess the predictive power of the model. Here the optimal value is 1. The model attained an efficiency coefficient of -2.10.

A positive Percent Bias (PBIAS) indicates a model's propensity towards under-prediction. Negative values indicate bias towards over-prediction. Again, the optimal value is 0. In the model, the PBIAS is 7.15.

The Observation Standard Deviation Ratio, RSR, is an error index. A perfect model attains a value of 0 when the error in the units of the valuable a quantified. The model has an RSR value of 1.76.

4.1.5 Dipalo Bridge, Pangasinan HMS Model Calibration Result

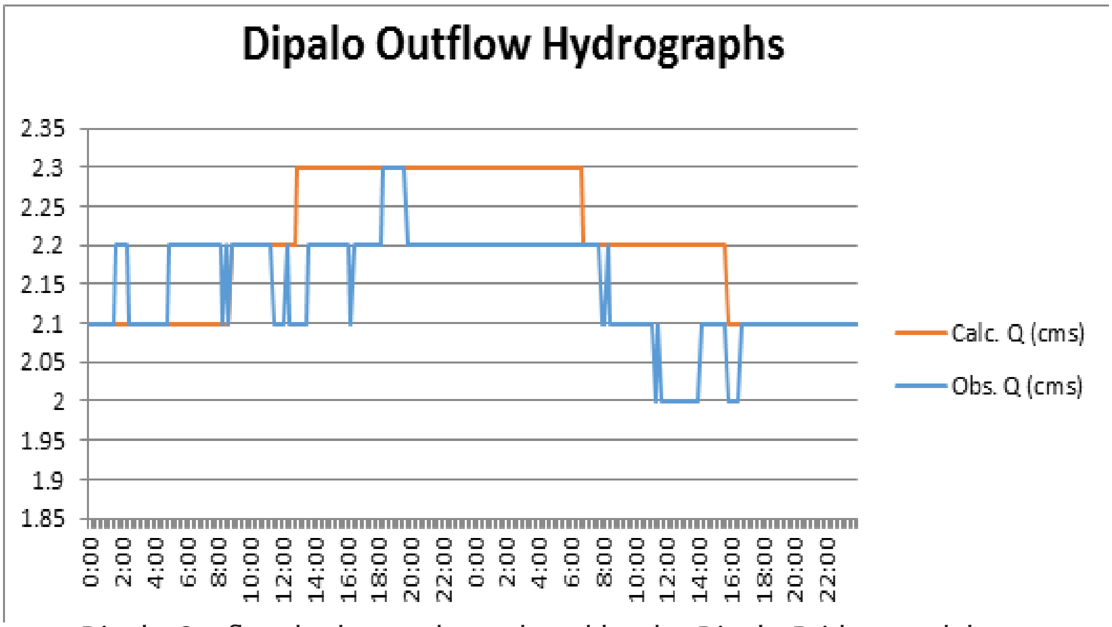

Figure 41. Dipalo Outflow hydrograph produced by the Dipalo Bridge model compared with observed outflow

After calibrating the Dipalo HEC-HMS river basin model, its accuracy was measured against the observed values. Figure 43 shows the comparison between the two discharge data.

The Root Mean Square Error (RMSE) method aggregates the individual differences of these two measurements. It was identified at 0.1.

The Pearson correlation coefficient (r2) assesses the strength of the linear relationship between the observations and the model. This value being close to 1 corresponds to an almost perfect match of the observed discharge and the resulting discharge from the HEC HMS model. Here, it measured 0.681.

The Nash-Sutcliffe (E) method was also used to assess the predictive power of the model. Here the optimal value is 1. The model attained an efficiency coefficient of -0.86.

A positive Percent Bias (PBIAS) indicates a model's propensity towards under-prediction. Negative values indicate bias towards over-prediction. Again, the optimal value is 0. In the model, the PBIAS is -2.40.

The Observation Standard Deviation Ratio, RSR, is an error index. A perfect model attains a value of 0 when the error in the units of the valuable a quantified. The model has an RSR value of 1.37.

The calibrated models of the other discharge points are used in flood forecasting. DREAM Program offers the LGUs and other disaster mitigation agencies a water level forecast tool, which can be found on the DREAM website.

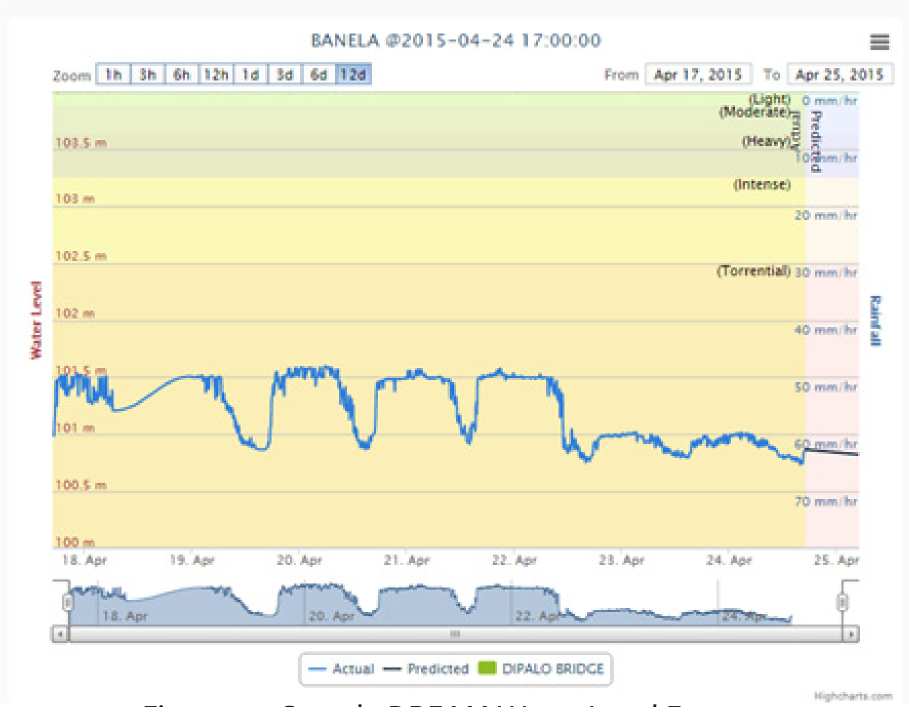

Figure 42. Sample DREAM Water Level Forecast

Given the predicted and real-time actual water level on specific AWLS, possible river flooding can be monitored and information can be disseminated to LGUs. This will help in the early evacuation of the probable affected communities. The calibrated models can also be used for flood inundation mapping.

4.2 Calculated Outflow hydrographs and Discharge Values for different Rainfall Return Periods

4.2.1 Hydrograph using the Rainfall-Runoff Model

4.2.1.1 Hector Mendoza/ Calvo Bridge Bridge, Pangasinan

The outflow of Hector Mendoza/Calvo Bridge using the Dagupan station Rainfall Intensity-Duration-Frequency curves (RIDF) in 5 different return periods (5-year, 10-year, 25-year, 50-year, and 100-year rainfall time series) based on PAGASA data are shown in Figures 43-47. The simulation results reveal significant increase in outflow magnitude as the rainfall intensity increases for a range of durations and return periods.

In the 5-year return period graph, the peak outflow is 1609.1 cms. This occurs after 10 hours and 10 minutes after the peak precipitation of 33.9 mm, as shown on Figure 43.

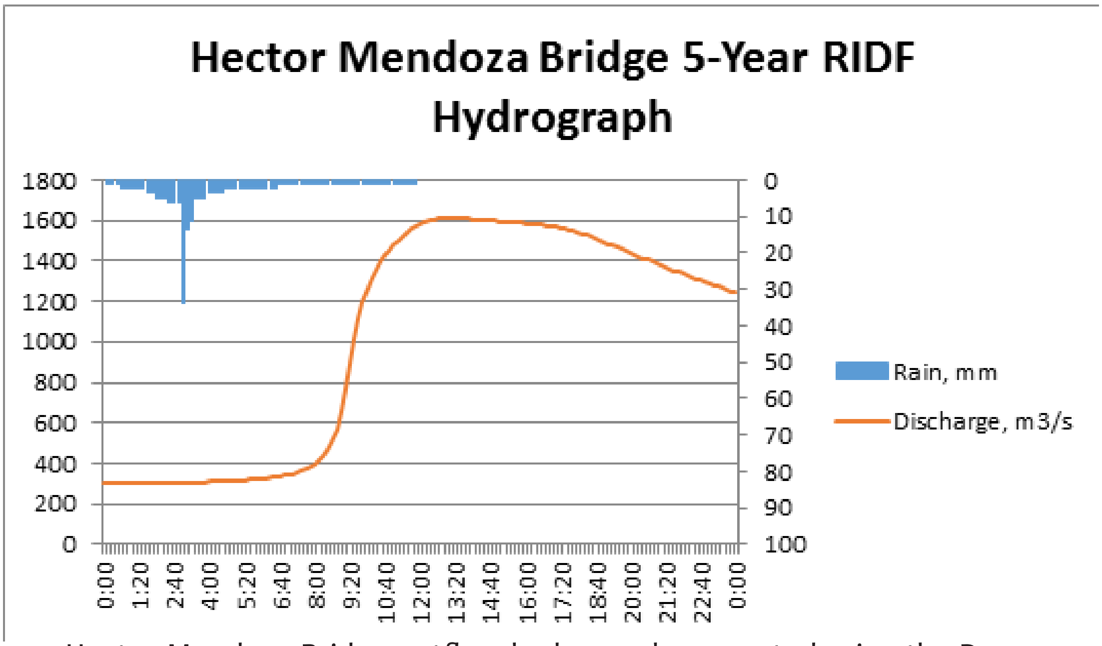

Figure 43. Hector Mendoza Bridge outflow hydrograph generated using the Dagupan 5-Year RIDF in HEC-HMS

In the 10-year return period graph, the peak outflow is 1880 cms. This occurs after 9 hours and 50 minutes after the peak precipitation of 40.5 mm, as shown on Figure 44.

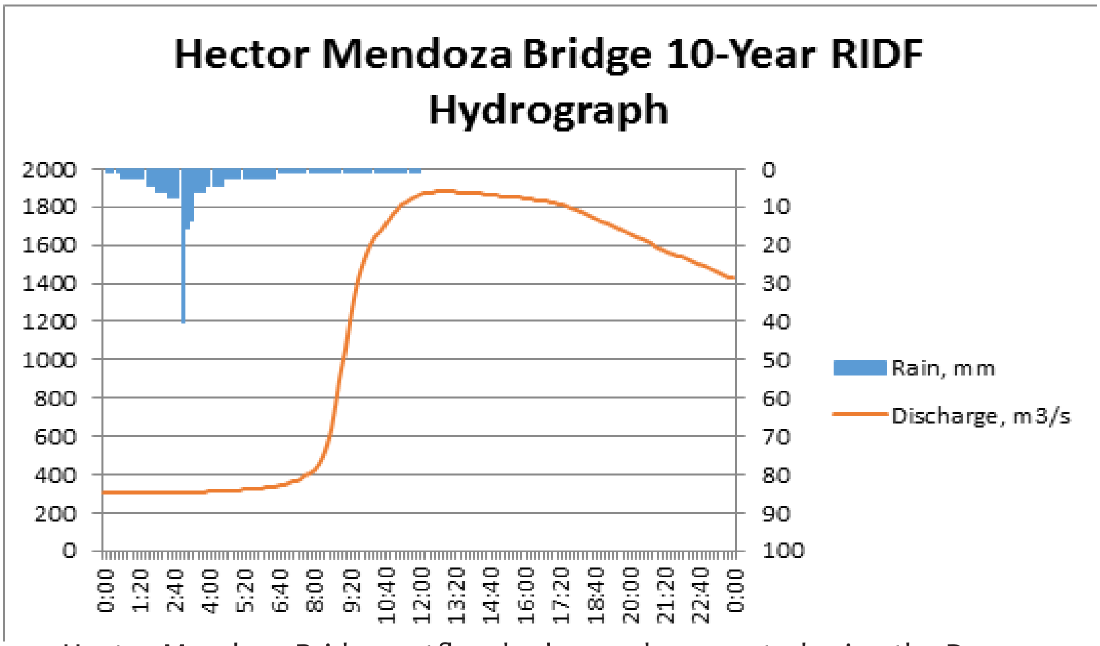

Figure 44. Hector Mendoza Bridge outflow hydrograph generated using the Dagupan 10-Year RIDF in HEC-HMS

In the 25-year return period graph, the peak outflow is 2221.2 cms. This occurs after 9 hours and 40 minutes after the peak precipitation of 48.9 mm, as shown on Figure 45.

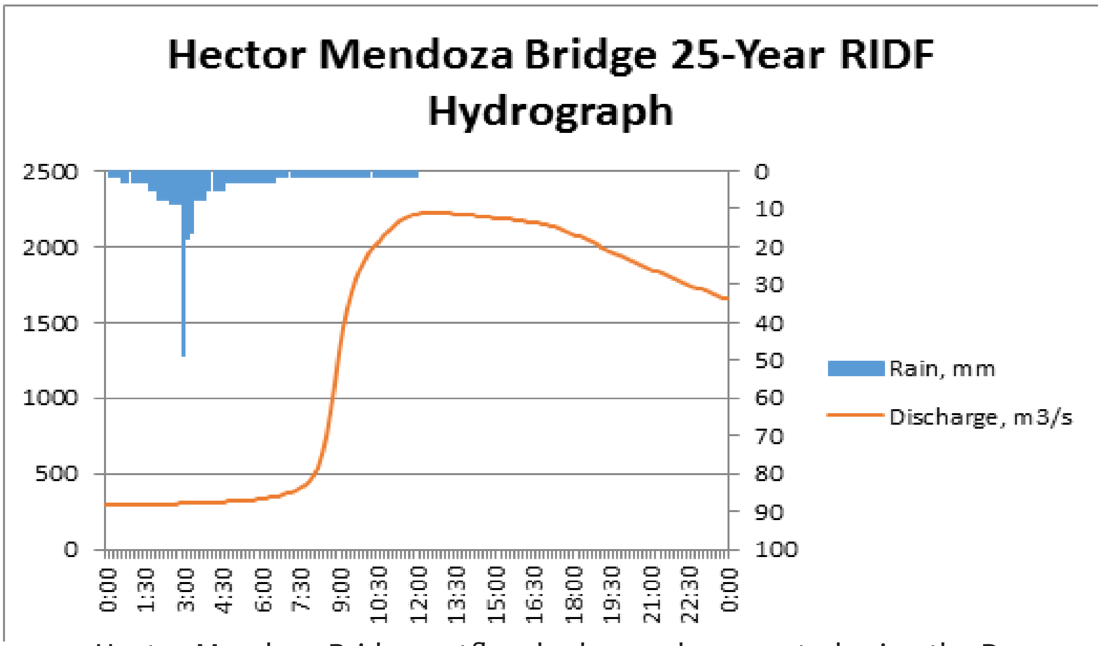

Figure 45. Hector Mendoza Bridge outflow hydrograph generated using the Dagupan 25-Year RIDF in HEC-HMS

In the 50-year return period graph, the peak outflow is 2474.8 cms. This occurs after 9 hours and 30 minutes after the peak precipitation of 55.1 mm, as shown on Figure 46.

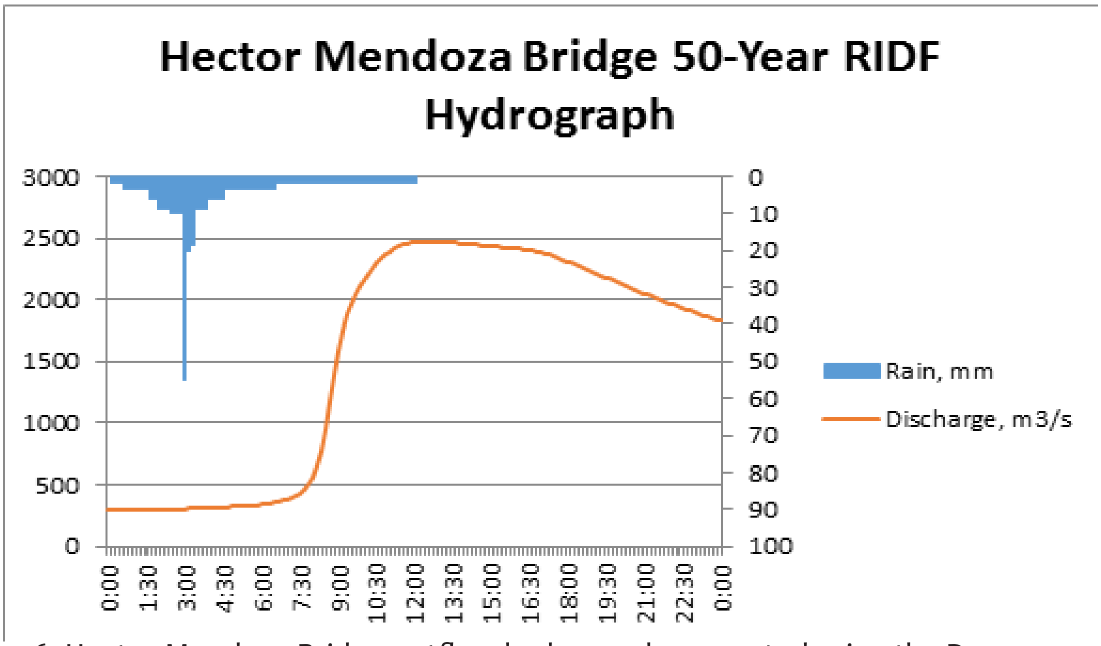

Figure 46. Hector Mendoza Bridge outflow hydrograph generated using the Dagupan 50-Year RIDF in HEC-HMS

In the 100-year return period graph, the peak outflow is 2726.7 cms. This occurs after 9 hours and 20 minutes after the peak precipitation of 61.2 mm, as shown on Figure 47.

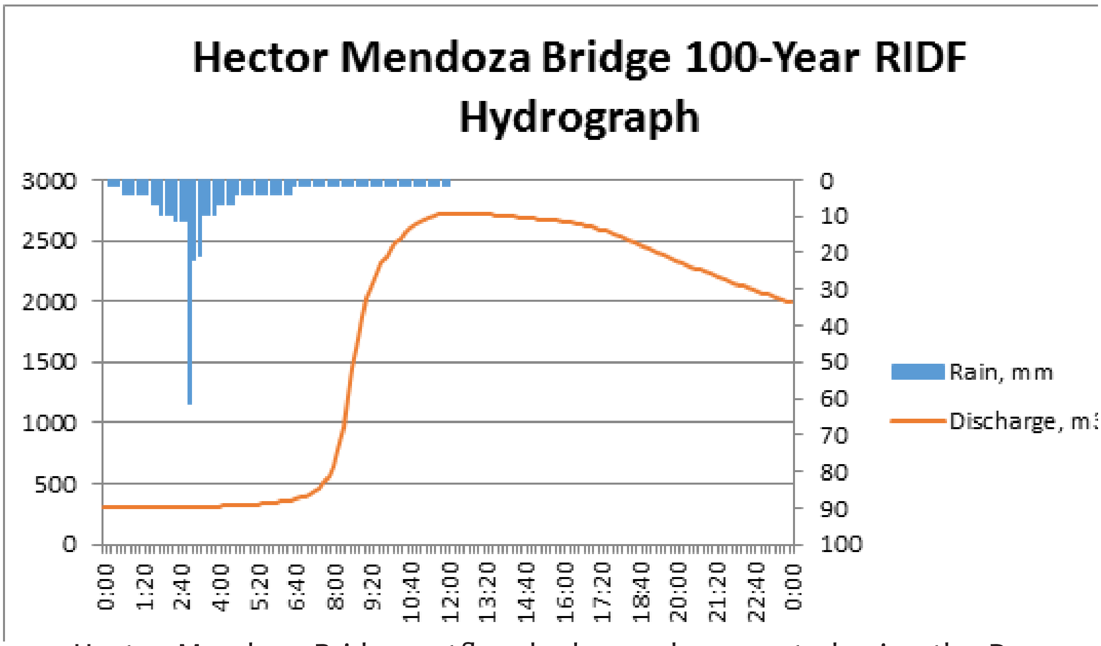

Figure 47. Hector Mendoza Bridge outflow hydrograph generated using the Dagupan 100-Year RIDF in HEC-HMS

A summary of the total precipitation, peak rainfall, peak outflow and time to peak of Hector Mendoza discharge using the Dagupan Rainfall Intensity-Duration-Frequency curves (RIDF) in five different return periods is shown in Table 2

Table 2. Summary of Hector Mendoza discharge using Dagupan Station Rainfall Intensity Duration Frequency (RIDF)

RIDF Period	Total Precipitation (mm)	Peak rainfall (mm)	Peak outflow (cms)	Time to Peak
5-Year	207.9	33.9	1609.7	10 Hours, 10 mins
10-Year	249.2	40.5	1880	9 Hours, 50 mins
25-Year	300	48.9	2221.2	9 Hours, 40 mins
50-Year	337.7	55.1	2474.8	9 Hours, 30 mins
100-Year	375.1	61.2	2726.7	9 Hours, 20 mins

4.2.1.2 Banela Bridge, Pangasinan

The outflow of Banela Bridge using the Baguio station Rainfall Intensity-Duration-Frequency curves (RIDF) in 5 different return periods (5-year, 10-year, 25-year, 50-year, and 100-year rainfall time series) based on PAGASA data are shown in Figures 48-52. The simulation results reveal significant increase in outflow magnitude as the rainfall intensity increases for a range of durations and return periods.

In the 5-year return period graph, the peak outflow is 393.7 cms. This occurs after 20 minutes after the peak precipitation of 49.9 mm, as shown on Figure 48.

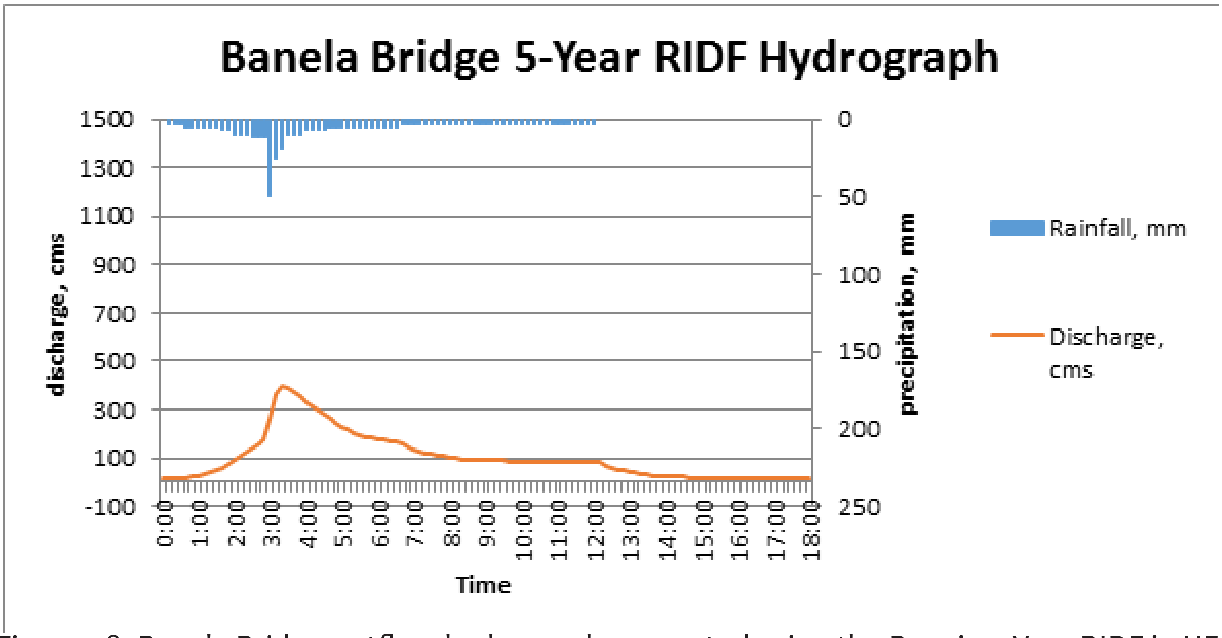

Figure 48. Banela Bridge outflow hydrograph generated using the Baguio 5-Year RIDF in HEC-HMS

In the 10-year return period graph, the peak outflow is 515 cms. This occurs after 30 after the peak precipitation of 63.8 mm, as shown on Figure 49.

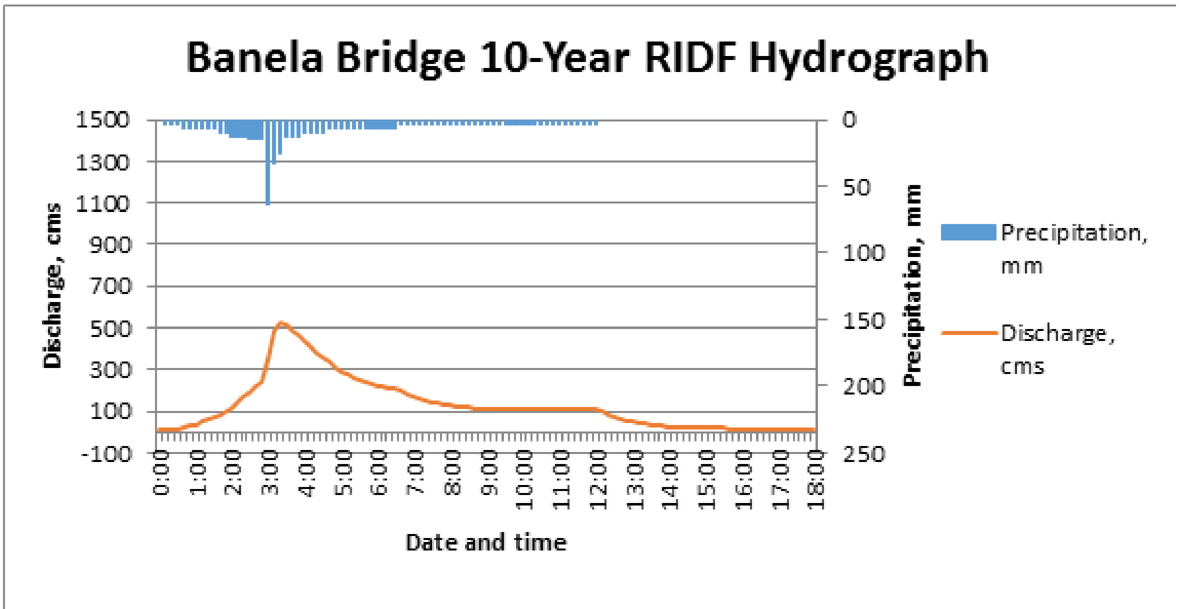

Figure 49. Banela Bridge outflow hydrograph generated using the Baguio 10-Year RIDF in HEC-HMS

In the 25-year return period graph, the peak outflow is 685.1 cms. This occurs after 20 after the peak precipitation of 82.2 mm, as shown on Figure 50.

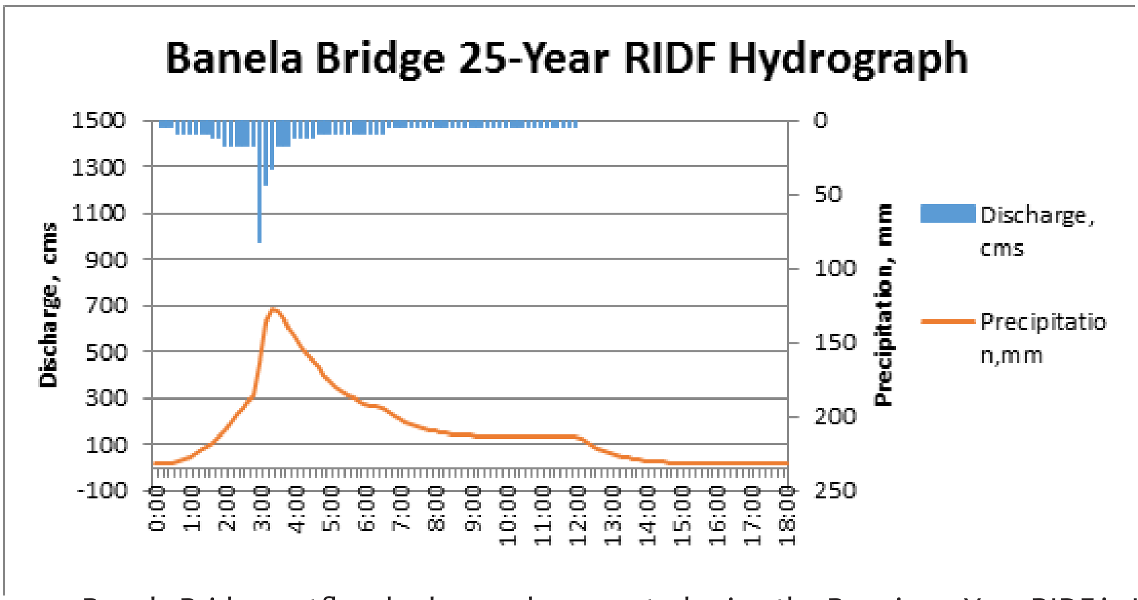

Figure 50. Banela Bridge outflow hydrograph generated using the Baguio 25-Year RIDF in HEC-HMS

In the 50-year return period graph, the peak outflow is 805.6 cms. This occurs after 20 minutes after the peak precipitation of 95.8 mm, as shown on Figure 51.

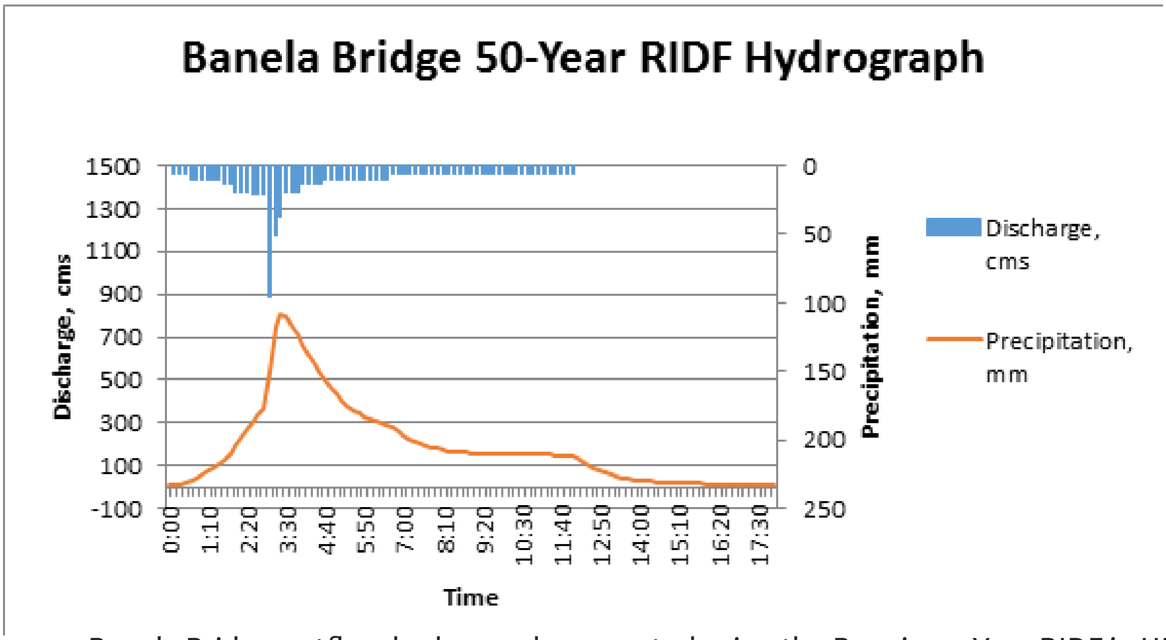

Figure 51. Banela Bridge outflow hydrograph generated using the Baguio 50-Year RIDF in HEC-HMS

In the 100-year return period graph, the peak outflow is 925.3 cms. This occurs after 20 minutes after the peak precipitation of 109.3 mm, as shown in Figure 52.

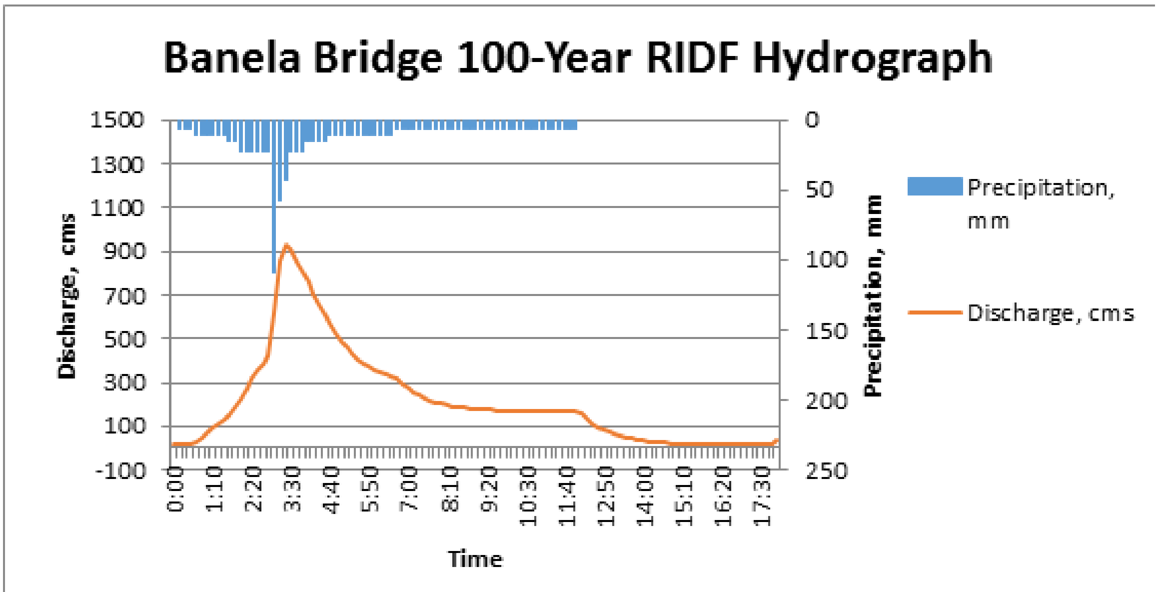

Figure 52. Banela Bridge outflow hydrograph generated using the Baguio 100-Year RIDF in HEC-HMS

A summary of the total precipitation, peak rainfall, peak outflow and time to peak of Banela Bridge discharge using the Baguio Rainfall Intensity-Duration-Frequency curves (RIDF) in five different return periods is shown in Table 3.

Table 3. Summary of Banela Bridge discharge using Baguio Station Rainfall Intensity Duration Frequency (RIDF)

RIDF Period	Total Precipitation (mm)	Peak rainfall (mm)	Peak outflow (cms)	Time to Peak
5-Year	436.9	49.9	393.7	20 mins
10-Year	555	63.8	515	30 mins
25-Year	704.1	82.2	685.1	20 mins
50-Year	814.8	95.8	805.6	20 mins
100-Year	924.7	109.3	925.3	20 mins

4.2.1.3 Magallanes Bridge, Pangasinan

The outflow of Magallanes Bridge using the Baguio station Rainfall Intensity-Duration-Frequency curves (RIDF) in 5 different return periods (5-year, 10-year, 25-year, 50-year, and 100-year rainfall time series) based on PAGASA data are shown in Figures 53-57. The simulation results reveal significant increase in outflow magnitude as the rainfall intensity increases for a range of durations and return periods.

In the 5-year return period graph, the peak outflow is 1866.1 cms. This occurs after 13 hours and 50 minutes after the peak precipitation of 49.3 mm, as shown on Figure 53.

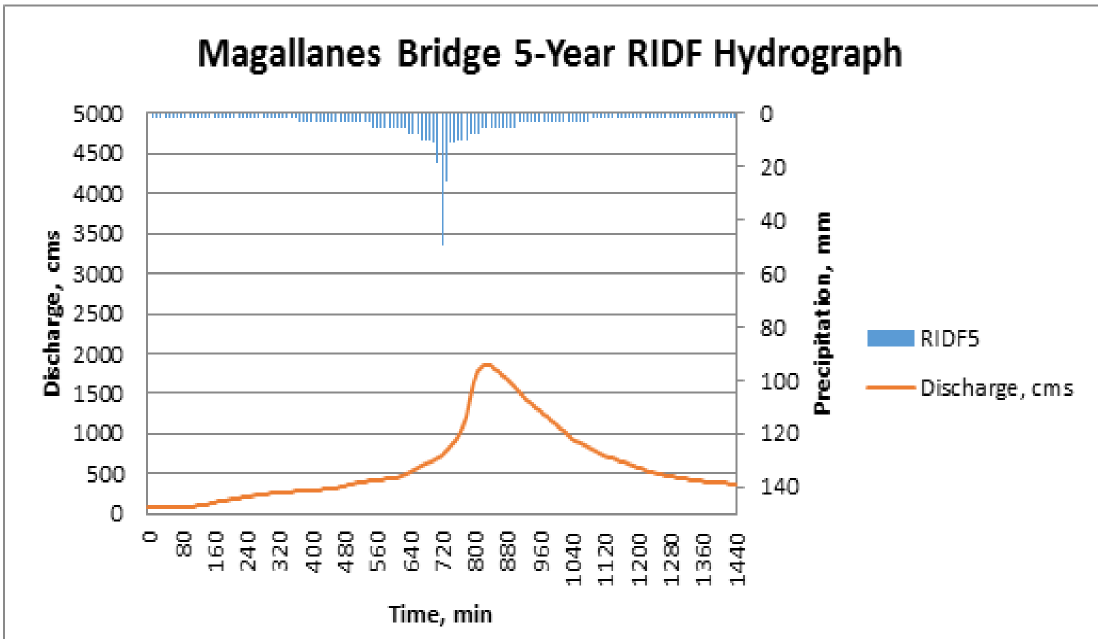

Figure 53. Magallanes Bridge outflow hydrograph generated using the Baguio 5-Year RIDF in HEC-HMS

In the 10-year return period graph, the peak outflow is 2362.9 cms. This occurs after 13 hours and 50 minutes after the peak precipitation of 63.8 mm, as shown on Figure 54.

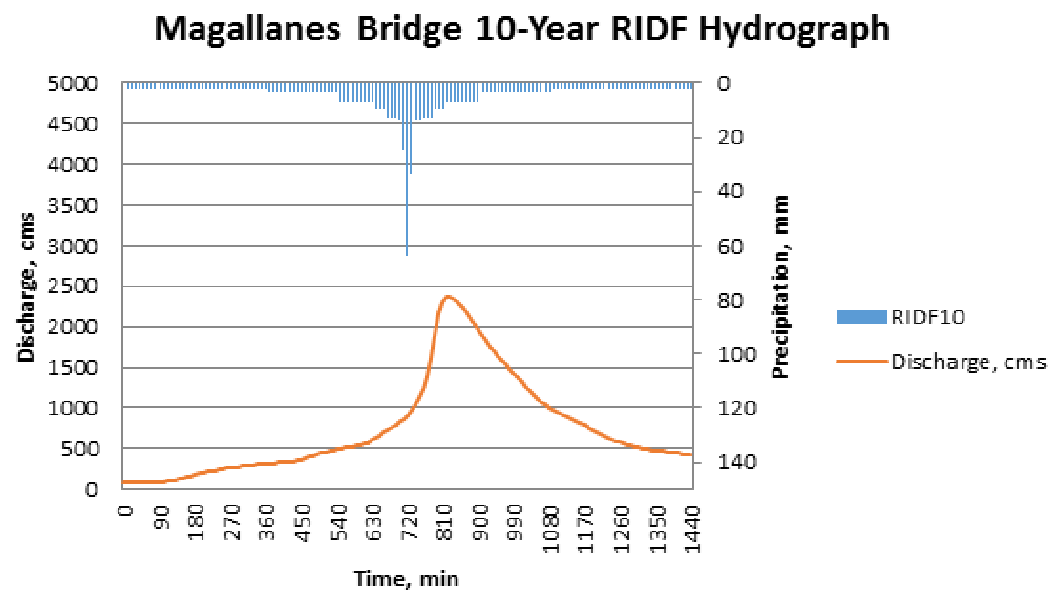

Figure 54. Magallanes Bridge outflow hydrograph generated using the Baguio 10-Year RIDF in HEC-HMS

In the 25-year return period graph, the peak outflow is 2987.8 cms. This occurs after 13 hours and 50 minutes after the peak precipitation of 82.1 mm, as shown in Figure 55.

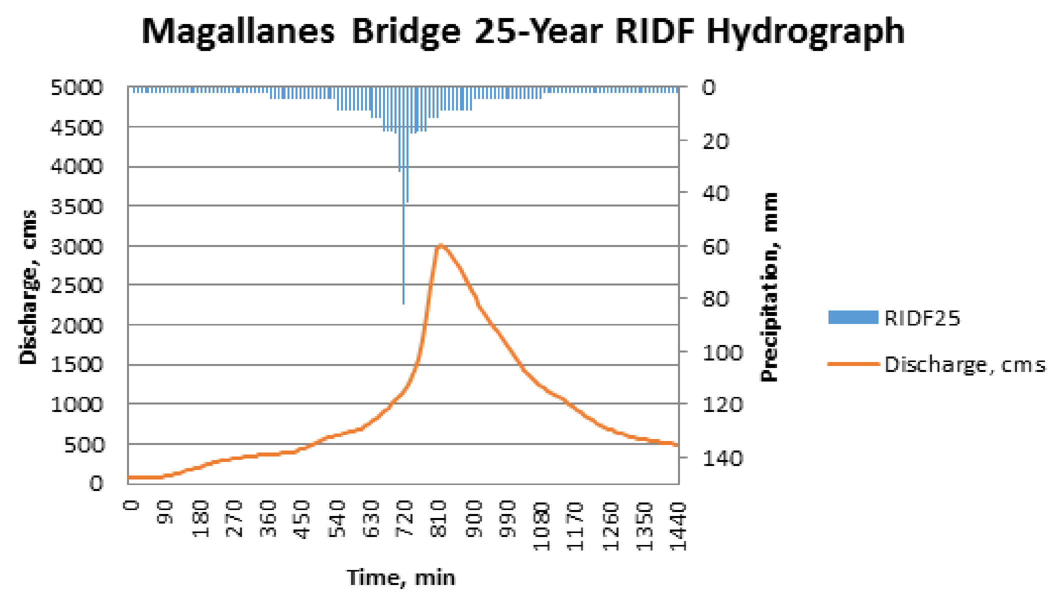

Figure 55. Magallanes Bridge outflow hydrograph generated using the Baguio 25-Year RIDF in HEC-HMS

In the 50-year return period graph, the peak outflow is 3449.5 cms. This occurs after 13 hours and 50 minutes after the peak precipitation of 95.8 mm, as shown on Figure 56.

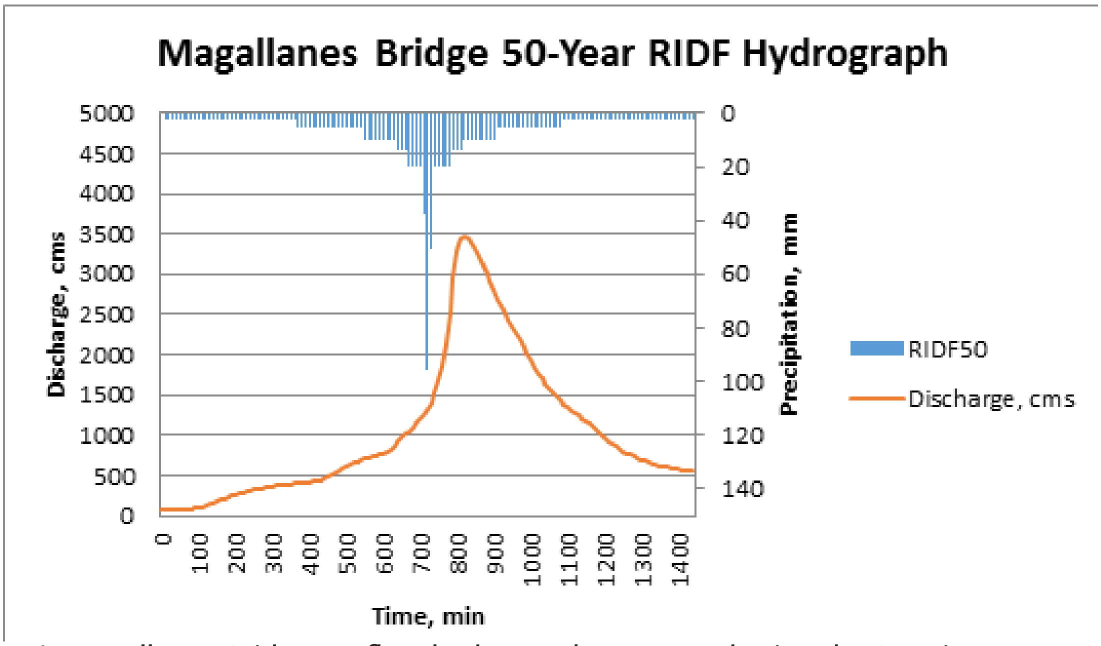

Figure 56. Magallanes Bridge outflow hydrograph generated using the Baguio 50-Year RIDF in HEC-HMS

In the 100-year return period graph shown in Figure 59, the peak outflow is 29620.7 cms. This occurs after 55 hours after the peak precipitation of 52.6 mm.

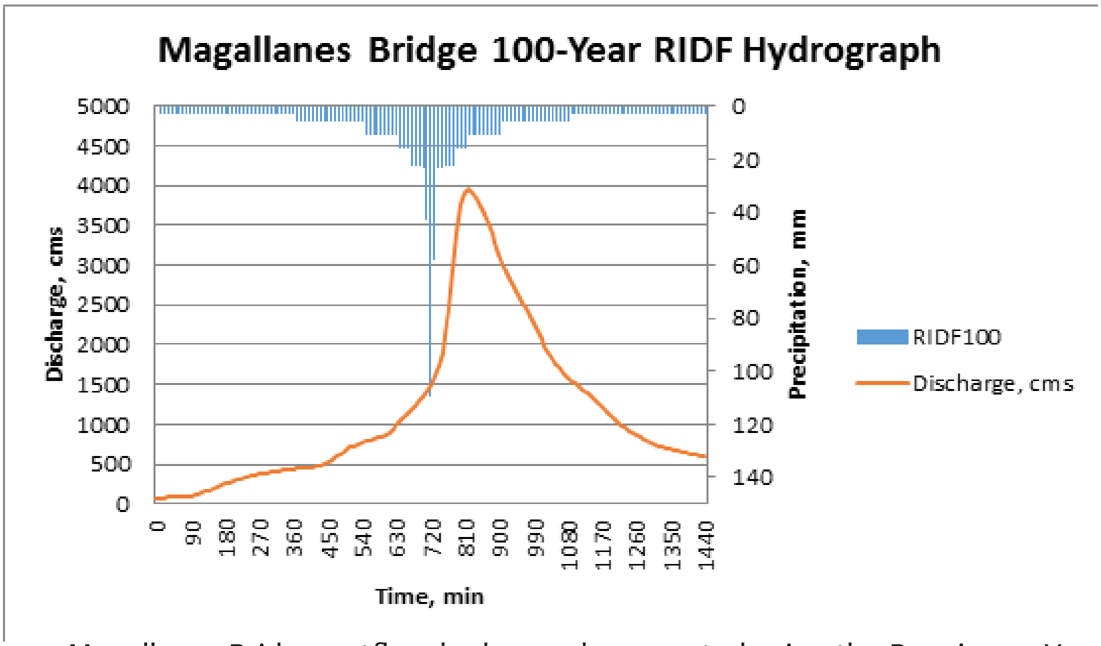

Figure 57. Magallanes Bridge outflow hydrograph generated using the Baguio 100-Year RIDF in HEC-HMS

A summary of the total precipitation, peak rainfall, peak outflow and time to peak of Magallanes Bridge discharge using the Baguio Rainfall Intensity-Duration-Frequency curves (RIDF) in five different return periods is shown in Table 4.

Table 4. Summary of Magallanes Bridge discharge using Baguio Station Rainfall Intensity Duration Frequency (RIDF)

RIDF Period	Total Precipitation (mm)	Peak rainfall (mm)	Peak outflow (cms)	Time to Peak
5-Year	563.6	49.3	1866.1	13 Hours, 50 mins
10-Year	701.7	63.8	2362.9	13 Hours, 50 mins
25-Year	876.1	82.1	2987.8	13 Hours, 50 mins
50-Year	1005.5	95.8	3449.5	13 Hours, 50 mins
100-Year	1134	109.3	3904.4	13 Hours, 50 mins

4.2.1.4 Viray Bridge, Pangasinan

The outflow of Viray Bridge using the Baguio station Rainfall Intensity-Duration-Frequency curves (RIDF) in 5 different return periods (5-year, 10-year, 25-year, 50-year, and 100-year rainfall time series) based on PAGASA data are shown in Figures 58-62. The simulation results reveal significant increase in outflow magnitude as the rainfall intensity increases for a range of durations and return periods.

In the 5-year return period graph, the peak outflow is 659.1 cms. This occurs after 16 hours and 30 minutes after the peak precipitation of 49.3 mm, as shown on Figure 58.

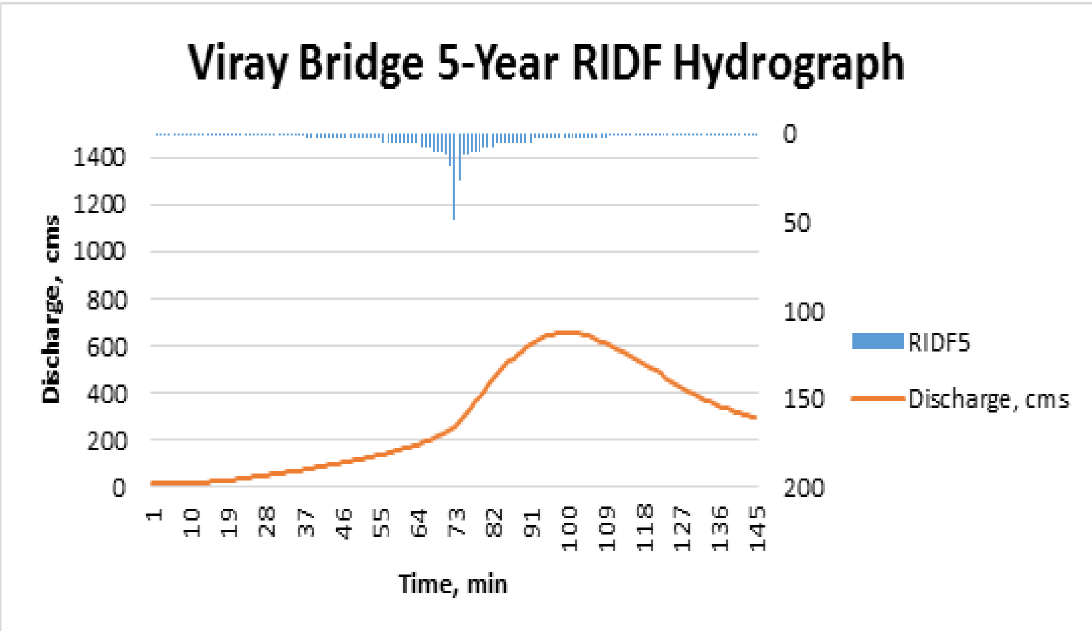

Figure 58. Viray Bridge outflow hydrograph generated using the Baguio 5-Year RIDF in HEC-HMS

In the 10-year return period graph, the peak outflow is 835.5 cms. This occurs after 16 hours and 30 minutes after the peak precipitation of 63.8 mm, as shown on Figure 59.

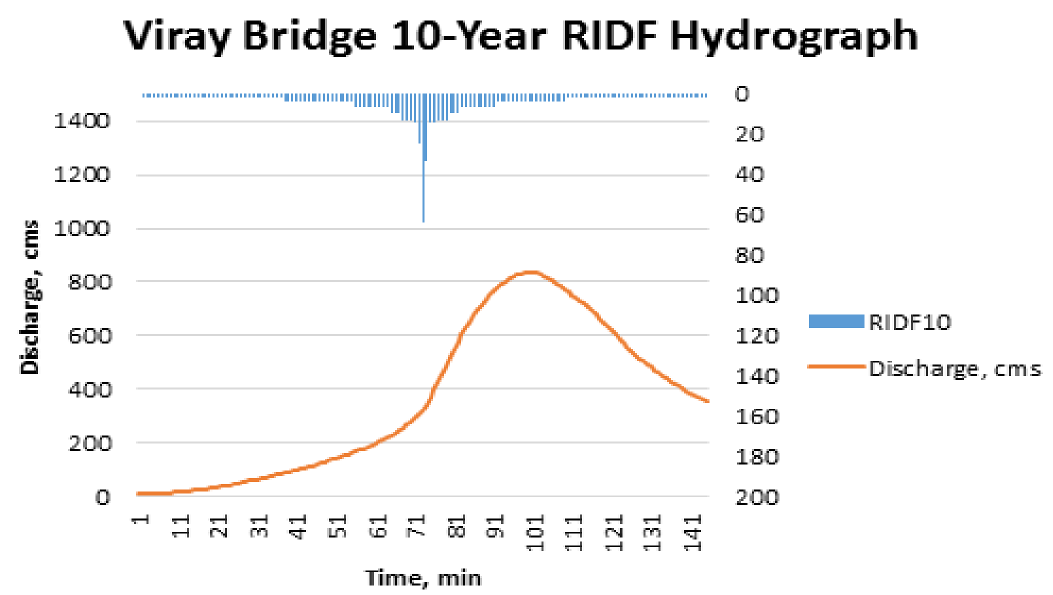

Figure 59. Viray Bridge outflow hydrograph generated using the Baguio 10-Year RIDF in HEC-HMS

In the 25-year return period graph, the peak outflow is 1058.4 cms. This occurs after 16 hours and 30 minutes after the peak precipitation of 82.1 mm, as shown on Figure 60.

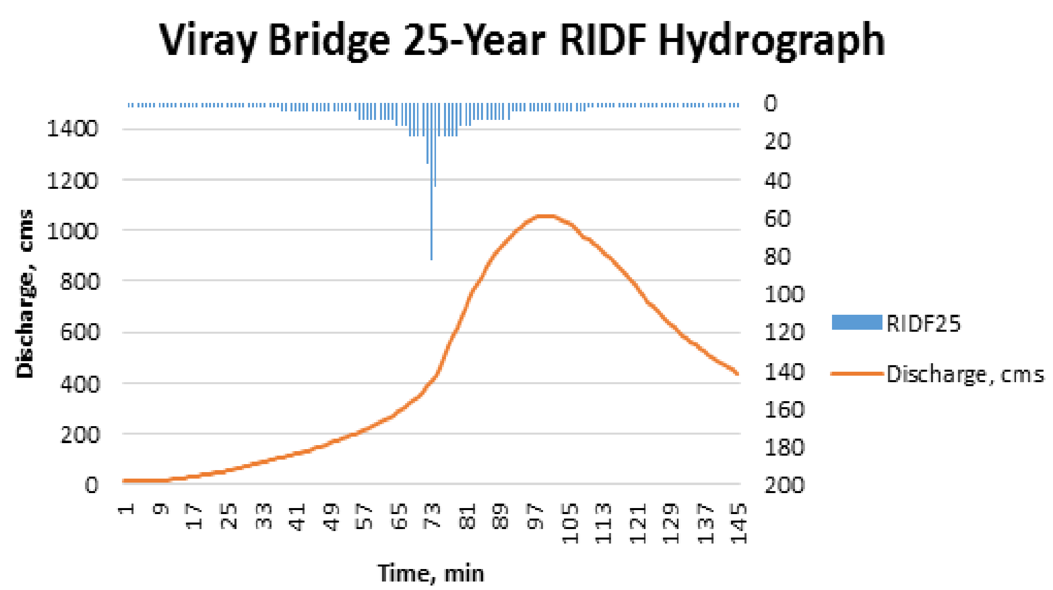

Figure 60. Viray Bridge outflow hydrograph generated using the Baguio 25-Year RIDF in HEC-HMS

In the 50-year return period graph, the peak outflow is 1223.7 cms. This occurs after 16 hours and 30 minutes after the peak precipitation of 95.8 mm, as shown on Figure 61.

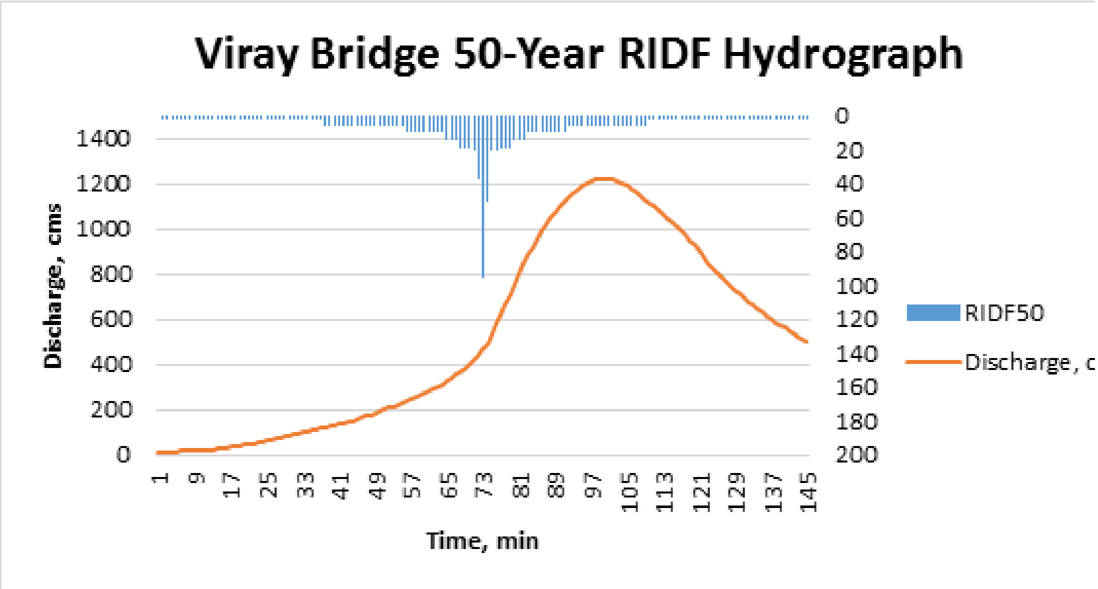

Figure 61. Viray Bridge outflow hydrograph generated using the Baguio 50-Year RIDF in HEC-HMS

In the 100-year return period graph, the peak outflow is 1387.9 cms. This occurs after 16 hours and 30 minutes after the peak precipitation of 109.3 mm, as shown in Figure 62.

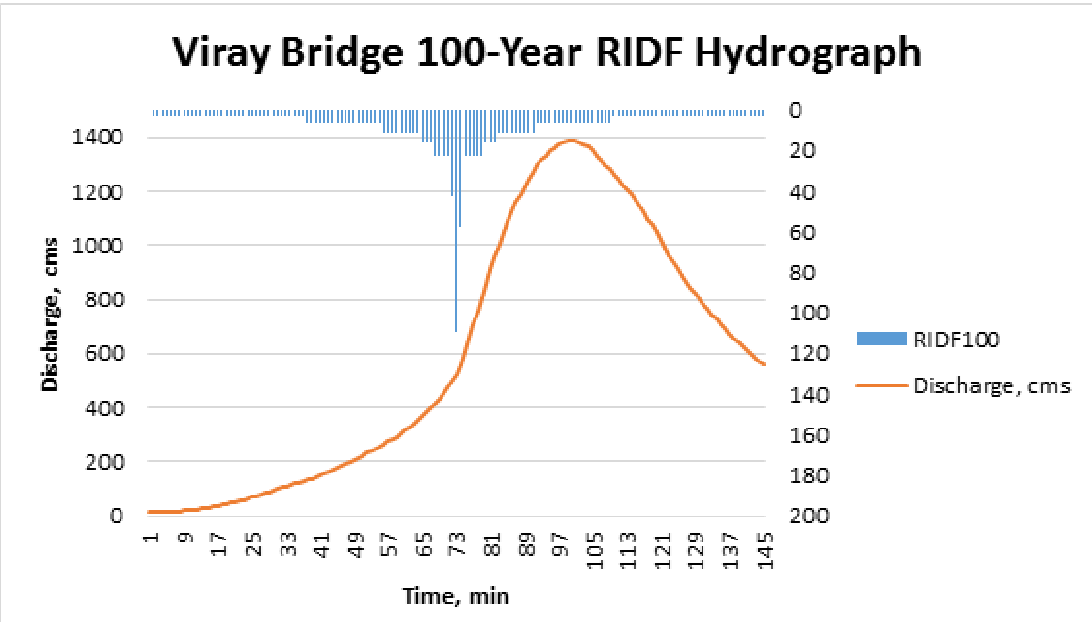

Figure 62. Viray Bridge outflow hydrograph generated using the Baguio 100-Year RIDF in HEC-HMS

A summary of the total precipitation, peak rainfall, peak outflow and time to peak of Viray Bridge discharge using the Baguio Rainfall Intensity-Duration-Frequency curves (RIDF) in five different return periods is shown in Table 5.

Table 5. Summary of Siffu outflow using Tuguegarao Station Rainfall Intensity Duration Frequency (RIDF)

RIDF Period	Total Precipitation (mm)	Peak rainfall (mm)	Peak outflow (cms)	Time to Peak
5-Year	563.6	49.3	659.1	16 Hours, 30 mins
10-Year	701.7	63.8	835.5	16 Hours, 30 mins
25-Year	876.1	82.1	1058.4	16 Hours, 30 mins
50-Year	1005.5	95.8	1223.7	16 Hours, 30 mins
100-Year	1134	109.3	1387.9	16 Hours, 30 mins

4.2.1.5 Dipalo Bridge, Pangasinan

The outflow of Dipalo Bridge using the Bsguio station Rainfall Intensity-Duration-Frequency curves (RIDF) in 5 different return periods (5-year, 10-year, 25-year, 50-year, and 100-year rainfall time series) based on PAGASA data are shown in Figures 63-67. The simulation results reveal significant increase in outflow magnitude as the rainfall intensity increases for a range of durations and return periods.

In the 5-year return period graph, the peak outflow is 25.4 cms. This occurs after 10 hours and 10 minutes after the peak precipitation of 49.3 mm, as shown on Figure 63.

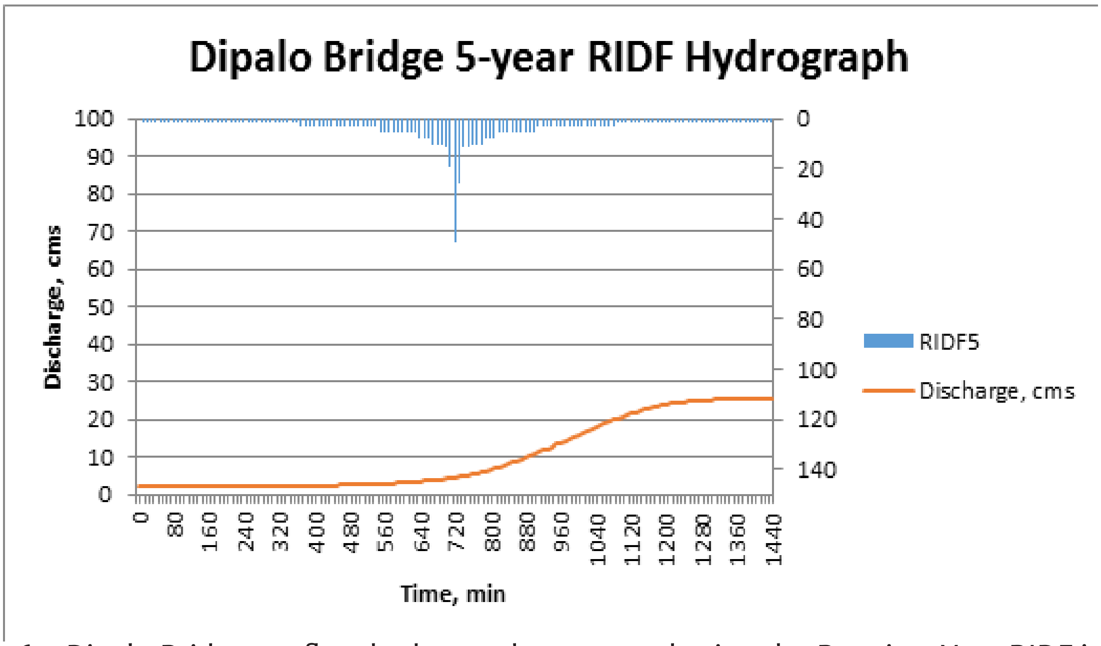

Figure 63. Dipalo Bridge outflow hydrograph generated using the Baguio 5-Year RIDF in HEC-HMS

In the 10-year return period graph, the peak outflow is 33.7 cms. This occurs after 10 hours and 10 minutes after the peak precipitation of 63.8 mm, as shown on Figure 64.

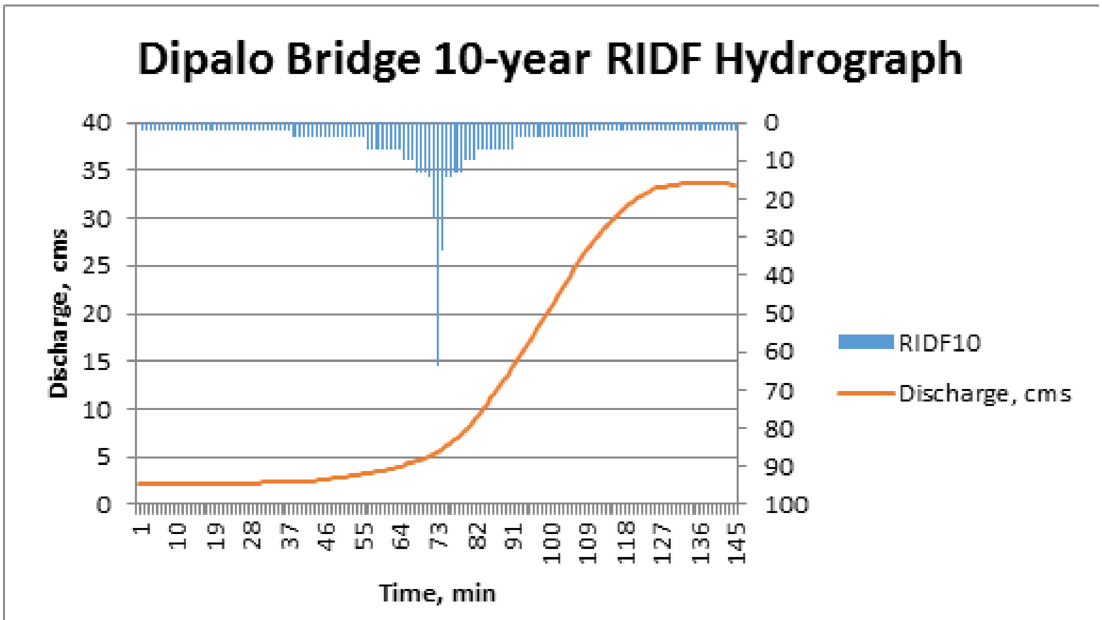

Figure 64. Dipalo Bridge outflow hydrograph generated using the Baguio 10-Year RIDF in HEC-HMS

In the 25-year return period graph, the peak outflow is 44.5 cms. This occurs after 9 hours and 50 minutes after the peak precipitation of 82.1 mm, as shown on Figure 65.

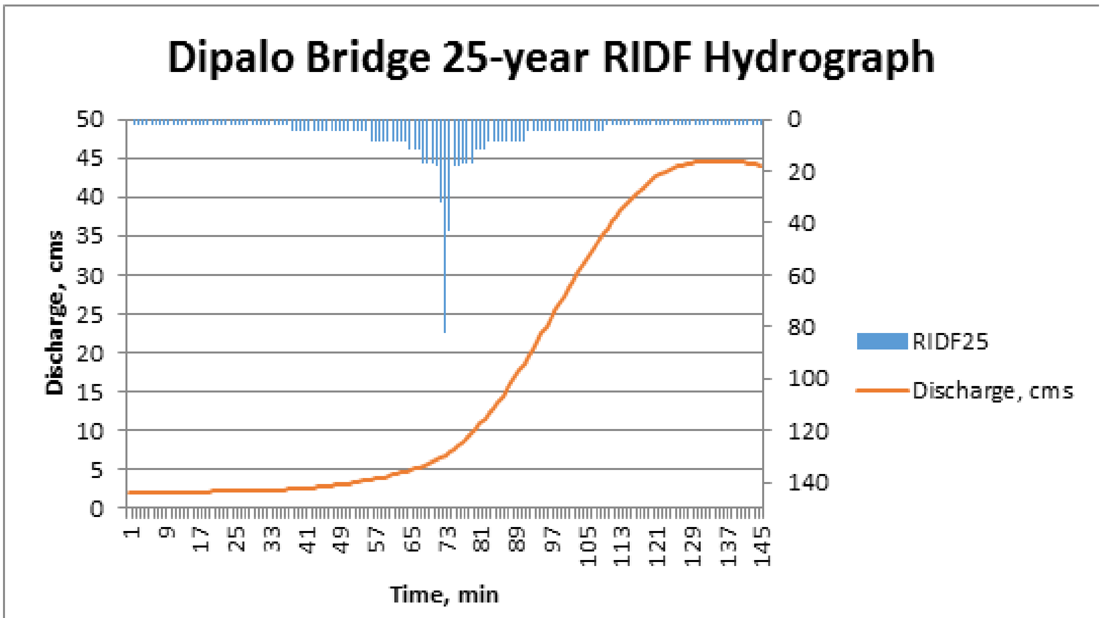

Figure 65. Dipalo Bridge outflow hydrograph generated using the Baguio 25-Year RIDF in HEC-HMS

In the 50-year return period graph, the peak outflow is 49.3 cms. This occurs after 8 hours and 40 minutes after the peak precipitation of 95.8 mm, as shown on Figure 66.

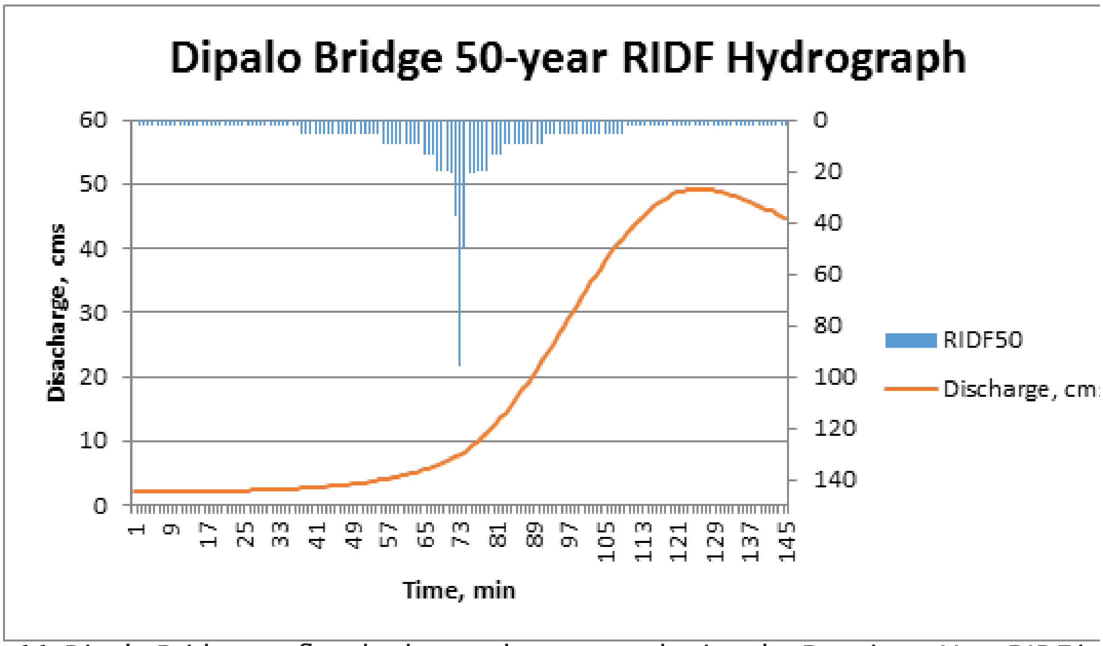

Figure 66. Dipalo Bridge outflow hydrograph generated using the Baguio 50-Year RIDF in HEC-HMS

In the 100-year return period graph, the peak outflow is 61 cms. This occurs after 9 hours and 40 minutes after the peak precipitation of 109.3 mm, as shown on Figure 67.

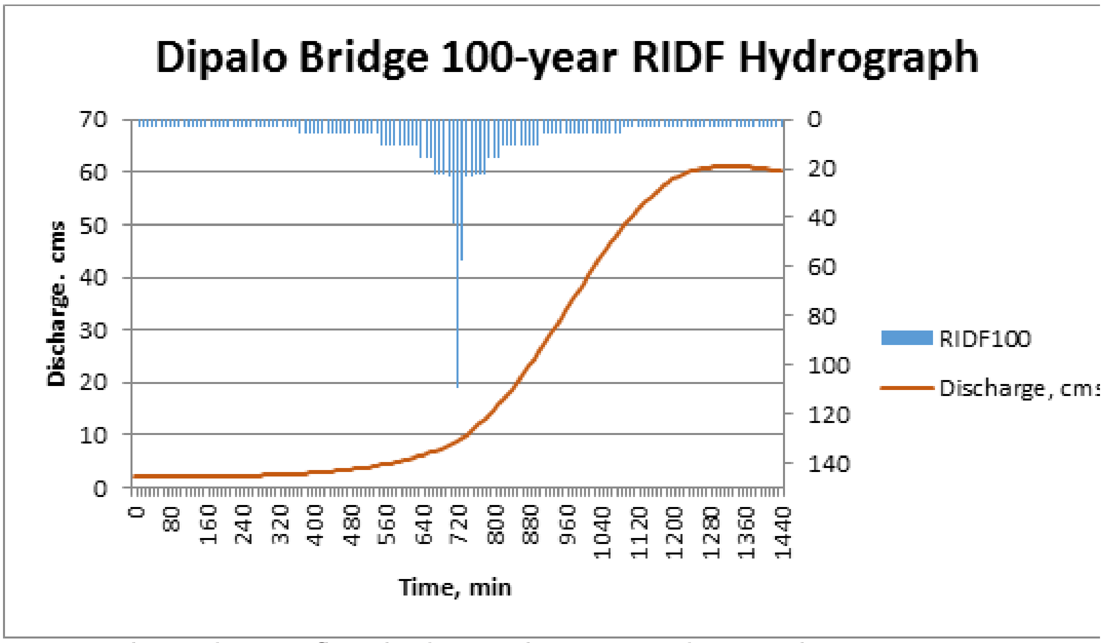

Figure 67. Dipalo Bridge outflow hydrograph generated using the Baguio 100-Year RIDF in HEC-HMS

A summary of the total precipitation, peak rainfall, peak outflow and time to peak of Dipalo Bridge discharge using the Baguio Rainfall Intensity-Duration-Frequency curves (RIDF) in five different return periods is shown in Table 6.

Table 6. Summary of Dipalo Bridge discharge using Baguio Station Rainfall Intensity Duration Frequency (RIDF)

RIDF Period	Total Precipitation (mm)	Peak rainfall (mm)	Peak outflow (cms)	Time to Peak
5-Year	214.9	28.5	477.4	10 hours, 10 minutes
10-Year	262.7	34.3	534	10 hours, 10 minutes
25-Year	323	41.7	696.3	9 hours and 50 minutes
50-Year	367.8	47.1	819.2	8 hours and 40 minutes
100-Year	412.2	52.6	941.3	9 hours and 50 minutes

4.2.2 Discharge Data using Dr. Horritt's Recommended Hydrological Method

The river discharge values using Dr. Horritt's recommended hydrological method are shown in Figure 68 and Figure 69 and the peak discharge values are summarized in Table 7 and Table 8.

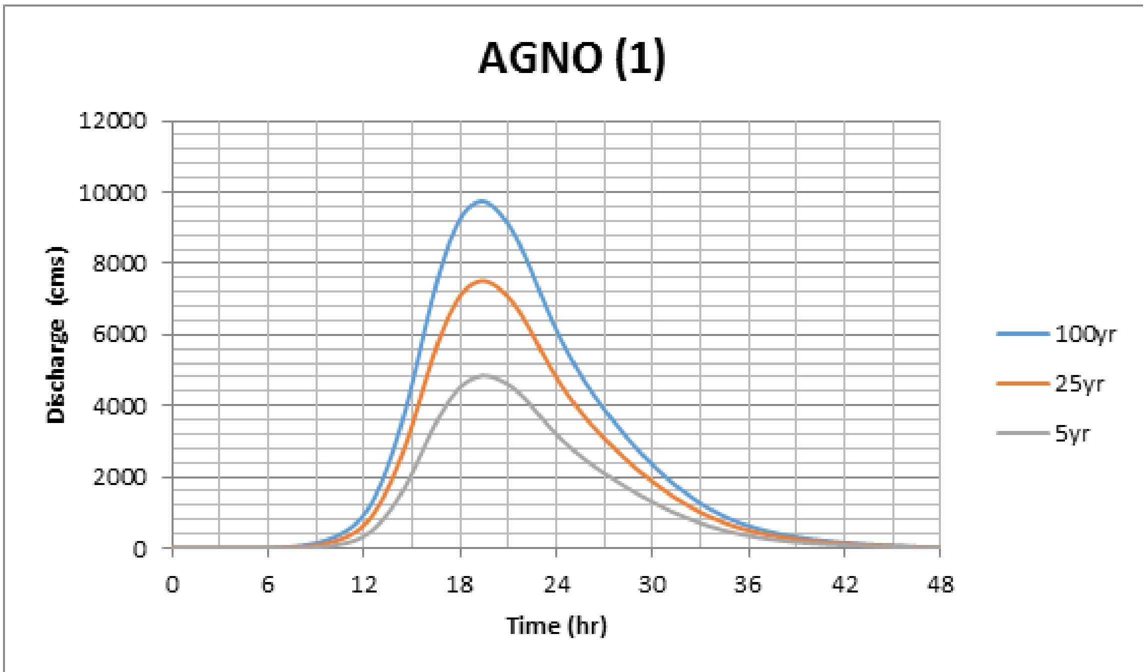

Figure 68. Outflow hydrograph generated for Agno (1) using the Iba 5-,25-, 100-Year rainfall scenarios in HEC-HMS

Table 7. Summary of Agno river (1) discharge using the recommended hydrological method by Dr. Horritt

RIDF Period	Peak discharge (cms)	Time-to-peak
5-Year	4844.2	19 hours, 30 minutes
25-Year	7511.6	19 hours, 20 minutes
100-Year	9746.0	19 hours, 20 minutes

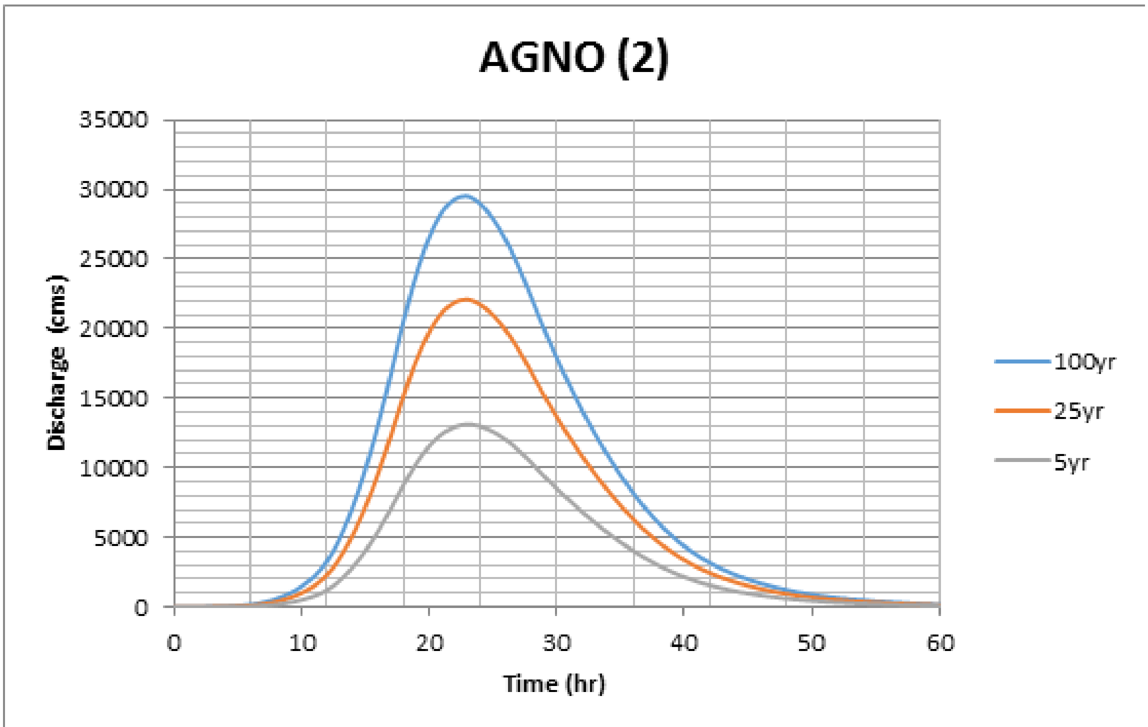

Figure 69. Outflow hydrograph generated for Agno (2) using the Iba 5-,25-, 100-Year rainfall scenarios in HEC-HMS

Table 8. Summary of Agno river (1) discharge using the recommended hydrological method by Dr. Horritt

RIDF Period	Peak discharge (cms)	Time-to-peak
5-Year	13124.9	23 hours
25-Year	22098.9	23 hours
100-Year	29531.2	22 hours, 50 minutes

The comparison of discharge values obtained from HEC-HMS, QMED, and from the bankful discharge method, Qbankful, are shown in Table 9. Using values from the DTM of Agno, the bankful discharge for the river was computed.

Table 9. Validation of river discharge estimate using the bankful method

Discharge Point	Qbankful, cms	QMED, cms	Validation
Agno river (1)	4,258.23	4,262.9	Pass
Agno river (2)	10,640.50	11,549.9	Pass

The values from the HEC-HMS discharge estimates were able to satisfy the condition for validating the computed discharge using the bankful method. The computed values were used for the two discharge points that did not have actual discharge data. The actual discharge data were also used for some areas in the floodplain that were modelled. It is recommended, therefore, to use the actual value of the river discharge for higher-accuracy modeling.

4.3 Flood Hazard and Flow Depth Maps

The following images are the hazard and flow depth maps for the 5-, 25-, and 100-year rain return scenarios of the Agno river basin.

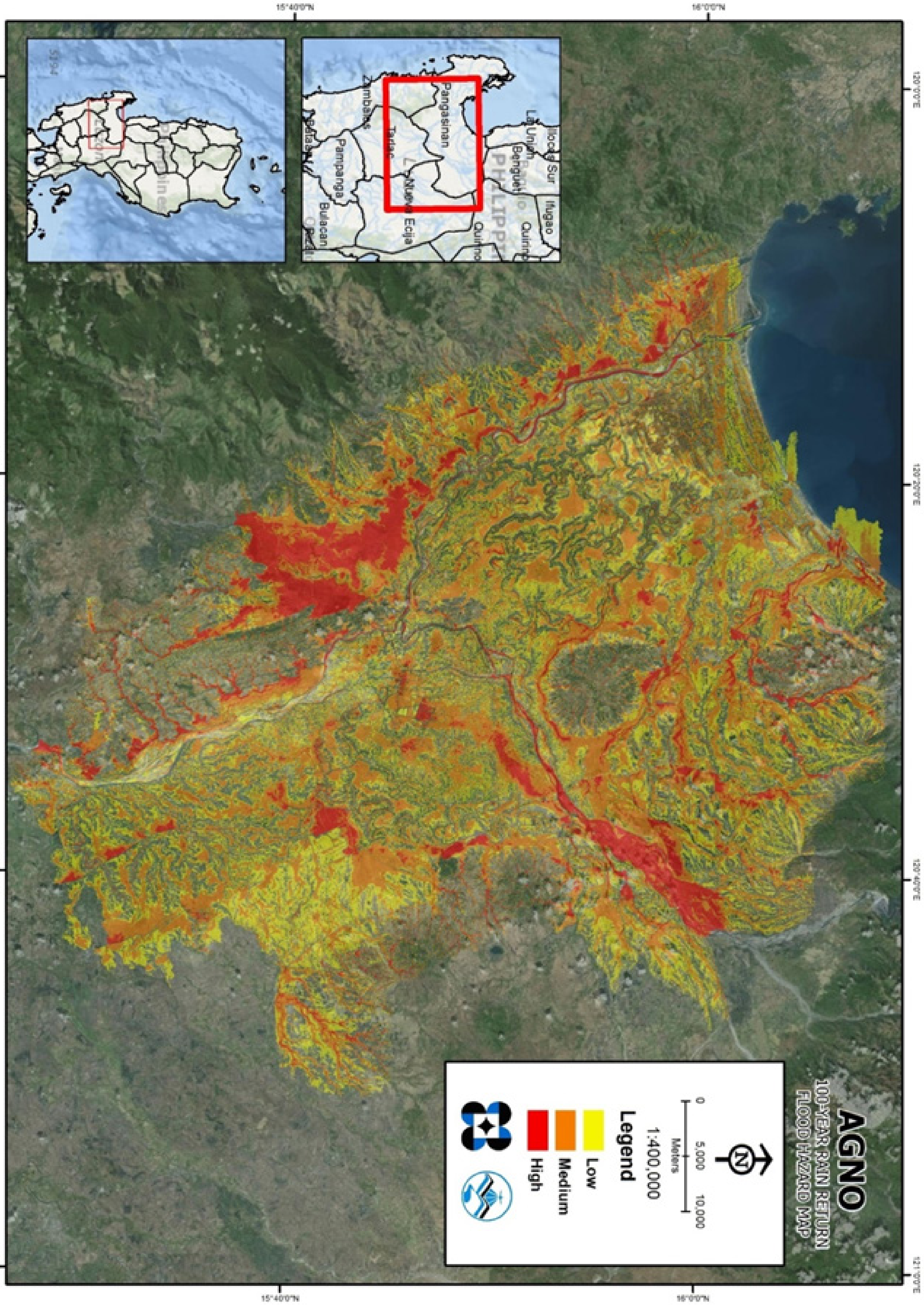

Figure 70. 100-year Flood Hazard Map for Agno River Basin

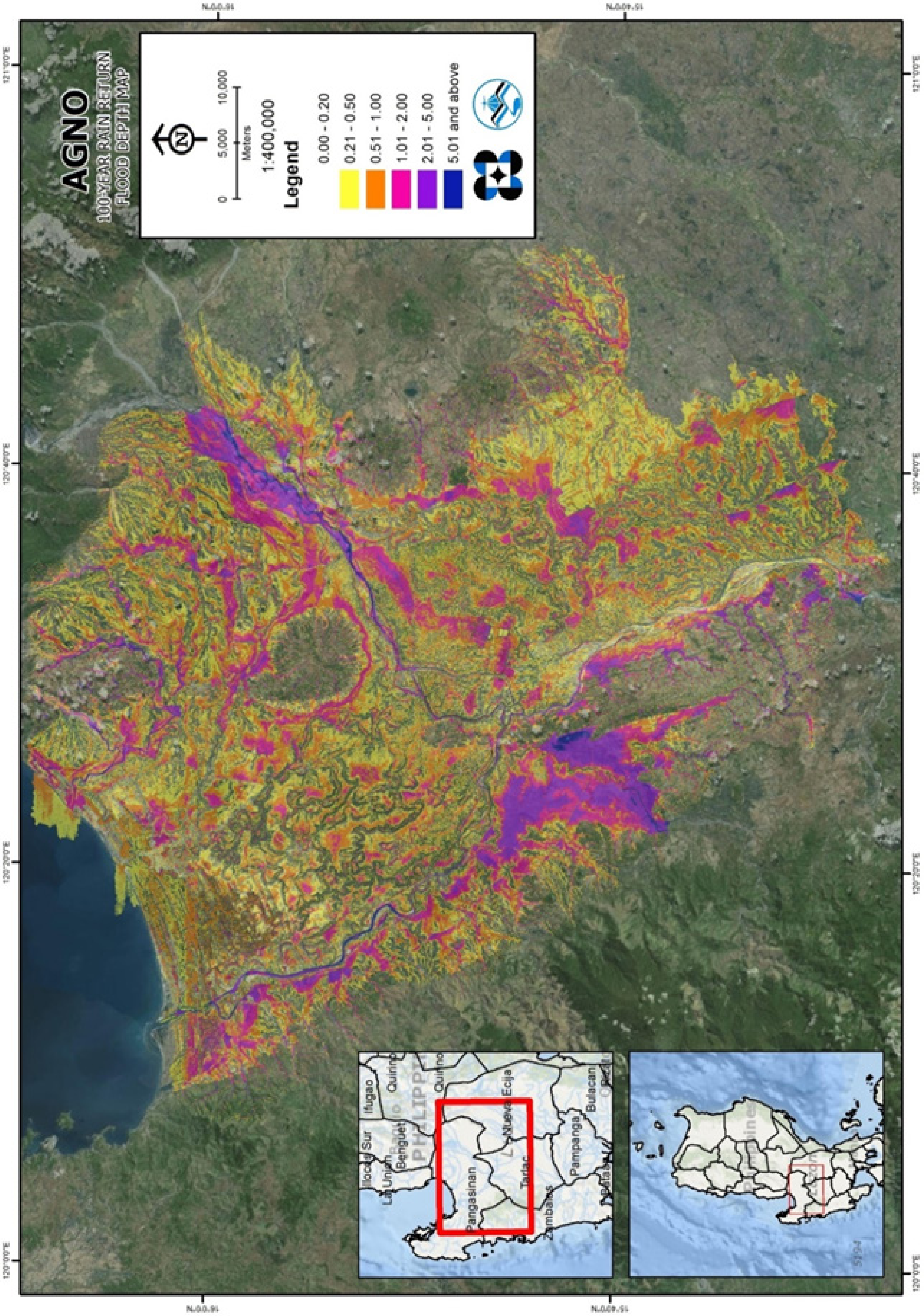

Figure 71. 100-year Flow Depth Map for Agno River Basin

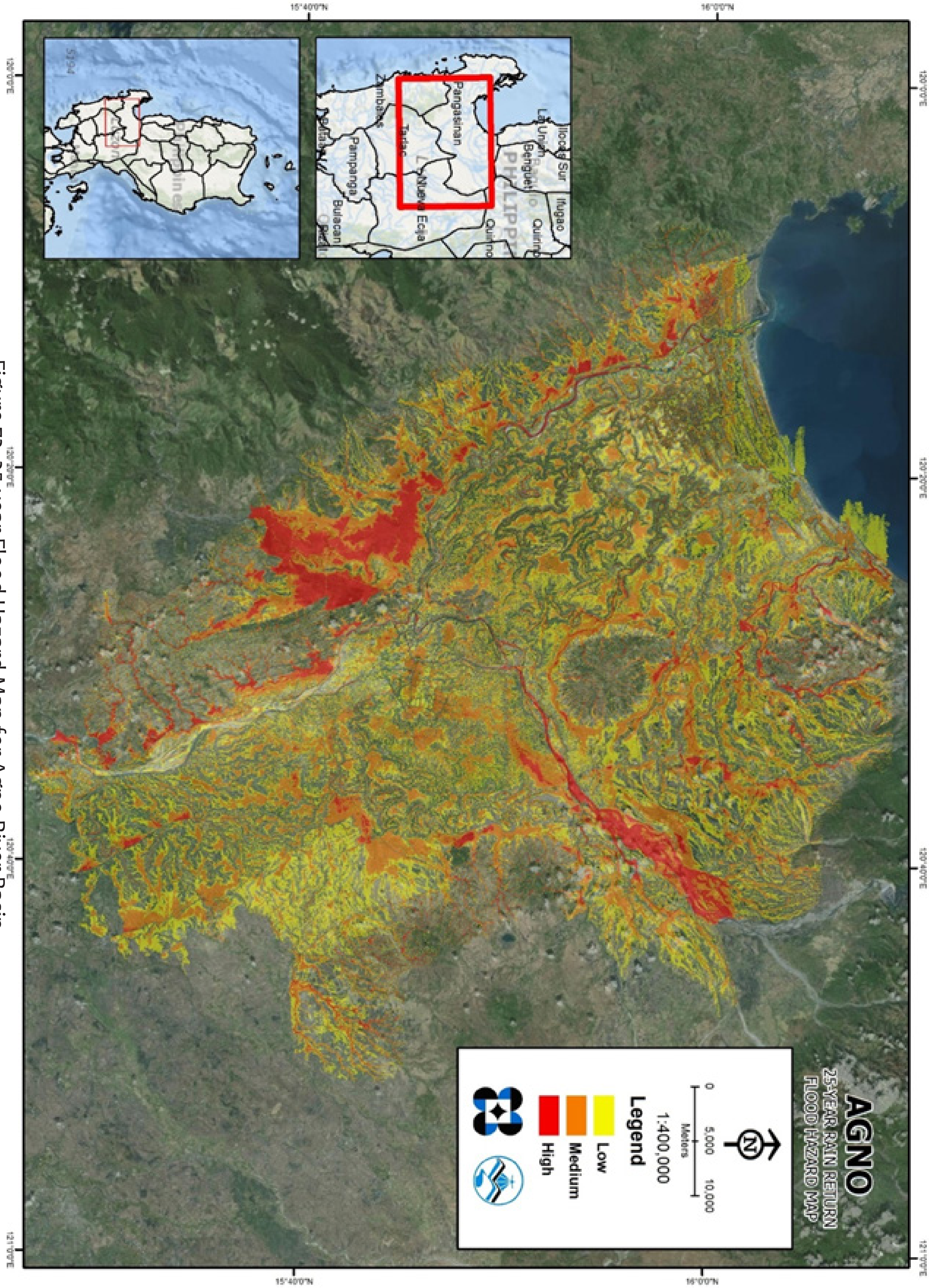

Figure 72. 25-year Flood Hazard Map for Agno River Basin

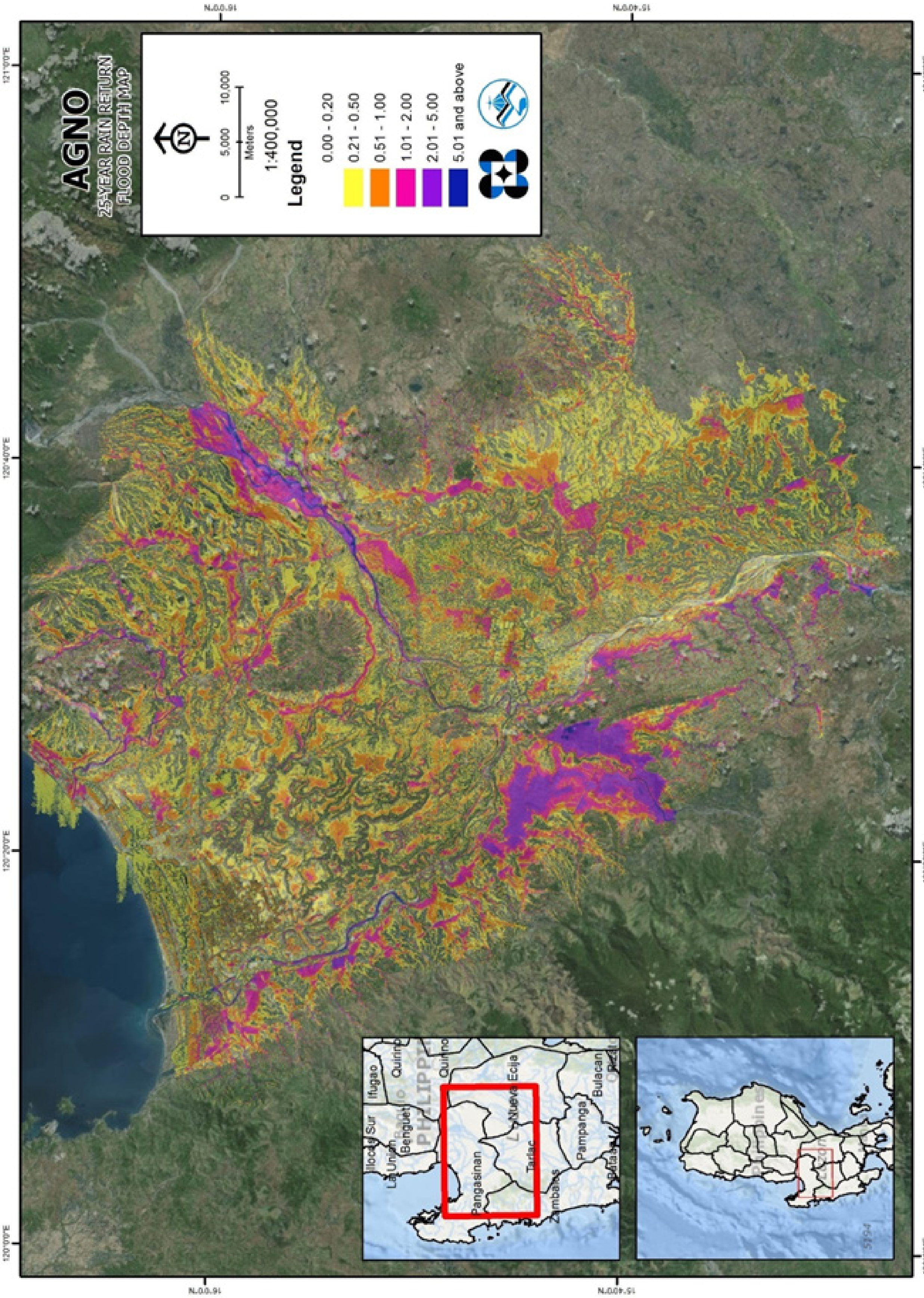

Figure 73. 25-year Flow Depth Map for Agno River Basin

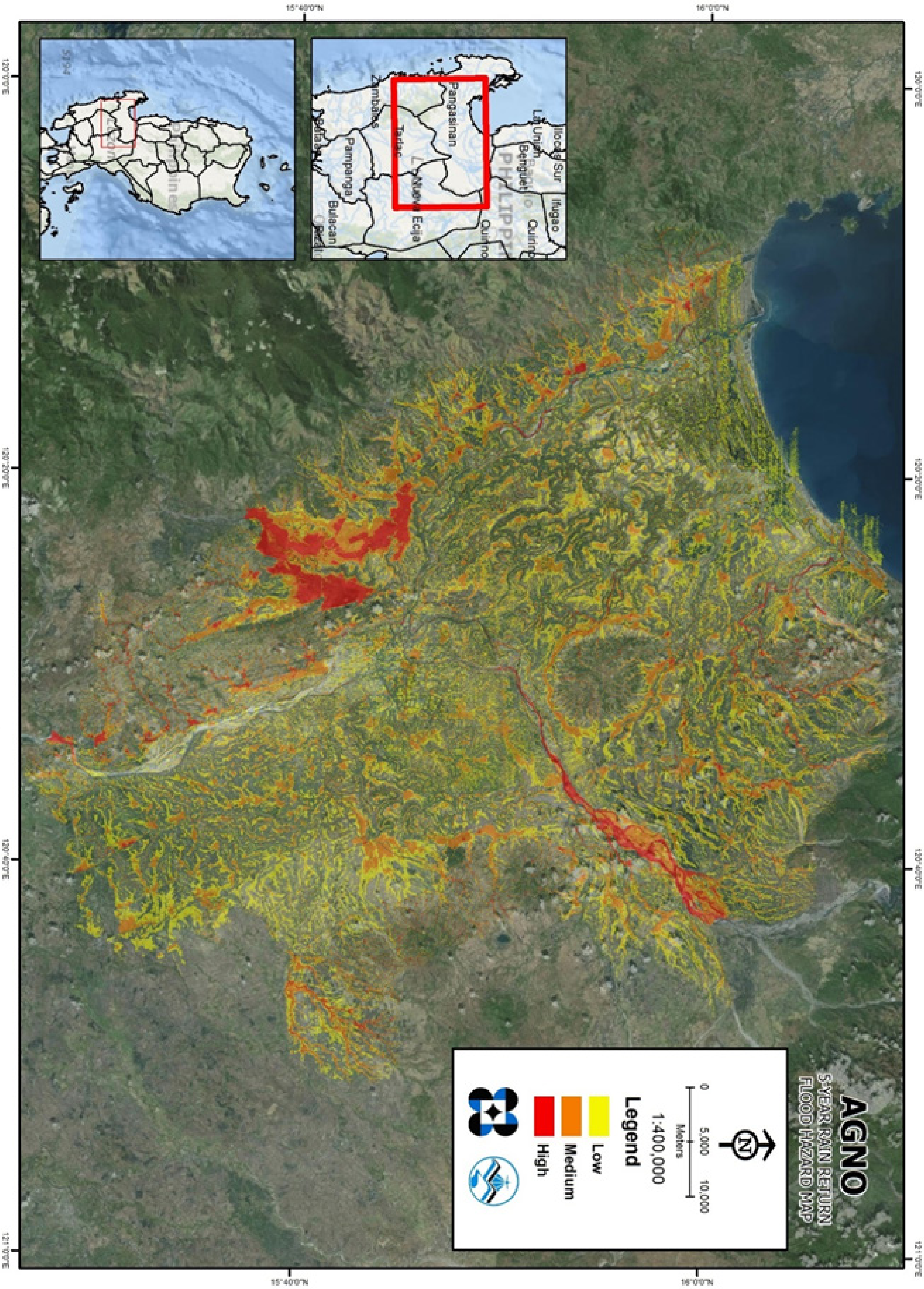

Figure 74. 5-year Flood Hazard Map for Agno River Basin

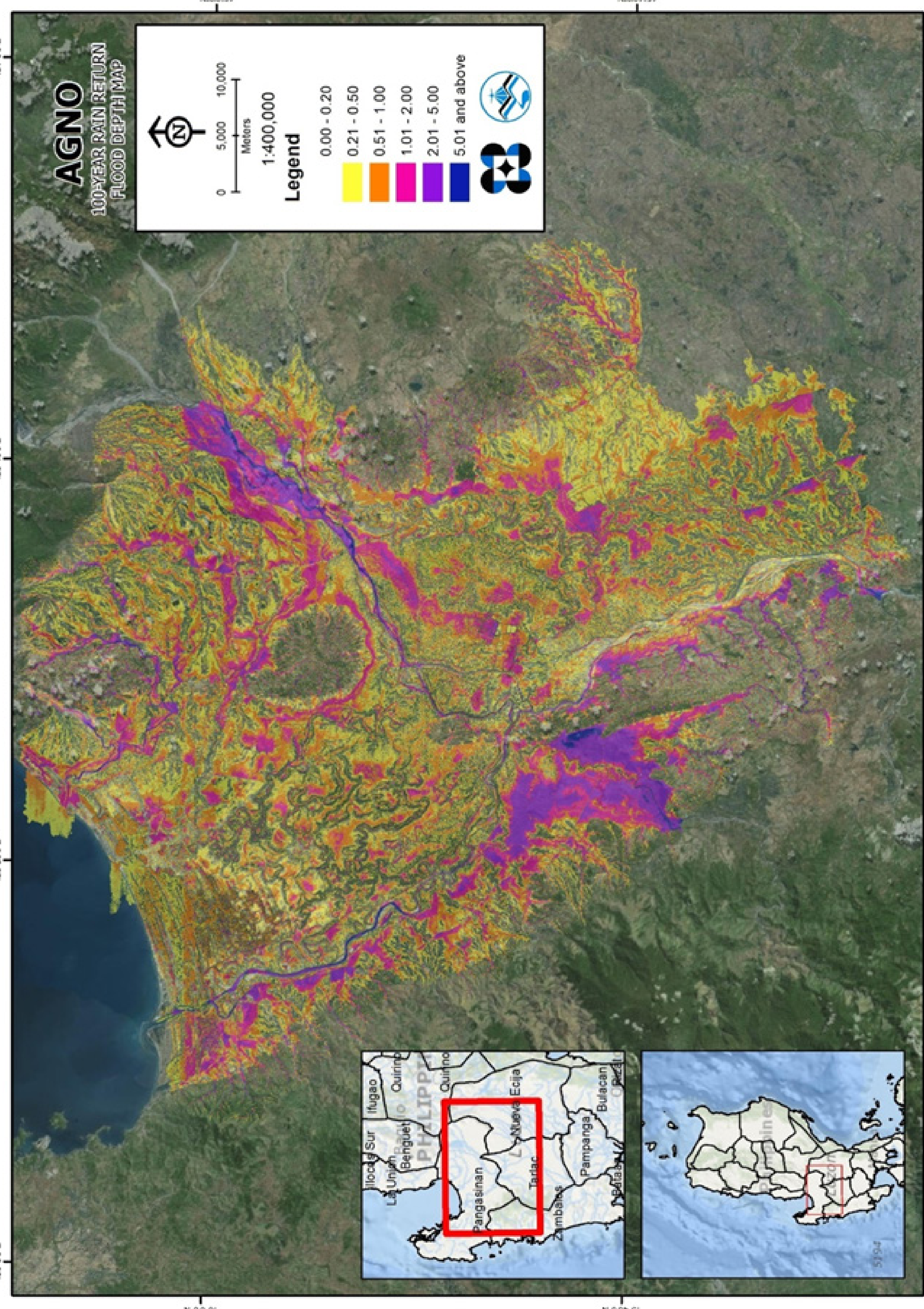

Figure 75. 5-year Flood Hazard Map for Agno River Basin

Bibliography

- Aquaveo. (2012). Watershed Modeling - HEC HMS Interface. Aquaveo.

- Feldman, A. D. (2000). Hydrologic Modeling System HEC-HMS Technical Reference Manual. Davis, CA: US Army Corps of Engineers - Hydrologic Engineering Center.

- FLO-2D Software, I. Flo-2D Reference Manual. FLO-2D Software, Inc.

- Kundell, J. (Ed.). (2008, April 3). Water profile of Philippines. Retrieved August 12, 2015, from http://www.eoearth.org/view/article/156982/#River_Basins_and_Water_Resources

- Merwade, V. (2012). Terrain Processing and HMS- Model Development using GeoHMS. Lafayette, Indiana.

- Santillan, J. (2011). Profile and Cross Section Surveys, Inflow measurement and flood modeling of Surigao River, Surigao City for Flood Hazard Assessment Purposes. Quezon City: Training Center for Applied Geodesy and Photogrammetry (TCAGP).

- Scharffenberg, W. A., & Fleming, M. J. (2010). Hydrologic Modeling System HEC-HMS User's Manual. Davis, California: U.S Army Corps of Engineers - Hydrologic Engineering Center

- Petr, T. (Ed.). (1985). Inland Fisheries in Multiple-purpose River Basin Planning and Development in Tropical Asian Countries: Three Case Studies. Retrieved August 12, 2015, from https://books.google.com.ph/books?id=ToA-XoHSUB4C&pg=PA20&dq=popon-to swamp&hl=en&sa=X&ei=JBVlUqaxFfGUiQfPpYHoCQ#v=onepage&q=poponto swamp&f=fa

- The Agno River Basin. (2009, October 23). Retrieved August 12, 2015, from http://www.abs-cbnnews.com/research/10/23/09/agno-river-basin

Appendix

Appendix A. Hector Mendoza Model Basin Parameters

Basin Number	SCS Curve Number Loss			Clark Unit Hydrograph Transform		Recession Baseflow				
	Initial Abstraction (mm)	Curve Number	Impervious (%)	Time of Concentration (HR)	Storage Coefficient (HR)	Initial Type	Initial Discharge (M3/S)	Recession Constant	Threshold Type	Ratio to Peak
10B	0.1366	92.4	0	0.365	7.722	1.7246	0.9702	0	Ratio to Peak	0.01
11B	0.1277	93.804	0	0.455	9.633	1.0104	0.993	0	Ratio to Peak	0.01
12B	0.1366	92.4	0	0.645	13.676	3.605	0.66	0	Ratio to Peak	0.01
13B	0.1366	92.4	0	0.175	3.7505	0.3989	0.99	0	Ratio to Peak	0.01
14B	0.1366	92.4	0	0.49	10.413	2.3846	0.66	0	Ratio to Peak	0.01
15B	0.1366	92.4	0	0.86	18.2	5.7908	0.9702	0	Ratio to Peak	0.01
16B	0.2138	91.476	0	2.24	47.548	24.328	0.9702	0	Ratio to Peak	0.01
17B	0.1617	97.104	0	0.69	14.599	3.7145	0.9702	0	Ratio to Peak	0.01
18B	0.1366	92.4	0	0.44	9.373	1.3216	0.9702	0	Ratio to Peak	0.01
19B	0.0879	93.144	0	0.715	15.191	2.6879	0.9702	0	Ratio to Peak	0.01
1B	0.1366	92.4	0	0.48	10.212	2.3208	0.9702	0	Ratio to Peak	0.01

Basin Number	SCS Curve Number Loss			Clark Unit Hydrograph Transform		Recession Baseflow				
	Initial Abstraction (mm)	Curve Number	Impervious (%)	Time of Concentration (HR)	Storage Coefficient (HR)	Initial Type	Initial Discharge (M3/S)	Recession Constant	Threshold Type	Ratio to Peak
20B	0.2136	92.4	0	0.495	10.485	3.4702	0.66	0	Ratio to Peak	0.01
21B	0.2456	81.792	0	1.69	35.809	1.6348	0.9702	0	Ratio to Peak	0.01
22B	0.1345	92.4	0	1.34	28.412	1.1348	0.9702	0	Ratio to Peak	0.01
23B	0.1002	98.424	0	1.155	24.466	3.7135	0.9702	0	Ratio to Peak	0.01
24B	0.0787	95.364	0	1.98	42.036	1.1148	0.66	0	Ratio to Peak	0.01
25B	0.1167	95.592	0	0.74	15.672	2.2166	0.9702	0	Ratio to Peak	0.01
26B	0.0853	99	0	1.855	39.306	0.9171	0.66	0	Ratio to Peak	0.01
27B	0.1165	95.628	0	0.65	13.806	2.9688	0.66	0	Ratio to Peak	0.01
28B	0.0658	98.7	0	0.775	16.413	0.3357	0.9702	0	Ratio to Peak	0.01
29B	0.1366	92.4	0	0.815	17.251	6.0543	0.9702	0	Ratio to Peak	0.01
2B	0.0871	92.4	0	0.515	10.946	1.8855	0.66	0	Ratio to Peak	0.01

Basin Number	SCS Curve Number Loss			Clark Unit Hydrograph Transform		Recession Baseflow				
	Initial Abstraction (mm)	Curve Number	Impervious (%)	Time of Concentration (HR)	Storage Coefficient (HR)	Initial Type	Initial Discharge (M3/S)	Recession Constant	Threshold Type	Ratio to Peak
30B	0.0871	92.4	0	0.345	7.28	2.6935	0.9702	0	Ratio to Peak	0.01
31B	0.1013	99	0	2.01	42.621	1.8653	0.9702	0	Ratio to Peak	0.01
32B	0.1502	99	0	1.67	35.386	1.9006	0.9702	0	Ratio to Peak	0.01
33B	0.0829	98.244	0	2.535	53.807	1.8388	0.9702	0	Ratio to Peak	0.01
34B	0.0581	93.336	0	3.365	71.37	3.2705	0.66	0	Ratio to Peak	0.01
35B	0.0871	99	0	2.055	43.583	1.8016	0.66	0	Ratio to Peak	0.01
36B	0.0924	99	0	2.51	53.242	1.7744	0.9702	0	Ratio to Peak	0.01
37B	0.114	99	0	1.46	30.947	0.569	0.9702	0	Ratio to Peak	0.01
38B	0.1364	99	0	1.27	26.949	1.3807	0.66	0	Ratio to Peak	0.01
39B	0.1184	96.048	0	0.88	18.675	5.8728	0.9702	0	Ratio to Peak	0.01
3B	0.1234	92.4	0	0.48	10.147	2.2449	0.9702	0	Ratio to Peak	0.01

Basin Number	SCS Curve Number Loss			Clark Unit Hydrograph Transform		Recession Baseflow				
	Initial Abstraction (mm)	Curve Number	Impervious (%)	Time of Concentration (HR)	Storage Coefficient (HR)	Initial Type	Initial Discharge (M3/S)	Recession Constant	Threshold Type	Ratio to Peak
40B	0.1817	95.316	0	0.38	8.099	1.6777	0.9702	0	Ratio to Peak	0.01
41B	0.0871	94.5	0	0.535	11.382	2.1174	0.9702	0	Ratio to Peak	0.01
42B	0.091	85.872	0	1.265	26.832	0.816	0.9702	0	Ratio to Peak	0.01
43B	0.0867	99	0	2.21	46.93	2.017	0.66	0	Ratio to Peak	0.01
44B	0.117	92.4	0	0.61	12.909	3.4784	0.9702	0	Ratio to Peak	0.01
45B	0.0871	99	0	1.57	33.345	0.6905	0.9702	0	Ratio to Peak	0.01
46B	0.058	95.556	0	2.525	53.521	1.9576	0.66	0	Ratio to Peak	0.01
47B	0.0486	99	0	1.15	24.421	0.278	0.9702	0	Ratio to Peak	0.01
48B	0.1338	99	0	3.99	84.578	7.7591	0.9702	0	Ratio to Peak	0.01
49B	0.0581	99	0	2.335	49.485	1.0008	0.9702	0	Ratio to Peak	0.01
4B	0.1247	92.4	0	0.345	7.28	1.3341	0.9702	0	Ratio to Peak	0.01

Basin Number	SCS Curve Number Loss			Clark Unit Hydrograph Transform		Recession Baseflow				
	Initial Abstraction (mm)	Curve Number	Impervious (%)	Time of Concentration (HR)	Storage Coefficient (HR)	Initial Type	Initial Discharge (M3/S)	Recession Constant	Threshold Type	Ratio to Peak
50B	0.1366	99	0	1.88	39.917	1.9897	0.66	0	Ratio to Peak	0.01
51B	0.0871	94.176	0	1.03	21.84	2.403	0.66	0	Ratio to Peak	0.01
52B	0.1105	92.4	0	0.75	15.919	5.985	0.66	0	Ratio to Peak	0.01
53B	0.0829	99	0	3.325	70.493	2.9481	0.9702	0	Ratio to Peak	0.01
54B	0.0615	96.648	0	3.18	67.444	4.5928	0.66	0	Ratio to Peak	0.01
55B	0.0871	99	0	2.95	62.608	3.695	0.9702	0	Ratio to Peak	0.01
56B	0.0581	99	0	4.195	88.959	2.6735	0.99	0	Ratio to Peak	0.01
57B	0.0871	99	0	2.85	60.444	1.5375	0.99	0	Ratio to Peak	0.01
58B	0.1366	99	0	1.975	41.899	0.7075	0.99	0	Ratio to Peak	0.01
59B	0.0987	99	0	2.435	51.61	1.7028	0.99	0	Ratio to Peak	0.01
5B	0.0871	92.4	0	0.645	13.689	4.4304	0.99	0	Ratio to Peak	0.01

Basin Number	SCS Curve Number Loss			Clark Unit Hydrograph Transform		Recession Baseflow				
	Initial Abstraction (mm)	Curve Number	Impervious (%)	Time of Concentration (HR)	Storage Coefficient (HR)	Initial Type	Initial Discharge (M3/S)	Recession Constant	Threshold Type	Ratio to Peak
60B	0.0871	98.688	0	5.55	117.77	76.163	0.99	0	Ratio to Peak	0.01
61B	0.0871	99	0	3.28	69.57	2.613	0.99	0	Ratio to Peak	0.01
62B	0.1241	99	0	1.935	41.087	0.7008	0.99	0	Ratio to Peak	0.01
63B	0.1562	99	0	2.345	49.777	1.2478	0.99	0	Ratio to Peak	0.01
64B	0.0975	94.38	0	0.465	9.8475	1.5233	0.99	0	Ratio to Peak	0.01
65B	0.0871	89.448	0	1.37	29.094	7.8113	0.99	0	Ratio to Peak	0.01
66B	0.0871	98.916	0	4.78	101.39	4.3985	0.99	0	Ratio to Peak	0.01
67B	0.0871	99	0	3.125	66.268	2.4275	0.99	0	Ratio to Peak	0.01
68B	0.0871	99	0	1.615	34.294	1.1517	0.99	0	Ratio to Peak	0.01
69B	0.0871	99	0	1.11	23.491	0.7262	0.99	0	Ratio to Peak	0.01
6B	0.091	92.4	0	0.53	11.271	2.8338	0.99	0	Ratio to Peak	0.01

Basin Number	SCS Curve Number Loss			Clark Unit Hydrograph Transform		Recession Baseflow				
	Initial Abstraction (mm)	Curve Number	Impervious (%)	Time of Concentration (HR)	Storage Coefficient (HR)	Initial Type	Initial Discharge (M3/S)	Recession Constant	Threshold Type	Ratio to Peak
70B	0.0871	99	0	2.02	42.874	0.744	0.99	0	Ratio to Peak	0.01
71B	0.0844	99	0	1.62	34.32	0.9589	0.99	0	Ratio to Peak	0.01
72B	0.0871	99	0	2.27	48.152	3.4936	0.99	0	Ratio to Peak	0.01
73B	0.0871	99	0	1.94	41.178	1.4779	0.99	0	Ratio to Peak	0.01
74B	0.0832	99	0	2.485	52.754	1.5701	0.99	0	Ratio to Peak	0.01
75B	0.0775	99	0	2.905	61.588	6.802	0.99	0	Ratio to Peak	0.01
76B	0.0767	99	0	2.245	47.639	1.7552	0.99	0	Ratio to Peak	0.01
77B	0.0792	99	0	3.295	69.849	1.9708	0.99	0	Ratio to Peak	0.01
78B	0.0871	99	0	0.97	20.534	0.464	0.99	0	Ratio to Peak	0.01
79B	0.0823	99	0	1.08	22.913	0.9311	0.99	0	Ratio to Peak	0.01
7B	0.0914	92.4	0	0.375	8.0015	2.9282	0.99	0	Ratio to Peak	0.01

Basin Number	SCS Curve Number Loss			Clark Unit Hydrograph Transform		Recession Baseflow				
	Initial Abstraction (mm)	Curve Number	Impervious (%)	Time of Concentration (HR)	Storage Coefficient (HR)	Initial Type	Initial Discharge (M3/S)	Recession Constant	Threshold Type	Ratio to Peak
80B	0.0813	99	0	2.51	53.216	1.8552	0.99	0	Ratio to Peak	0.01
81B	0.1616	99	0	2.315	49.153	3.921	0.99	0	Ratio to Peak	0.01
82B	0.0871	99	0	2.645	56.154	1.736	0.99	0	Ratio to Peak	0.01
83B	0.1366	99	0	6.985	148.12	5.109	0.99	0	Ratio to Peak	0.01
84B	0.1366	99	0	1.075	22.848	0.8273	0.99	0	Ratio to Peak	0.01
85B	0.1616	88.668	0	1.765	37.388	0.8112	0.99	0	Ratio to Peak	0.01
86B	0.0871	99	0	1.335	28.282	0.5357	0.99	0	Ratio to Peak	0.01
87B	0.1366	99	0	1.615	34.203	0.8174	0.99	0	Ratio to Peak	0.01
88B	0.1366	99	0	2.55	54.074	1.0012	0.99	0	Ratio to Peak	0.01
89B	0.1366	99	0	1.57	33.28	1.1301	0.99	0	Ratio to Peak	0.01
8B	0.1366	92.4	0	0.9	19.13	5.9157	0.99	0	Ratio to Peak	0.01

Basin Number	SCS Curve Number Loss			Clark Unit Hydrograph Transform		Recession Baseflow				
	Initial Abstraction (mm)	Curve Number	Impervious (%)	Time of Concentration (HR)	Storage Coefficient (HR)	Initial Type	Initial Discharge (M3/S)	Recession Constant	Threshold Type	Ratio to Peak
90B	0.1366	99	0	1.73	36.693	0.757	0.99	0	Ratio to Peak	0.01
9B	0.1366	92.4	0	0.305	6.461	1.4538	0.99	0	Ratio to Peak	0.01

Appendix B. Hector Mendoza Model Reach Parameters

Reach Number	Muskingum Cunge Channel Routing						
	Time Step Method	Length (m)	Slope	Manning's n	Shape	Width	Side Slope
100R	Automatic Fixed Interval	20695	0.0373	0.0036	Trapezoid	30	45
101R	Automatic Fixed Interval	3152.4	0.0366	0.0036	Trapezoid	30	45
102R	Automatic Fixed Interval	27209	0.0063	0.0054	Trapezoid	30	45
103R	Automatic Fixed Interval	14273	0.007	0.0036	Trapezoid	30	45
104R	Automatic Fixed Interval	21158	0.0685	0.0036	Trapezoid	30	45
105R	Automatic Fixed Interval	3754.9	0.0173	0.0036	Trapezoid	30	45
106R	Automatic Fixed Interval	6667.4	0.006	0.0035	Trapezoid	30	45
107R	Automatic Fixed Interval	11210	0.0044	0.0035	Trapezoid	30	45
108R	Automatic Fixed Interval	9648.1	0.0115	0.0036	Trapezoid	30	45
109R	Automatic Fixed Interval	34749	0.0045	0.0035	Trapezoid	30	45
110R	Automatic Fixed Interval	23128	0.0561	0.0036	Trapezoid	30	45
111R	Automatic Fixed Interval	13138	0.0004	0.0037	Trapezoid	30	45
112R	Automatic Fixed Interval	4312.5	0.0032	0.0054	Trapezoid	30	45
113R	Automatic Fixed Interval	3950.3	0.0016	0.0054	Trapezoid	30	45
114R	Automatic Fixed Interval	4026.8	0.0037	0.0036	Trapezoid	30	45
115R	Automatic Fixed Interval	43840	0.0032	0.0036	Trapezoid	30	45
116R	Automatic Fixed Interval	2650.2	0.0089	0.0036	Trapezoid	30	45
117R	Automatic Fixed Interval	43813	0.0036	0.0035	Trapezoid	30	45
118R	Automatic Fixed Interval	6042.6	0.0031	0.0036	Trapezoid	30	45
119R	Automatic Fixed Interval	22514	0.0134	0.0036	Trapezoid	30	45
120R	Automatic Fixed Interval	6410.1	0.0731	0.0036	Trapezoid	30	45
121R	Automatic Fixed Interval	16271	0.0027	0.0036	Trapezoid	30	45
122R	Automatic Fixed Interval	12484	0.0035	0.0036	Trapezoid	30	45
123R	Automatic Fixed Interval	3040.9	0.0011	0.0054	Trapezoid	30	45
124R	Automatic Fixed Interval	7120.3	0.0025	0.0036	Trapezoid	30	45
125R	Automatic Fixed Interval	2473.9	0.0006	0.0032	Trapezoid	30	45
126R	Automatic Fixed Interval	7396.3	0.0027	0.0036	Trapezoid	30	45
127R	Automatic Fixed Interval	17615	0.0033	0.0036	Trapezoid	30	45
128R	Automatic Fixed Interval	31544	0.0023	0.0054	Trapezoid	30	45
129R	Automatic Fixed Interval	9229.6	0.0028	0.0036	Trapezoid	30	45
130R	Automatic Fixed Interval	12612	0.0038	0.0036	Trapezoid	30	45
131R	Automatic Fixed Interval	14038	0.0061	0.0036	Trapezoid	30	45
132R	Automatic Fixed Interval	8202	0.0013	0.0024	Trapezoid	30	45
133R	Automatic Fixed Interval	1411.4	0.0029	0.0036	Trapezoid	30	45
134R	Automatic Fixed Interval	20122	0.0639	0.0036	Trapezoid	30	45

Appendix

Reach Number	Muskingum Cunge Channel Routing						
	Time Step Method	Length (m)	Slope	Manning's n	Shape	Width	Side Slope
135R	Automatic Fixed Interval	38309	0.0019	0.0054	Trapezoid	30	45
136R	Automatic Fixed Interval	1481	0.0005	0.0024	Trapezoid	30	45
137R	Automatic Fixed Interval	1139.2	0.0009	0.0032	Trapezoid	30	45
138R	Automatic Fixed Interval	4790.2	0.0048	0.0036	Trapezoid	30	45
139R	Automatic Fixed Interval	21302	0.0019	0.0024	Trapezoid	30	45
140R	Automatic Fixed Interval	17424	0.0021	0.0036	Trapezoid	30	45
141R	Automatic Fixed Interval	33928	0.0041	0.0054	Trapezoid	30	45
142R	Automatic Fixed Interval	90642	0.0065	0.0036	Trapezoid	30	45
143R	Automatic Fixed Interval	8376.2	0.0022	0.0036	Trapezoid	30	45
144R	Automatic Fixed Interval	4088.3	0.0014	0.0024	Trapezoid	30	45
145R	Automatic Fixed Interval	20885	0.0012	0.0036	Trapezoid	30	45
146R	Automatic Fixed Interval	17687	0.0018	0.0024	Trapezoid	30	45
147R	Automatic Fixed Interval	16380	0.0008	0.0035	Trapezoid	30	45
148R	Automatic Fixed Interval	5226.1	0.0008	0.0036	Trapezoid	30	45
149R	Automatic Fixed Interval	4709.7	0.001	0.0035	Trapezoid	30	45
150R	Automatic Fixed Interval	8026.9	0.0011	0.0036	Trapezoid	30	45
151R	Automatic Fixed Interval	10769	0.0021	0.0036	Trapezoid	30	45
152R	Automatic Fixed Interval	6080.7	0.0008	0.0036	Trapezoid	30	45
153R	Automatic Fixed Interval	1337.3	0.0014	0.0036	Trapezoid	30	45
154R	Automatic Fixed Interval	80489	0.0043	0.0036	Trapezoid	30	45
155R	Automatic Fixed Interval	99422	0.0053	0.0036	Trapezoid	30	45
156R	Automatic Fixed Interval	16426	0.0011	0.0036	Trapezoid	30	45
157R	Automatic Fixed Interval	4101.1	0.0106	0.0036	Trapezoid	30	45
158R	Automatic Fixed Interval	15745	0.0028	0.0036	Trapezoid	30	45
159R	Automatic Fixed Interval	1448.8	0.0273	0.0036	Trapezoid	30	45
160R	Automatic Fixed Interval	7520.7	0.0007	0.0036	Trapezoid	30	45
161R	Automatic Fixed Interval	11075	0.0009	0.0036	Trapezoid	30	45
162R	Automatic Fixed Interval	14008	0.0005	0.0036	Trapezoid	30	45
163R	Automatic Fixed Interval	1535	0.0029	0.0036	Trapezoid	30	45
164R	Automatic Fixed Interval	12479	0.0004	0.0036	Trapezoid	30	45
165R	Automatic Fixed Interval	22246	0.001	0.0036	Trapezoid	30	45
166R	Automatic Fixed Interval	2872.6	0.0015	0.0036	Trapezoid	30	45
167R	Automatic Fixed Interval	6444.7	0.0038	0.0036	Trapezoid	30	45
168R	Automatic Fixed Interval	8766.2	0.0004	0.0036	Trapezoid	30	45
169R	Automatic Fixed Interval	44864	0.0005	0.0036	Trapezoid	30	45
170R	Automatic Fixed Interval	3961.7	0.0074	0.0036	Trapezoid	30	45
171R	Automatic Fixed Interval	1299.3	0.0065	0.0036	Trapezoid	30	45
172R	Automatic Fixed Interval	38912	0.0007	0.0036	Trapezoid	30	45

Appendix

Reach Number	Muskingum Cunge Channel Routing						
	Time Step Method	Length (m)	Slope	Manning's n	Shape	Width	Side Slope
173R	Automatic Fixed Interval	4832.8	0.0005	0.0036	Trapezoid	30	45
174R	Automatic Fixed Interval	10028	0.0036	0.0036	Trapezoid	30	45
175R	Automatic Fixed Interval	2899.4	0.0071	0.0036	Trapezoid	30	45
177R	Automatic Fixed Interval	9268	0.0006	0.0036	Trapezoid	30	45
178R	Automatic Fixed Interval	5198.9	0.0012	0.0036	Trapezoid	30	45
179R	Automatic Fixed Interval	3254.5	0.0028	0.0036	Trapezoid	30	45
92R	Automatic Fixed Interval	4411.6	0.0094	0.0036	Trapezoid	30	45
93R	Automatic Fixed Interval	18221	0.0555	0.0036	Trapezoid	30	45
94R	Automatic Fixed Interval	14267	0.0099	0.0036	Trapezoid	30	45
95R	Automatic Fixed Interval	9482.5	0.0695	0.0036	Trapezoid	30	45
96R	Automatic Fixed Interval	9329.6	0.0123	0.0036	Trapezoid	30	45
97R	Automatic Fixed Interval	11035	0.0472	0.0036	Trapezoid	30	45
98R	Automatic Fixed Interval	5391.6	0.0695	0.0036	Trapezoid	30	45
99R	Automatic Fixed Interval	8449.6	0.002	0.0036	Trapezoid	30	45

Appendix C. Banela Model Basin Parameters

Basin Number	SCS Curve Number Loss			Clark Unit Hydrograph Transform		Recession Baseflow				
	Initial Abstraction (mm)	Curve Number	Impervious (%)	Time of Concentration (HR)	Storage Coefficient (HR)	Initial Type	Initial Discharge (M3/S)	Recession Constant	Threshold Type	Ratio to Peak
10B	40	77.693	0	0.171	4.0326	9.1569	0.918	0	Ratio to Peak	0
11B	40	81.2245	0	0.5418	12.7673	3.3397	0.918	0	Ratio to Peak	0
12B	40	85.08897	0	0.3699	8.7243	2.2459	0.918	0	Ratio to Peak	0
13B	40	84.11024	0	0.2286	5.382	1.6723	0.918	0	Ratio to Peak	0
14B	40	77.1885	0	0.2421	5.7135	1.1884	0.918	0	Ratio to Peak	0
15B	40	86.2695	0	0.3933	9.269	1.5787	0.918	0	Ratio to Peak	0
16B	40	84.756	0	0.3438	8.1029	2.4193	0.918	0	Ratio to Peak	0
17B	40	85.29077	0	0.2673	6.2972	1.3508	0.918	0	Ratio to Peak	0
18B	40	84.756	0	0.2979	7.0317	1.1168	0.918	0	Ratio to Peak	0
19B	40	84.756	0	0.2916	6.8783	1.1077	0.918	0	Ratio to Peak	0
1B	40	77.693	0	0.0711	1.6809	3.762	0.918	0	Ratio to Peak	0

Basin Number	SCS Curve Number Loss			Clark Unit Hydrograph Transform		Recession Baseflow				
	Initial Abstraction (mm)	Curve Number	Impervious (%)	Time of Concentration (HR)	Storage Coefficient (HR)	Initial Type	Initial Discharge (M3/S)	Recession Constant	Threshold Type	Ratio to Peak
20B	40	84.756	0	0.3186	7.501	1.6444	0.918	0	Ratio to Peak	0
21B	40	84.756	0	0.1953	4.5994	0.70625	0.918	0	Ratio to Peak	0
22B	40	83.68646	0	0.3663	8.6411	2.7549	0.918	0	Ratio to Peak	0
23B	40	84.756	0	0.2583	6.0892	1.9474	0.918	0	Ratio to Peak	0
24B	40	84.756	0	0.1008	2.3751	0.81376	0.918	0	Ratio to Peak	0
25B	40	81.99134	0	0.1242	2.9211	1.75	0.918	0	Ratio to Peak	0
26B	40	78.702	0	0.2367	5.5679	1.1785	0.918	0	Ratio to Peak	0
27B	40	80.12469	0	0.1323	3.1226	2.4766	0.918	0	Ratio to Peak	0
28B	40	81.2245	0	0.1143	2.6975	2.0157	0.918	0	Ratio to Peak	0
29B	40	83.39385	0	0.0846	1.9851	1.8841	0.918	0	Ratio to Peak	0
2B	40	77.84435	0	0.9144	21.5553	107.9675	0.918	0	Ratio to Peak	0

Basin Number	SCS Curve Number Loss			Clark Unit Hydrograph Transform		Recession Baseflow				
	Initial Abstraction (mm)	Curve Number	Impervious (%)	Time of Concentration (HR)	Storage Coefficient (HR)	Initial Type	Initial Discharge (M3/S)	Recession Constant	Threshold Type	Ratio to Peak
30B	40	79.83208	0	0.0999	2.3478	2.5864	0.918	0	Ratio to Peak	0
31B	40	78.702	0	0.0882	2.0722	1.6309	0.918	0	Ratio to Peak	0
32B	40	80.66955	0	0.0945	2.2178	1.4121	0.918	0	Ratio to Peak	0
33B	40	79.01479	0	0.054	1.2805	1.2653	0.918	0	Ratio to Peak	0
34B	40	77.693	0	0.1926	4.5435	11.41	0.918	0	Ratio to Peak	0
35B	40	77.693	0	0.0522	1.2389	1.219	0.918	0	Ratio to Peak	0
36B	40	77.693	0	0.0639	1.5106	3.4207	0.918	0	Ratio to Peak	0
37B	40	77.693	0	0.081	1.9045	4.2207	0.918	0	Ratio to Peak	0
38B	40	84.53402	0	0.5391	12.7023	5.5439	0.918	0	Ratio to Peak	0
39B	40	83.29295	0	1.0593	24.9639	11.128	0.918	0	Ratio to Peak	0
3B	40	77.693	0	0.0945	2.2269	3.1346	0.918	0	Ratio to Peak	0

Basin Number	SCS Curve Number Loss			Clark Unit Hydrograph Transform		Recession Baseflow				
	Initial Abstraction (mm)	Curve Number	Impervious (%)	Time of Concentration (HR)	Storage Coefficient (HR)	Initial Type	Initial Discharge (M3/S)	Recession Constant	Threshold Type	Ratio to Peak
40B	40	84.756	0	0.7119	16.77	4.8506	0.918	0	Ratio to Peak	0
41B	40	84.756	0	0.405	9.5498	1.3344	0.918	0	Ratio to Peak	0
42B	40	84.756	0	0.531	12.5203	2.086	0.918	0	Ratio to Peak	0
43B	40	84.756	0	0.4635	10.9213	2.3396	0.918	0	Ratio to Peak	0
44B	40	83.79745	0	0.9792	23.0789	35.304	0.918	0	Ratio to Peak	0
45B	40	84.756	0	0.4779	11.2658	2.4098	0.918	0	Ratio to Peak	0
46B	40	84.756	0	0.3573	8.4292	1.252	0.918	0	Ratio to Peak	0
47B	40	84.756	0	0.4563	10.7601	4.5681	0.918	0	Ratio to Peak	0
48B	40	84.756	0	0.4545	10.7042	2.4732	0.918	0	Ratio to Peak	0
49B	40	84.756	0	0.6525	15.3829	4.1625	0.918	0	Ratio to Peak	0
4B	40	75.99788	0	2.3796	56.0872	471.4339	0.918	0	Ratio to Peak	0

Basin Number	SCS Curve Number Loss			Clark Unit Hydrograph Transform		Recession Baseflow				
	Initial Abstraction (mm)	Curve Number	Impervious (%)	Time of Concentration (HR)	Storage Coefficient (HR)	Initial Type	Initial Discharge (M3/S)	Recession Constant	Threshold Type	Ratio to Peak
50B	40	84.756	0	0.3816	9.0038	2.1129	0.918	0	Ratio to Peak	0
51B	40	84.756	0	0.5013	11.8131	3.0761	0.918	0	Ratio to Peak	0
52B	40	84.756	0	0.3636	8.567	2.6446	0.918	0	Ratio to Peak	0
53B	40	84.756	0	0.2601	6.1373	2.8174	0.918	0	Ratio to Peak	0
54B	40	84.756	0	0.6219	14.6562	3.9235	0.918	0	Ratio to Peak	0
55B	40	84.756	0	0.3582	8.4357	4.104	0.918	0	Ratio to Peak	0
56B	40	84.756	0	0.3573	8.4175	1.9707	0.918	0	Ratio to Peak	0
57B	40	85.07888	0	0.5193	12.2356	4.442	0.918	0	Ratio to Peak	0
58B	40	84.756	0	0.378	8.8998	2.615	0.918	0	Ratio to Peak	0
59B	40	81.8299	0	0.3249	7.6466	2.4154	0.918	0	Ratio to Peak	0
5B	40	82.68755	0	0.2538	5.9735	8.2132	0.918	0	Ratio to Peak	0

Basin Number	SCS Curve Number Loss			Clark Unit Hydrograph Transform		Recession Baseflow				
	Initial Abstraction (mm)	Curve Number	Impervious (%)	Time of Concentration (HR)	Storage Coefficient (HR)	Initial Type	Initial Discharge (M3/S)	Recession Constant	Threshold Type	Ratio to Peak
60B	40	82.86917	0	0.5157	12.1576	3.348	0.918	0	Ratio to Peak	0
61B	40	84.756	0	0.3384	7.9807	2.4177	0.918	0	Ratio to Peak	0
62B	40	84.756	0	0.3141	7.4074	2.1302	0.918	0	Ratio to Peak	0
63B	40	85.04861	0	0.3942	9.2833	2.6506	0.918	0	Ratio to Peak	0
64B	40	84.756	0	0.2601	6.1204	1.9021	0.918	0	Ratio to Peak	0
65B	40	84.756	0	0.2952	6.9615	1.3079	0.918	0	Ratio to Peak	0
66B	40	80.04397	0	0.2268	5.3482	1.5729	0.918	0	Ratio to Peak	0
67B	40	83.76718	0	0.4329	10.205	4.0189	0.918	0	Ratio to Peak	0
68B	40	84.2515	0	0.1422	3.3618	1.2157	0.918	0	Ratio to Peak	0
69B	40	72.50674	0	0.1917	4.511	2.8033	0.918	0	Ratio to Peak	0
6B	40	74.1615	0	0.4653	10.9642	2.3645	0.918	0	Ratio to Peak	0

Basin Number	SCS Curve Number Loss			Clark Unit Hydrograph Transform		Recession Baseflow				
	Initial Abstraction (mm)	Curve Number	Impervious (%)	Time of Concentration (HR)	Storage Coefficient (HR)	Initial Type	Initial Discharge (M3/S)	Recession Constant	Threshold Type	Ratio to Peak
70B	40	84.756	0	0.2583	6.0879	1.9071	0.918	0	Ratio to Peak	0
71B	40	79.2065	0	0.3132	7.3879	1.9136	0.918	0	Ratio to Peak	0
72B	40	84.4533	0	0.1611	3.8025	2.0662	0.918	0	Ratio to Peak	0
73B	40	84.756	0	0.2781	6.5624	2.5933	0.918	0	Ratio to Peak	0
74B	40	78.87353	0	0.1449	3.4151	2.337	0.918	0	Ratio to Peak	0
75B	40	84.756	0	0.2628	6.1854	2.211	0.918	0	Ratio to Peak	0
76B	5.2676	78.97443	0	0.0173016	0.934895	5.5787	0.9642978	0	Ratio to Peak	0
77B	40	79.17623	0	0.0792	1.8564	1.8545	0.918	0	Ratio to Peak	0
78B	40	77.693	0	0.117	2.7599	4.5491	0.918	0	Ratio to Peak	0
79B	40	77.693	0	0.0882	2.0813	2.4466	0.9363702	0	Ratio to Peak	0
7B	40	82.25368	0	0.6408	15.1034	4.4199	0.918	0	Ratio to Peak	0

Appendix

Basin Number	SCS Curve Number Loss			Clark Unit Hydrograph Transform		Recession Baseflow				
	Initial Abstraction (mm)	Curve Number	Impervious (%)	Time of Concentration (HR)	Storage Coefficient (HR)	Initial Type	Initial Discharge (M3/S)	Recession Constant	Threshold Type	Ratio to Peak
80B	40	77.693	0	0.1125	2.6468	6.113	0.918	0	Ratio to Peak	0
81B	40	76.03824	0	0.099	2.3244	3.858	0.9363192	0	Ratio to Peak	0
82B	40	77.693	0	0.0495	1.1661	1.4626	0.918	0	Ratio to Peak	0
83B	40	77.693	0	0.0369	0.8775	0.62087	0.91341	0	Ratio to Peak	0
84B	40	77.693	0	0.0828	1.9435	2.6745	0.91341	0	Ratio to Peak	0
85B	40	84.756	0	0.2223	5.2312	1.6517	0.918	0	Ratio to Peak	0
86B	40	84.756	0	0.3546	8.3668	3.8783	0.918	0	Ratio to Peak	0
87B	40	85.08897	0	0.4122	9.7214	2.1196	0.918	0	Ratio to Peak	0
88B	40	84.756	0	0.4392	10.3467	4.9392	0.918	0	Ratio to Peak	0
89B	40	85.04861	0	0.423	9.971	2.4823	0.918	0	Ratio to Peak	0
8B	40	78.07642	0	0.1566	3.6985	4.569	0.918	0	Ratio to Peak	0

Basin Number	SCS Curve Number Loss			Clark Unit Hydrograph Transform		Recession Baseflow				
	Initial Abstraction (mm)	Curve Number	Impervious (%)	Time of Concentration (HR)	Storage Coefficient (HR)	Initial Type	Initial Discharge (M3/S)	Recession Constant	Threshold Type	Ratio to Peak
90B	40	85.9668	0	0.2826	6.6664		0.918	0	Ratio to Peak	0
9B	40	77.693	0	0.0864	2.0371			0	Ratio to Peak	0

Appendix D. Banela Model Reach Parameters

Reach Number	Muskingum Cunge Channel Routing						
	Time Step Method	Length (m)	Slope	Manning's n	Shape	Width	Side Slope
100R	Automatic Fixed Interval	37935.697	0.00443	0.5	Trapezoid	30	45
101R	Automatic Fixed Interval	8066.869	0.01244	0.5	Trapezoid	30	45
102R	Automatic Fixed Interval	4381.072	0.01572	0.5	Trapezoid	30	45
103R	Automatic Fixed Interval	7448.896	0.00121	0.5	Trapezoid	30	45
104R	Automatic Fixed Interval	22031.254	0.00364	0.5	Trapezoid	30	45
105R	Automatic Fixed Interval	13898.271	0.00324	0.5	Trapezoid	30	45
106R	Automatic Fixed Interval	15999.295	0.00125	0.5	Trapezoid	30	45
107R	Automatic Fixed Interval	6362.932	0.00432	0.5	Trapezoid	30	45
108R	Automatic Fixed Interval	4854.057	0.00524	0.5	Trapezoid	30	45
109R	Automatic Fixed Interval	12410.047	0.00286	0.5	Trapezoid	30	45
110R	Automatic Fixed Interval	6147.173	0.00239	0.5	Trapezoid	30	45
111R	Automatic Fixed Interval	2961.438	0.00125	0.5	Trapezoid	30	45
112R	Automatic Fixed Interval	4935.022	0.00044	0.5	Trapezoid	30	45
113R	Automatic Fixed Interval	5311.072	0.00275	0.5	Trapezoid	30	45
114R	Automatic Fixed Interval	10067.16	0.00264	0.5	Trapezoid	30	45
115R	Automatic Fixed Interval	2300.442	0.00239	0.5	Trapezoid	30	45
116R	Automatic Fixed Interval	6984.245	0.00654	0.5	Trapezoid	30	45
117R	Automatic Fixed Interval	10561.647	0.00269	0.5	Trapezoid	30	45
118R	Automatic Fixed Interval	2456.408	0.00383	0.5	Trapezoid	30	45
119R	Automatic Fixed Interval	5032.031	0.00378	0.5	Trapezoid	30	45
120R	Automatic Fixed Interval	5324.622	0.00839	0.5	Trapezoid	30	45
121R	Automatic Fixed Interval	2808.665	0.00128	0.5	Trapezoid	30	45
122R	Automatic Fixed Interval	19038.274	0.00531	0.5	Trapezoid	30	45
123R	Automatic Fixed Interval	4361.844	0.01616	0.5	Trapezoid	30	45
124R	Automatic Fixed Interval	6551.912	0.01217	0.5	Trapezoid	30	45
125R	Automatic Fixed Interval	8044.621	0.00856	0.5	Trapezoid	30	45
126R	Automatic Fixed Interval	10864.419	0.01528	0.5	Trapezoid	30	45
127R	Automatic Fixed Interval	8933.357	0.06799	0.5	Trapezoid	30	45
128R	Automatic Fixed Interval	7555.296	0.05916	0.5	Trapezoid	30	45
129R	Automatic Fixed Interval	4850.403	0.00045	0.5	Trapezoid	30	45
130R	Automatic Fixed Interval	25984.702	0.05385	0.5	Trapezoid	30	45
131R	Automatic Fixed Interval	32761.598	0.00098	0.5	Trapezoid	30	45
133R	Automatic Fixed Interval	22917.494	0.00251	0.5	Trapezoid	30	45
134R	Automatic Fixed Interval	12941.815	0.00045	0.5	Trapezoid	30	45
135R	Automatic Fixed Interval	4850.403	0.00107	0.5	Trapezoid	30	45

Appendix

Reach Number	Muskingum Cunge Channel Routing						
	Time Step Method	Length (m)	Slope	Man-ning's n	Shape	Width	Side Slope
136R	Automatic Fixed Interval	18010.984	0.00064	0.5	Trapezoid	30	45
137R	Automatic Fixed Interval	4161.141	0.00056	0.5	Trapezoid	30	45
138R	Automatic Fixed Interval	47053.622	0.0017	0.5	Trapezoid	30	45
139R	Automatic Fixed Interval	7569.986	0.0001	0.5	Trapezoid	30	45
140R	Automatic Fixed Interval	1868.321	0.00026	0.5	Trapezoid	30	45
141R	Automatic Fixed Interval	12275.827	0.0016	0.5	Trapezoid	30	45
142R	Automatic Fixed Interval	7697.851	0.00038	0.5	Trapezoid	30	45
143R	Automatic Fixed Interval	12343.406	0.00057	0.5	Trapezoid	30	45
144R	Automatic Fixed Interval	5511.486	0.00165	0.5	Trapezoid	30	45
145R	Automatic Fixed Interval	11674.57	0.00126	0.5	Trapezoid	30	45
146R	Automatic Fixed Interval	16729.006	0.00262	0.5	Trapezoid	30	45
147R	Automatic Fixed Interval	13829.121	0.0017	0.5	Trapezoid	30	45
148R	Automatic Fixed Interval	19563.568	0.00332	0.5	Trapezoid	30	45
149R	Automatic Fixed Interval	10448.231	0.00165	0.5	Trapezoid	30	45
150R	Automatic Fixed Interval	10757.092	0.00058	0.5	Trapezoid	30	45
151R	Automatic Fixed Interval	13008.772	0.00211	0.5	Trapezoid	30	45
152R	Automatic Fixed Interval	8162.372	0.00325	0.5	Trapezoid	30	45
153R	Automatic Fixed Interval	14035.063	0.00374	0.5	Trapezoid	30	45
154R	Automatic Fixed Interval	16370.399	0.00257	0.5	Trapezoid	30	45
155R	Automatic Fixed Interval	9122.295	0.00407	0.5	Trapezoid	30	45
156R	Automatic Fixed Interval	7479.789	0.00267	0.5	Trapezoid	30	45
157R	Automatic Fixed Interval	19872.304	0.00133	0.5	Trapezoid	30	45
158R	Automatic Fixed Interval	8408.395	0.00124	0.5	Trapezoid	30	45
159R	Automatic Fixed Interval	6835.235	0.00626	0.5	Trapezoid	30	45
160R	Automatic Fixed Interval	8579.841	0.00383	0.5	Trapezoid	30	45
161R	Automatic Fixed Interval	9684.666	0.00381	0.5	Trapezoid	30	45
162R	Automatic Fixed Interval	15802.831	0.00567	0.5	Trapezoid	30	45
163R	Automatic Fixed Interval	13227.093	0.00496	0.5	Trapezoid	30	45
164R	Automatic Fixed Interval	15185.76	0.00397	0.5	Trapezoid	30	45
165R	Automatic Fixed Interval	9530.623	0.00472	0.5	Trapezoid	30	45
166R	Automatic Fixed Interval	10058.91	0.00489	0.5	Trapezoid	30	45
167R	Automatic Fixed Interval	8072.914	0.00565	0.5	Trapezoid	30	45
168R	Automatic Fixed Interval	8362.237	0.00661	0.5	Trapezoid	30	45
169R	Automatic Fixed Interval	32434.031	0.00447	0.5	Trapezoid	30	45
170R	Automatic Fixed Interval	11859.662	0.01387	0.5	Trapezoid	30	45
171R	Automatic Fixed Interval	17632.406	0.02148	0.5	Trapezoid	30	45
172R	Automatic Fixed Interval	24427.424	0.0333333	0.76881	Trapezoid	30	45
173R	Automatic Fixed Interval	14511.59	0.05183	0.5	Trapezoid	30	45

Reach Number	Muskingum Cunge Channel Routing						
	Time Step Method	Length (m)	Slope	Manning's n	Shape	Width	Side Slope
174R	Automatic Fixed Interval	11242.647	0.05	0.51002	Trapezoid	30	45
175R	Automatic Fixed Interval	19377.159	0.08739	0.5	Trapezoid	30	45
176R	Automatic Fixed Interval	16392.795	0.05	0.26595	Trapezoid	30	45
177R	Automatic Fixed Interval	2258.694	0.05	0.33333	Trapezoid	30	45
178R	Automatic Fixed Interval	2605.881	0.00385	0.5	Trapezoid	30	45
180R	Automatic Fixed Interval	13707.079	0.00107	0.5	Trapezoid	30	45
181R	Automatic Fixed Interval	3769.407	0.00261	0.5	Trapezoid	30	45
93R	Automatic Fixed Interval	25920.77	0.04381	0.5	Trapezoid	30	45
94R	Automatic Fixed Interval	5252.206	0.00501	0.5	Trapezoid	30	45
95R	Automatic Fixed Interval	16885.505	0.00622	0.5	Trapezoid	30	45
96R	Automatic Fixed Interval	3999.583	0.00492	0.5	Trapezoid	30	45
97R	Automatic Fixed Interval	6343.086	0.00182	0.5	Trapezoid	30	45
98R	Automatic Fixed Interval	6104.151	0.00142	0.5	Trapezoid		
99R	Automatic Fixed Interval				Trapezoid		

Appendix E. Magallanes Model Basin Parameters

Basin Number	SCS Curve Number Loss			Clark Unit Hydrograph Transform		Recession Baseflow				
	Initial Abstraction (mm)	Curve Number	Impervious (%)	Time of Concentration (HR)	Storage Coefficient (HR)	Initial Type	Initial Discharge (M3/S)	Recession Constant	Threshold Type	Ratio to Peak
13B	0.1366	92.4	0	0.2625	0.53579	5.9882	0.66	0	Ratio to Peak	0
14B	0.1366	92.4	0	0.735	1.4876	4.4709	0.9702	0	Ratio to Peak	0
20B	0.2136	92.4	0	0.7425	1.4978	6.393	0.9702	0	Ratio to Peak	0
25B	0.1167	95.592	0	1.11	2.2388	5.0656	0.9702	0	Ratio to Peak	0
27B	0.1165	95.628	0	0.975	1.9723	8.1324	0.9702	0	Ratio to Peak	0
29B	0.1366	92.4	0	1.2225	2.4644	10.478	0.66	0	Ratio to Peak	0
30B	0.0871	92.4	0	0.5175	1.04	7.1999	0.66	0	Ratio to Peak	0
38B	0.1364	99	0	1.905	3.8499	1.2045	0.99	0	Ratio to Peak	0
39B	0.1184	96.048	0	1.32	2.6678	18.28	0.9702	0	Ratio to Peak	0
40B	0.1817	95.316	0	0.57	1.157	17.732	0.9702	0	Ratio to Peak	0
41B	0.0871	94.5	0	0.8025	1.6259	4.1687	0.66	0	Ratio to Peak	0
48B	0.1338	99	0	5.985	12.083	15.65	0.9702	0		

Appendix F. Magallanes Model Basin Parameters

Reach Num-ber	Muskingum Cunge Channel Routing						
	Time Step Method	Length (m)	Slope	Manning's n	Shape	Width	Side Slope
104R	Automatic Fixed Interval	21158	0.0685	0.009	Trapezoid	30	45
110R	Automatic Fixed Interval	23128	0.0561	0.009	Trapezoid	30	45
115R	Automatic Fixed Interval	43840	0.0032	0.009	Trapezoid	30	45
117R	Automatic Fixed Interval	43813	0.0036	0.0088	Trapezoid	30	45
119R	Automatic Fixed Interval	22514	0.0134	0.009	Trapezoid	30	45
120R	Automatic Fixed Interval	6410.1	0.0731	0.009	Trapezoid	30	45
128R	Automatic Fixed Interval	31544	0.0023	0.0135	Trapezoid	30	45
129R	Automatic Fixed Interval	9229.6	0.0028	0.009	Trapezoid	30	45
130R	Automatic Fixed Interval	12612	0.0038	0.009	Trapezoid	30	45
131R	Automatic Fixed Interval	14038	0.0061	0.009	Trapezoid	30	45

Appendix G. Viray Model Basin Parameters

Basin Number	SCS Curve Number Loss			Clark Unit Hydrograph Transform		Recession Baseflow				
	Initial Abstraction (mm)	Curve Number	Impervious (%)	Time of Concentration (HR)	Storage Coefficient (HR)	Initial Type	Initial Discharge (M3/S)	Recession Constant	Threshold Type	Ratio to Peak
13B	0.1366	93.247	0	2.8	0.039511	0.39894	1	0	Ratio to Peak	0.05
14B	0.1366	89.4	0	7.84	0.84699	2.3846	0.6507	0	Ratio to Peak	0.05
20B	0.2136	91.441	0	7.92	0.85169	3.4702	0.64992	0	Ratio to Peak	0.05
29B	0.1366	91.429	0	13.04	1.3992	6.0543	0.91153	0	Ratio to Peak	0.05
30B	0.0871	91.183	0	5.52	0.57743	2.6935	0.91225	0	Ratio to Peak	0.05
38B	0.1364	99	0	20.32	2.15592	1.3807	0.66	0	Ratio to Peak	0.05
39B	0.1184	98.92944	0	14.08	1.49396	5.8728	0.9702	0	Ratio to Peak	0.05
40B	0.1817	98.17548	0	6.08	0.64792	1.6777	0.9702	0	Ratio to Peak	0.05
41B	0.0871	97.335	0	8.56	0.91052	2.1174	0.9702	0	Ratio to Peak	0.05

Appendix H. Viray Model Reach Parameters

Reach Number	Muskingum Cunge Channel Routing						
	Time Step Method	Length (m)	Slope	Manning's n	Shape	Width	Side Slope
104R	Automatic Fixed Interval	21158.274	0.06851	0.0027	Trapezoid	30	45
110R	Automatic Fixed Interval	23128.317	0.05606	0.0027	Trapezoid	30	45
119R	Automatic Fixed Interval	22513.754	0.01336	0.0027	Trapezoid	30	45
120R	Automatic Fixed Interval	6410.124	0.07312	0.0027	Trapezoid	30	45
129R	Automatic Fixed Interval	9229.623	0.00279	0.0027	Trapezoid	30	45
130R	Automatic Fixed Interval	12612.106	0.00381	0.0027	Trapezoid	30	45
131R	Automatic Fixed Interval	14037.817	0.00612	0.0027	Trapezoid	30	45

Appendix I. Dipalo Model Basin Parameters

Basin Number	SCS Curve Number Loss			Clark Unit Hydrograph Transform		Recession Baseflow				
	Initial Abstraction (mm)	Curve Number	Impervious (%)	Time of Concentration (HR)	Storage Coefficient (HR)	Initial Type	Initial Discharge (M3/S)	Recession Constant	Threshold Type	Ratio to Peak
41B	0.0870858	45	0	8.6	20	2.1174	0.9702	0	Ratio to Peak	0.76157

Appendix J. Dipalo Model Reach Parameters

Reach Number	Muskingum Cunge Channel Routing						
	Time Step Method	Length (m)	Slope	Manning's n	Shape	Width	Side Slope
131R	Automatic Fixed Interval	14037.82	0.00612	0.0036	Trapezoid	30	45

Appendix K. Agno (1) HEC-HMS Discharge Simulation

DIRECT FLOW (cms)							
Time (hr)	100-yr	25-yr	5-year	Time (hr)	100-yr	25-yr	5-year
0	0	0	0	6	9.4	3.5	0.4
0.1666667	0	0	0	6.1666667	11.4	4.4	0.6
0.3333333	0	0	0	6.3333333	13.7	5.5	0.9
0.5	0	0	0	6.5	16.5	6.9	1.2
0.6666667	0	0	0	6.6666667	19.7	8.5	1.7
0.8333333	0	0	0	6.8333333	23.5	10.5	2.3
1	0	0	0	7	27.9	12.8	3
1.1666667	0	0	0	7.1666667	33	15.6	4
1.3333333	0	0	0	7.3333333	38.9	18.9	5.1
1.5	0	0	0	7.5	45.5	22.6	6.4
1.6666667	0	0	0	7.6666667	52.9	26.9	8
1.8333333	0	0	0	7.8333333	61.2	31.8	9.9
2	0	0	0	8	70.5	37.3	12
2.1666667	0	0	0	8.1666667	80.8	43.5	14.5
2.3333333	0	0	0	8.3333333	92.1	50.4	17.4
2.5	0	0	0	8.5	104.5	58	20.6
2.6666667	0	0	0	8.6666667	118	66.5	24.2
2.8333333	0	0	0	8.8333333	132.7	75.8	28.3
3	0	0	0	9	149.1	86.3	33.1
3.1666667	0	0	0	9.1666667	167.2	98.1	38.5
3.3333333	0	0	0	9.3333333	187.1	111	44.6
3.5	0.1	0	0	9.5	208.8	125.4	51.4
3.6666667	0.1	0	0	9.6666667	232.7	141.3	59.2
3.8333333	0.2	0	0	9.8333333	259.1	159.1	68
4	0.3	0	0	10	288	178.7	77.8
4.1666667	0.5	0.1	0	10.166667	319.4	200.1	88.7
4.3333333	0.8	0.1	0	10.333333	353.4	223.4	100.8
4.5	1.1	0.2	0	10.5	390.6	249.2	114.3
4.6666667	1.5	0.3	0	10.666667	430.9	277.3	129.3
4.8333333	2	0.5	0	10.833333	474.5	307.8	145.7
5	2.6	0.7	0	11	522.1	341.5	164
5.1666667	3.3	0.9	0	11.166667	574.6	378.7	184.4
5.3333333	4.2	1.3	0.1	11.333333	632	419.7	207.1
5.5	5.2	1.7	0.1	11.5	694.5	464.6	232.3
5.6666667	6.4	2.2	0.2	11.666667	764.8	515.5	261.3
5.8333333	7.8	2.7	0.3	11.833333	851.2	578.9	298.5

DIRECT FLOW (cms)							
Time (hr)	100-yr	25-yr	5-year	Time (hr)	100-yr	25-yr	5-year
12	948.5	650.8	341.2	18.333333	9461.2	7262.9	4642.2
12.166667	1053.1	728.4	387.6	18.5	9545.2	7332.4	4692.8
12.333333	1167.1	813.4	438.9	18.666667	9616.5	7392.2	4737.2
12.5	1299.3	912.6	499.4	18.833333	9670.5	7438.7	4773.2
12.666667	1446.8	1023.8	568	19	9708.1	7472.6	4801.2
12.833333	1604.2	1142.7	641.5	19.166667	9733.1	7496.8	4823
13	1770.2	1268.4	719.6	19.333333	9746	7511.6	4838.7
13.166667	1948.4	1403.7	803.9	19.5	9739	7510.9	4844.2
13.333333	2139.5	1549	894.8	19.666667	9709.8	7492.7	4838.2
13.5	2340	1701.7	990.5	19.833333	9667	7464.1	4825.3
13.666667	2548.4	1860.7	1090.5	20	9614.8	7427.9	4807.5
13.833333	2768.7	2029.1	1196.7	20.166667	9551.9	7383.5	4784.3
14	3004.3	2209.5	1311	20.333333	9476.9	7329.6	4755
14.166667	3249.8	2397.9	1430.7	20.5	9391.8	7267.9	4720.6
14.333333	3502.5	2592.1	1554.3	20.666667	9299	7200.3	4682.2
14.5	3765.7	2794.7	1683.7	20.833333	9198	7126.1	4639.6
14.666667	4047	3011.7	1822.9	21	9086.5	7043.8	4591.5
14.833333	4339.1	3237.4	1968.2	21.166667	8966.5	6954.7	4539.1
15	4636.5	3467.5	2116.6	21.333333	8840.6	6861	4483.4
15.166667	4939.5	3702.4	2268.6	21.5	8707.3	6761.4	4423.9
15.333333	5253.2	3946	2426.8	21.666667	8562.6	6652.9	4358.3
15.5	5573.5	4195.1	2589.2	21.833333	8408.5	6536.8	4287.6
15.666667	5895.1	4445.6	2753	22	8248.1	6415.8	4213.5
15.833333	6214.2	4694.6	2916.1	22.166667	8082	6290.1	4136.2
16	6524.1	4936.7	3075.1	22.333333	7907.5	6157.7	4054.1
16.166667	6824.6	5171.7	3229.9	22.5	7725	6018.9	3967.6
16.333333	7119	5402.3	3382.2	22.666667	7538.1	5876.4	3878.4
16.5	7406	5627.4	3531.1	22.833333	7349.8	5732.6	3788.3
16.666667	7677	5840.5	3672.6	23	7163.7	5590.6	3699
16.833333	7927.4	6037.6	3804.1	23.166667	6982.3	5451.9	3611.8
17	8163.9	6224.4	3929.1	23.333333	6802.8	5314.6	3525.4
17.166667	8390	6403.2	4049.4	23.5	6624.4	5178.2	3439.3
17.333333	8599.7	6569.6	4161.8	23.666667	6450.7	5045.2	3355.4
17.5	8784.2	6716.6	4261.8	23.833333	6287.5	4920.4	3276.8
17.666667	8951.9	6850.7	4353.8	24	6130.2	4800.1	3201
17.833333	9107.9	6976	4440.2	24.166667	5975.1	4681.4	3126.2
18	9249.7	7090.2	4519.5	24.333333	5823.2	4565.1	3052.7
18.166667	9365	7183.9	4585.6	24.5	5676.9	4453.1	2981.9

DIRECT FLOW (cms)							
Time (hr)	100-yr	25-yr	5-year	Time (hr)	100-yr	25-yr	5-year
24.666667	5534.9	4344.2	2912.9	31	1934.2	1544.1	1075.5
24.833333	5395.7	4237.4	2845.2	31.166667	1869.9	1493.1	1040.4
25	5259.1	4132.5	2778.5	31.333333	1806.9	1443	1005.9
25.166667	5127.1	4031.2	2713.9	31.5	1745.9	1394.5	972.4
25.333333	4999.4	3933	2651.4	31.666667	1686.8	1347.5	939.8
25.5	4874.3	3836.8	2589.9	31.833333	1629	1301.5	908
25.666667	4751.8	3742.6	2529.6	32	1572.5	1256.5	876.8
25.833333	4634.1	3652	2471.7	32.166667	1517.2	1212.4	846.3
26	4522.2	3565.8	2416.5	32.333333	1463.1	1169.3	816.4
26.166667	4413.5	3482.2	2362.9	32.5	1410.3	1127.2	787.1
26.333333	4306.8	3399.9	2310.1	32.666667	1358.8	1086.1	758.5
26.5	4202	3319.1	2258.1	32.833333	1308.8	1046.2	730.7
26.666667	4099.2	3239.7	2206.9	33	1261.1	1008.1	704.2
26.833333	3998.1	3161.6	2156.3	33.166667	1215	971.2	678.5
27	3898	3084.1	2106	33.333333	1170	935.3	653.4
27.166667	3798.9	3007.4	2056.1	33.5	1126.2	900.3	629
27.333333	3702.8	2932.8	2007.5	33.666667	1083.7	866.3	605.2
27.5	3608.4	2859.6	1959.6	33.833333	1042.3	833.2	582.1
27.666667	3514.5	2786.6	1911.8	34	1002.1	801.1	559.6
27.833333	3421.4	2714.1	1864.2	34.166667	963.3	770.1	537.9
28	3329.1	2642.2	1816.7	34.333333	926.3	740.4	517.1
28.166667	3237.7	2570.8	1769.5	34.5	890.8	712	497.3
28.333333	3147.3	2500.2	1722.6	34.666667	856.7	684.7	478.1
28.5	3058.1	2430.4	1676.1	34.833333	823.8	658.4	459.7
28.666667	2971.9	2362.8	1631	35	792.2	633.1	442
28.833333	2888.9	2297.8	1587.5	35.166667	761.8	608.8	425
29	2807.7	2234	1544.7	35.333333	732.6	585.4	408.7
29.166667	2727.5	2171.1	1502.4	35.5	704.5	563	393
29.333333	2648.5	2108.9	1460.6	35.666667	677.6	541.5	378
29.5	2570.6	2047.6	1419.1	35.833333	652.2	521.2	363.8
29.666667	2494	1987.1	1378.2	36	628	501.8	350.3
29.833333	2418.6	1927.7	1337.8	36.166667	604.5	483.1	337.2
30	2344.6	1869.2	1298	36.333333	581.9	465	324.6
30.166667	2273	1812.6	1259.4	36.5	560	447.5	312.4
30.333333	2203	1757.2	1221.6	36.666667	538.9	430.7	300.6
30.5	2134.1	1702.7	1184.3	36.833333	518.6	414.4	289.3
30.666667	2066.3	1649	1147.5	37	498.9	398.7	278.3
30.833333	1999.7	1596.1	1111.3	37.166667	480.2	383.7	267.9

DIRECT FLOW (cms)							
Time (hr)	100-yr	25-yr	5-year	Time (hr)	100-yr	25-yr	5-year
37.333333	462.3	369.5	257.9	43.666667	105.9	84.8	59.5
37.5	445.1	355.7	248.3	43.833333	101.3	81.2	57
37.666667	428.5	342.4	239	44	96.8	77.6	54.5
37.833333	412.4	329.6	230.1	44.166667	92.4	74.1	52.1
38	396.9	317.2	221.4	44.333333	88.1	70.7	49.8
38.166667	381.9	305.2	213.1	44.5	84	67.4	47.5
38.333333	367.4	293.6	205	44.666667	80	64.3	45.3
38.5	353.5	282.6	197.3	44.833333	76	61.1	43.1
38.666667	340.4	272	189.9	45	72.2	58.1	41.1
38.833333	327.7	261.9	182.9	45.166667	68.5	55.2	39
39	315.5	252.2	176.1	45.333333	64.9	52.3	37.1
39.166667	303.8	242.8	169.5	45.5	61.4	49.5	35.1
39.333333	292.4	233.7	163.1	45.666667	57.9	46.7	33.2
39.5	281.5	225	157	45.833333	54.6	44.1	31.4
39.666667	270.9	216.5	151.1	46	51.3	41.5	29.6
39.833333	260.8	208.4	145.5	46.166667	48.2	39	27.9
40	251.2	200.7	140.1	46.333333	45.1	36.6	26.2
40.166667	242.1	193.5	135	46.5	42.2	34.3	24.6
40.333333	233.3	186.5	130.1	46.666667	39.5	32	23.1
40.5	224.9	179.7	125.4	46.833333	36.8	29.9	21.6
40.666667	216.7	173.2	120.9	47	34.5	28.1	20.3
40.833333	208.9	166.9	116.5	47.166667	32.5	26.5	19.2
41	201.3	160.9	112.3	47.333333	30.7	25	18.1
41.166667	194	155	108.2	47.5	28.9	23.6	17.2
41.333333	186.8	149.3	104.2	47.666667	27.3	22.3	16.3
41.5	179.9	143.8	100.4	47.833333	25.8	21.1	15.4
41.666667	173.2	138.5	96.7	48	24.5	20	14.6
41.833333	166.7	133.3	93.1				
42	160.4	128.2	89.5				
42.166667	154.2	123.3	86.1				
42.333333	148.2	118.6	82.8				
42.5	142.4	113.9	79.6				
42.666667	136.7	109.4	76.5				
42.833333	131.2	105	73.4				
43	125.8	100.7	70.5				
43.166667	120.6	96.5	67.6				
43.333333	115.5	92.5	64.8				
43.5	110.6	88.6	62.1				

Appendix L. Agno (2) HEC-HMS Discharge Simulation

DIRECT FLOW (cms)							
Time (hr)	100-yr	25-yr	5-year	Time (hr)	100-yr	25-yr	5-year
0	0	0	0	6	173.1	107.2	45.4
0.1666667	0	0	0	6.1666667	193.5	120.5	51.7
0.3333333	0	0	0	6.3333333	215.8	135.2	58.7
0.5	0	0	0	6.5	240.1	151.3	66.4
0.6666667	0	0	0	6.6666667	266.6	168.9	74.8
0.8333333	0	0	0	6.8333333	295.3	188	84.1
1	0	0	0	7	326.7	208.9	94.3
1.1666667	0	0	0	7.1666667	361	231.9	105.5
1.3333333	0.1	0	0	7.3333333	398.3	256.9	117.7
1.5	0.2	0	0	7.5	438.6	284.1	131.1
1.6666667	0.4	0.1	0	7.6666667	482	313.4	145.6
1.8333333	0.7	0.2	0	7.8333333	528.4	345	161.3
2	1.1	0.4	0	8	578.2	378.9	178.3
2.1666667	1.7	0.7	0.1	8.1666667	631.5	415.3	196.5
2.3333333	2.6	1	0.1	8.3333333	688.2	454.2	216.2
2.5	3.6	1.5	0.2	8.5	748.4	495.6	237.1
2.6666667	5	2.2	0.4	8.6666667	812	539.6	259.5
2.8333333	6.8	3.1	0.6	8.8333333	879.2	586	283.3
3	9	4.3	1	9	950.7	635.8	309
3.1666667	11.6	5.7	1.4	9.1666667	1026.8	688.8	336.6
3.3333333	14.7	7.4	1.9	9.3333333	1107.6	745.3	366.1
3.5	18.4	9.5	2.6	9.5	1192.9	805.3	397.5
3.6666667	22.6	12	3.5	9.6666667	1282.9	868.6	430.9
3.8333333	27.5	14.8	4.5	9.8333333	1377.4	935.3	466.3
4	33.1	18.1	5.8	10	1477.4	1006.2	504.1
4.1666667	39.4	21.9	7.3	10.166667	1583.4	1081.5	544.6
4.3333333	46.5	26.3	9	10.333333	1695.5	1161.3	587.6
4.5	54.4	31.1	11	10.5	1814.4	1246.2	633.6
4.6666667	63.2	36.6	13.3	10.666667	1940.1	1336.2	682.5
4.8333333	73	42.7	15.9	10.833333	2072.6	1431.2	734.5
5	83.7	49.5	18.9	11	2213.2	1532.4	790
5.1666667	95.5	57	22.2	11.166667	2362.4	1640	849.2
5.3333333	108.4	65.3	25.9	11.333333	2520.4	1754	912.2
5.5	122.6	74.4	30.1	11.5	2688	1875.3	979.4
5.6666667	137.9	84.3	34.7	11.666667	2868.7	2006.3	1052.2
5.8333333	154.6	95.1	39.7	11.833333	3073.8	2155.4	1135.5

DIRECT FLOW (cms)							
Time (hr)	100-yr	25-yr	5-year	Time (hr)	100-yr	25-yr	5-year
12	3296.1	2317.3	1226.2	18.333333	21701.5	16057.6	9302.1
12.166667	3530.1	2488	1322.1	18.5	22276.3	16492.2	9564.5
12.333333	3775.7	2667.4	1423.3	18.666667	22839.6	16918.4	9822.2
12.5	4033.1	2855.8	1529.7	18.833333	23387	17333	10073.5
12.666667	4306.2	3055.9	1643	19	23902.7	17724.4	10311.6
12.833333	4607.9	3277.3	1768.8	19.166667	24390	18094.7	10537.8
13	4931.2	3515	1904	19.333333	24858.7	18451.2	10756.2
13.166667	5268	3762.9	2045.6	19.5	25311.8	18796.3	10967.9
13.333333	5616.6	4020	2192.8	19.666667	25749.6	19129.9	11173.1
13.5	5976.4	4285.6	2345.4	19.833333	26168.5	19449.6	11370.2
13.666667	6349.1	4561.1	2504	20	26555.9	19746	11554.1
13.833333	6740.2	4850.5	2670.9	20.166667	26909.5	20017.4	11723.5
14	7148.2	5152.6	2845.6	20.333333	27239.5	20271.1	11882.6
14.166667	7569	5464.7	3026.4	20.5	27550.4	20510.6	12033.4
14.333333	8000.9	5785.4	3212.7	20.666667	27843.1	20736.5	12176.1
14.5	8443.1	6114.1	3404.2	20.833333	28115.8	20947.4	12310.1
14.666667	8897.7	6452.4	3601.6	21	28358.5	21136.1	12431.2
14.833333	9371.4	6805.1	3807.9	21.166667	28564	21297.2	12536.3
15	9865.7	7173.5	4023.6	21.333333	28745.6	21440.4	12631
15.166667	10373.2	7551.9	4245.5	21.5	28909.7	21570.5	12717.9
15.333333	10889.8	7937.6	4472.1	21.666667	29056.9	21688	12797.3
15.5	11415.2	8330.2	4703.2	21.833333	29186.5	21792.3	12869
15.666667	11951	8730.9	4939.5	22	29295.3	21881.1	12931.6
15.833333	12504.2	9144.7	5183.8	22.166667	29378.4	21950.9	12983.3
16	13081.8	9577	5439.1	22.333333	29441.3	22005.6	13026.3
16.166667	13672.4	10019.3	5700.4	22.5	29487.5	22047.9	13062
16.333333	14269.3	10466.6	5965.2	22.666667	29517.2	22078	13090.6
16.5	14872.2	10918.7	6233.2	22.833333	29531.2	22096.2	13112.2
16.666667	15480	11374.7	6503.8	23	29524.3	22098.9	13124.9
16.833333	16096.3	11837.2	6778.6	23.166667	29478.4	22072.8	13120.9
17	16730.3	12313.2	7061.4	23.333333	29407.2	22027.9	13106.2
17.166667	17370.6	12794.2	7347.4	23.5	29320.5	21971.4	13084.7
17.333333	18010	13274.8	7633.8	23.666667	29219.2	21903.9	13056.6
17.5	18648.2	13755	7920.3	23.833333	29103.6	21825.7	13022.4
17.666667	19283.1	14232.9	8206	24	28972.4	21735.9	12981.3
17.833333	19911.4	14706.3	8489.4	24.166667	28823.5	21632.8	12932.3
18	20521.7	15166.6	8765.6	24.333333	28660.4	21519.1	12877.2
18.166667	21116.8	15615.9	9035.9	24.5	28485.2	21396.3	12816.7

DIRECT FLOW (cms)							
Time (hr)	100-yr	25-yr	5-year	Time (hr)	100-yr	25-yr	5-year
24.666667	28298.3	21264.7	12750.8	31	15945.5	12201.4	7656.2
24.833333	28100.8	21125.1	12680.2	31.166667	15629	11964.1	7514.9
25	27891.3	20976.5	12604.2	31.333333	15318.1	11730.9	7375.6
25.166667	27667.9	20817.3	12521.8	31.5	15013	11501.7	7238.4
25.333333	27431.2	20648.1	12433.4	31.666667	14711.6	11275.1	7102.4
25.5	27183.8	20470.9	12340	31.833333	14412.8	11050.2	6967.2
25.666667	26926.8	20286.2	12242.1	32	14116.5	10827.1	6832.6
25.833333	26660.2	20094.2	12139.7	32.166667	13823.4	10606.2	6699.2
26	26382.6	19893.9	12032.2	32.333333	13536.6	10389.7	6568.1
26.166667	26090	19682.3	11917.8	32.5	13258.1	10179.3	6440.3
26.333333	25782	19459	11796.5	32.666667	12984	9972.1	6314
26.5	25463.9	19228.1	11670.5	32.833333	12712.5	9766.6	6188.5
26.666667	25138.5	18991.5	11540.9	33	12443.4	9562.7	6063.8
26.833333	24805.9	18749.4	11407.9	33.166667	12176.9	9360.7	5939.9
27	24466.1	18501.7	11271.3	33.333333	11913.8	9161.1	5817.3
27.166667	24116	18246.2	11129.9	33.5	11654	8963.8	5695.8
27.333333	23751.7	17979.9	10981.9	33.666667	11397.4	8768.8	5575.5
27.5	23380.1	17708	10830.3	33.833333	11144.2	8576.2	5456.4
27.666667	23004.6	17432.8	10676.3	34	10894.2	8385.9	5338.5
27.833333	22625.3	17154.5	10520.2	34.166667	10647.4	8197.8	5221.7
28	22243.3	16874	10362.3	34.333333	10404.5	8012.6	5106.4
28.166667	21860.5	16592.5	10203.5	34.5	10167.4	7831.6	4993.5
28.333333	21484.9	16316.2	10047	34.666667	9934.6	7653.7	4882.3
28.5	21112.7	16042	9891.3	34.833333	9704.8	7477.9	4772.2
28.666667	20740.4	15767.3	9734.9	35	9477.8	7304.2	4663.2
28.833333	20368.1	15492.4	9577.9	35.166667	9253.7	7132.6	4555.3
29	19996.4	15217.7	9420.5	35.333333	9033.5	6963.9	4449.1
29.166667	19627.7	14944.9	9263.6	35.5	8816.8	6797.8	4344.4
29.333333	19272.9	14682	9111.9	35.666667	8603	6633.8	4240.9
29.5	18927.1	14425.4	8963.3	35.833333	8392.5	6472.3	4138.9
29.666667	18584.2	14170.7	8815.3	36	8185.3	6313.3	4038.4
29.833333	18243.1	13917.1	8667.6	36.166667	7981.3	6156.6	3939.2
30	17903.4	13664.2	8519.8	36.333333	7781.1	6002.7	3841.7
30.166667	17566.4	13413.1	8372.5	36.5	7587.1	5853.6	3746.9
30.333333	17235.1	13166	8227.2	36.666667	7399.7	5709.3	3655
30.5	16909	12922.4	8083.5	36.833333	7216.5	5568.2	3565.1
30.666667	16585.8	12680.7	7940.7	37	7036.5	5429.5	3476.6
30.833333	16264.8	12440.5	7798.3	37.166667	6859.8	5293.3	3389.6

DIRECT FLOW (cms)							
Time (hr)	100-yr	25-yr	5-year	Time (hr)	100-yr	25-yr	5-year
37.333333	6686.5	5159.7	3304.1	43.666667	2442.4	1884.1	1205.6
37.5	6516.7	5028.6	3220.3	43.833333	2379.6	1835.7	1174.7
37.666667	6349.8	4899.9	3137.9	44	2318.3	1788.4	1144.4
37.833333	6186	4773.5	3056.9	44.166667	2258.5	1742.3	1115
38	6025.3	4649.5	2977.4	44.333333	2200.2	1697.3	1086.2
38.166667	5867.6	4527.7	2899.3	44.5	2143.2	1653.4	1058.2
38.333333	5712.9	4408.2	2822.7	44.666667	2087.7	1610.6	1030.8
38.5	5562.1	4291.7	2747.9	44.833333	2034.2	1569.3	1004.4
38.666667	5416.5	4179.2	2675.6	45	1982.3	1529.2	978.7
38.833333	5274.6	4069.5	2605.1	45.166667	1931.4	1490	953.6
39	5135.8	3962.2	2536.1	45.333333	1881.7	1451.6	929
39.166667	4999.9	3857.2	2468.6	45.5	1833.2	1414.2	905
39.333333	4867.2	3754.7	2402.7	45.666667	1785.8	1377.6	881.6
39.5	4737.8	3654.8	2338.6	45.833333	1739.6	1342	858.8
39.666667	4611.8	3557.4	2276.1	46	1694.4	1307.1	836.5
39.833333	4488.8	3462.4	2215.2	46.166667	1650.3	1273.1	814.7
40	4369	3370	2156	46.333333	1607.2	1239.9	793.5
40.166667	4252.4	3280	2098.3	46.5	1565.2	1207.5	772.7
40.333333	4138.8	3192.4	2042.3	46.666667	1524.3	1175.9	752.5
40.5	4028.4	3107.2	1987.8	46.833333	1484.7	1145.3	732.9
40.666667	3922.2	3025.2	1935.3	47	1446.5	1115.8	714
40.833333	3819.7	2946.1	1884.6	47.166667	1409.2	1087	695.5
41	3720	2869.3	1835.4	47.333333	1372.8	1058.9	677.5
41.166667	3623.1	2794.5	1787.6	47.5	1337.2	1031.5	660
41.333333	3528.8	2721.8	1741.2	47.666667	1302.6	1004.8	642.8
41.5	3436.9	2651	1695.9	47.833333	1268.9	978.7	626.2
41.666667	3347.2	2581.8	1651.8	48	1235.9	953.3	609.9
41.833333	3259.6	2514.3	1608.6	48.166667	1203.9	928.6	594.1
42	3174.2	2448.4	1566.5	48.333333	1172.6	904.5	578.7
42.166667	3090.9	2384.2	1525.5	48.5	1142.2	881	563.7
42.333333	3009.7	2321.6	1485.5	48.666667	1112.6	858.2	549.1
42.5	2930.6	2260.7	1446.6	48.833333	1083.7	835.9	534.8
42.666667	2854.2	2201.8	1408.9	49	1055.9	814.5	521.1
42.833333	2780.9	2145.2	1372.7	49.166667	1028.8	793.6	507.7
43	2709.7	2090.3	1337.5	49.333333	1002.3	773.1	494.6
43.166667	2640.3	2036.7	1303.3	49.5	976.4	753.1	481.8
43.333333	2572.7	1984.5	1269.9	49.666667	951.1	733.6	469.3
43.5	2506.7	1933.7	1237.3	49.833333	926.4	714.5	457.1

DIRECT FLOW (cms)							
Time (hr)	100-yr	25-yr	5-year	Time (hr)	100-yr	25-yr	5-year
50	902.3	695.9	445.2	56.333333	338	260.9	167
50.166667	878.8	677.8	433.6	56.5	328.8	253.8	162.5
50.333333	855.8	660.1	422.2	56.666667	319.8	246.9	158.1
50.5	833.5	642.8	411.2	56.833333	310.9	240.1	153.8
50.666667	811.7	626	400.5	57	302.2	233.4	149.5
50.833333	790.4	609.7	390	57.166667	293.5	226.7	145.3
51	770.1	594	380	57.333333	285	220.2	141.2
51.166667	750.5	578.8	370.2	57.5	276.7	213.8	137.2
51.333333	731.3	564.1	360.8	57.666667	268.4	207.5	133.2
51.5	712.6	549.6	351.5	57.833333	260.3	201.3	129.3
51.666667	694.4	535.5	342.5	58	252.4	195.2	125.4
51.833333	676.6	521.8	333.7	58.166667	244.7	189.2	121.7
52	659.3	508.5	325.2	58.333333	237.1	183.4	118
52.166667	642.4	495.5	316.8	58.5	229.7	177.8	114.4
52.333333	626	482.8	308.7	58.666667	222.5	172.2	110.9
52.5	610	470.4	300.8	58.833333	215.4	166.8	107.5
52.666667	594.4	458.4	293.2	59	208.4	161.4	104.1
52.833333	579.2	446.7	285.7	59.166667	201.6	156.2	100.8
53	564.6	435.5	278.5	59.333333	194.8	151	97.5
53.166667	550.6	424.7	271.6	59.5	188.2	145.9	94.3
53.333333	537	414.2	264.8	59.666667	181.6	140.8	91.1
53.5	523.7	403.9	258.3	59.833333	175.1	135.8	87.9
53.666667	510.8	393.9	251.9	60	168.7	130.9	84.8
53.833333	498.2	384.2	245.6				
54	485.9	374.7	239.6				
54.166667	473.9	365.5	233.6				
54.333333	462.2	356.5	227.9				
54.5	450.7	347.6	222.2				
54.666667	439.5	339	216.7				
54.833333	428.6	330.6	211.3				
55	417.8	322.3	206				
55.166667	407.2	314.1	200.8				
55.333333	396.8	306.1	195.7				
55.5	386.5	298.2	190.7				
55.666667	376.5	290.5	185.8				
55.833333	366.6	282.9	180.9				
56	356.9	275.4	176.2				
56.166667	347.4	268.1	171.5				

D R E A M

Disaster RIsk and Exposure Assessment for Mitigation